universität wien

MASTERARBEIT

Titel der Masterarbeit

„Chemical derivatization and cellular imaging of immunosuppressive peptides“

verfasst von

Mina Vasileva, BSc

angestrebter akademischer Grad

Master of Science (MSc)

Wien, 2014

Studienkennzahl lt. Studienblatt:	A066834
Studienrichtung lt. Studienblatt:	Masterstudium Molekulare Biologie
Betreut von:	Dr. Gernot Schabbauer

Acknowledgement

First of all I would like to express my gratitude to my supervisors Dr. Christian Gruber and Dr. Gernot Schabbauer for supervising my thesis and for the useful comments and remarks.

Furthermore I would like to thank Roland Hellinger and Kathrin Thell, PhD students in Gruber's group, for introducing me to the topic as well for the advice and guidance on the way.

Moreover, I would like to thank all the members of Dr. Gruber's research group for the friendly and motivating atmosphere.

I also would like to thank my family for the encouragement through my life, for their support and for their valuable motivation.

Table of contents

List of Figures and Tables

List of Figures

List of Tables

Abbreviations

AcN	acetonitrile
Ala	alanine
APC	antigen presenting cell
Arg	arginine
Asn	asparagines
ATP	adenosine triphosphate
BCE	before common era
CCK	cyclic cystine knot
CD	cluster of differentiation
cyO2	cycloviolacin O2
Cys	cysteine
CPP	cell penetrating peptide
CRAC	Ca^{2+} release-activated Ca^{2+} channel
Da	dalton
ddH_20	double distilled water
DMSO	dimethylsulfoxide
DNA	deoxyribonucleic acid
FACS	fluorescent-assisted cell sorting
FBS	fetal bovine serum
FITC	fluorescein isothiocyanate
Glu	glutamine

HeNe laser	helium-neon laser
HFT UV	Haupt-Farb Teiler (main dichroic beam splitter) Ultraviolet
HIV	human immunodeficiency virus
HPLC	high performance liquid chromatography
HTS	high throughput screening
IFN–γ	interferon-γ
IL-2	interleukin-2
JNK	c-Jun N-terminal kinase
kB1	kalata B1
Leu	leucine
LC–MS	liquid chromatography-mass spectrometry
Lys	lysine
LSM	laser scanning microscope
MACS	magnetic cell isolation and cell separation
MALDI-TOF	matrix assisted laser desorption ionization–time of flight
MeOH	methanol
MHC	major histocompatibility complex
MS	mass spectrometry
m/z	mass-to-charge ration
NFAT	nuclear factor of activated T-cells
NK cells	natural killer cells
NMR	nuclear magnetic resonance
PBMC	peripheral blood mononuclear cells

PBS	phosphate buffered saline
PC	phospatidylcholine
PE	phosphatidylethanolamine
PG	phosphatidylglycerol
PMA	phorbol myristate acetate
Pro	proline
PS	phospahtidylserine
PTEN	phosphatase and tensin homologue
Rcf	relative centrifugal force
RP-HPLC	revesed-phase high-performance liquid chromatography
Rpm	revolutions per minute
SHIP	SH_2–domain-containing inositol polyphosphate 5'phosphatase
Tat	trans-activating regulatory protein
TCR	T-cell receptor
TFA	trifluoroacetic acid
TNF–α	tumor necrosis factor-α
Trp	tryptophan
Val	valine
WHO	world health organization

1. Introduction

Natural products have been an essential source of medicinal compounds for over two millennia. The earliest evidence for the implementation of plant-derived substances in traditional medicine dates back to around 2600 BCE in the region of Mesopotamia (Cragg and Newman, 2013). Natural products have the ability to interact with many specific targets in the cells and they are an important source for bioactive molecules (Firn and Jones, 2003). Rich origins for such chemical compounds are not just animals and microbes, but also plants (Koehn and Carter, 2005). The World Health Organisation (WHO) surveyed that 65% of the world population is implementing plant-derived medicines as a source material to treat diseases (Newman and Cragg, 2013).

Over the last years there has been a fast increase in the development of methods for detection of molecular targets. This could be applied for the discovery of novel drugs for prevention and treatment of human diseases (Newman et al., 2003). Moreover, due to better selectivity of molecular targets through implementation of methods from the molecular or cellular biology, the focus of the pharmaceutical industry switched away from natural products (Koehn and Carter, 2005). Additionally, automated technologies like high throughput screening (HTS) enabled the search of molecular targets in synthetic chemical databases (Koehn and Carter, 2005).

Nevertheless, the discovery of novel natural products continues to play an important role in the healthcare nowadays and is a main source for innovative pharmaceutical agents (Mischra and Tiwari, 2011). Additionally, natural product compounds such as plant-derived bioactive peptides are essential for the pharmacological industry due to their wide range of pharmacological effects which can be implemented for the development of therapeutic products.

1.1 Bioactive peptides from natural sources

Bioactive peptides are produced in all species of life from bacteria to mammals (St Georgiev, 1990; Hancock and Diamond, 2000). They are protein fragments which have a positive effect on living organisms (Korhonen and Philanto, 2007). They possess a wide variety of properties – antimicrobial (Tam et al., 1999), antioxidative (Sarmadi and Ismail, 2010) and immunomodulatory activities (St Georgiev, 1990). They inflect physiological functions and have a drug like activity (Sharma et al., 2011).

With the change and development in screening and drug design technologies higher efficiency and faster effect are desired. In the last century drugs have been developed from small natural products with a molecular weight of <500 Da, which is beneficial for their oral bioavailability. However, their small size is the cause for reduced target selectivity which triggers side-effects (Craik et al., 2013). This problem could be overcome with protein therapeutics whereby there are three main sources of therapeutic peptides (Lantham, 1999; Sato et al. 2006)

a) Plants, animals or human-derived bioactive peptides
b) Recombinant peptides
c) Peptides derived through chemical synthesis

However, there are some drawbacks with the implementation of these peptides, which are connected with membrane impermeability, low bioavailability, and negligible activity when administered orally, metabolic instability and high cost (Vlieghe et al., 2010). Overcoming these problems could lead to more targeted approach and to the discovery of novel drugs with better efficacy in the treatment of diseases.

Sources for such bioactive compounds are venom toxins from spiders (Escoubas, 2006; Escoubas et al., 2006), scorpions (Possani et al., 1999), snakes (Fox and Serrano, 2007; Theakston and Kamiguti, 2002) and marine animals, in particular cone-snails (Alewood et al., 2003; Norton and Olivera, 2006; Olivera et al., 1990). Most isolated peptides are rich in cysteines to

stabilize their active conformation (Arnison et al., 2013). Previous studies focused on the venom of cone-snails, because of the presence of bioactive peptides known as conotoxins within it. These are molecules with the length of 6 to 50 amino acids which have highly conserved cysteine frameworks. The pharmacology industry concentrated on these bioactive peptides due to their effect against chronic pain. This resulted in the marketing of a synthetic conopeptide, namely ziconotide (Prialt®), as a drug (Pope and Deer, 2013). However, its application was restricted because of cytotoxicity (Webster et al., 2008), but pharmaceutical developments provided protection against serious side effects (Mitchell et al., 2013).

Another rich source of naturally occurring bioactive peptides are plants which contain 19 000 to 59 000 active compounds (Gruber et al., 2010). Furthermore, this class of peptides has extracellular and intracellular activities. Peptides, located outside the cell surface, play an important role in signaling and defense. On the other hand, intracellular peptides are crucial for a variety of physiological functions or could be the products of proteolysis (Farrokhi et al., 2008).

Special emphasis in the class of plant derived bioactive peptides is placed on circular peptides, so called cyclotides, due to their stability, bioactivity, abundance and sequence diversity (Gruber et al., 2010). They are ribosomally synthesized gene product and can be produced by recombinant techniques (Kimura et al., 2006) or in plant suspension culture (Seydel et al., 2007)

1.2 Cyclotides

1.2.1 Discovery of cyclotides

The history of cyclotides may be traced back to the 1960s when Sandberg reported that some indigenous African tribes have been using extract from the plant *Oldenlandia affinis* to facilitate childbirth (Sandberg, 1965). Later, the Norwegian doctor Lorents Gran made a Red Cross relief mission in the Republic of Congo and observed that African women have been using the plant

called “kalata-kalata” for medicinal purposes (Gran, 1973). The uterotonic substance from this *Oldenlandia affinis* plant has been isolated and analyzed. Gran determined that it contained cyclic peptides which are responsible for the strong activity. The fraction B1 has been the most fully characterized one. In this way the first cyclotide has been discovered and the peptide kalata B1 has been identified as an active ingredient (Gerlach and Mondal, 2012).

In the year 1995 the structure of the isolated peptides has been determined and in this way a class of new cyclic peptides has been discovered (Saether et al., 1995). Cyclotides are a class of plant peptides which are isolated from plants of the families *Rubiaceae* (coffee), *Violaceae* (violet), and *Cucurbitaceae* (Simonsen et al., 2005; Gruber et al., 2008).

1.2.2 Structure of cyclotides

Cyclotides are a class of plant-derived cyclic peptides which are characterized by a head-to-tail cyclic backbone and a cystine knot core composed of three highly conserved disulfide bonds (Craik, 2011). In Figure 1-1 a typical Möbius cyclotide called kalata B1, which is a representative cyclotide from *Rubiaceae* family, is illustrated. The three disulfide bonds are shown in yellow in Figure 1-1 and are formed as C_I-C_{IV}, C_{II}-C_V and C_{III}-C_{VI}. The ring-shaped structure of the peptide is organized by the disulfide bridges between C_I-C_{IV} and C_{II}-$C_{V.}$ Additionally, the third disulfide bond C_{III}-C_{VI} strands the ring. The structure shown in Figure 1-1 is responsible for the stability and for the resistance of the cyclotides to thermal and chemical denaturants and to peptidases (Colgrave and Craik, 2004).

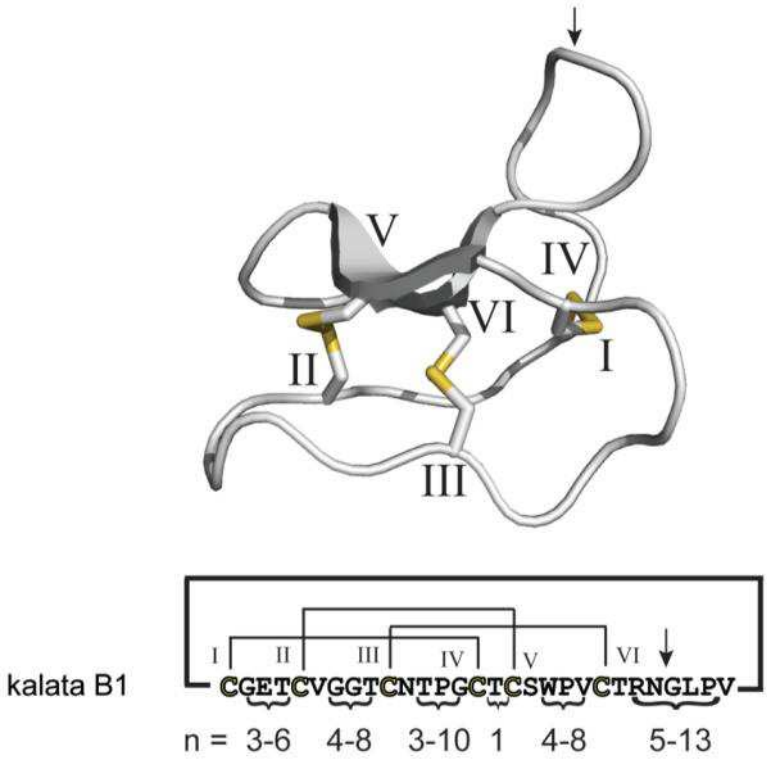

Figure 1-1: Structure and sequence diversity of cyclotides. In gray is illustrated the structure of the cyclotide kalata B1. With roman numerals are labeled the six conserved cysteines and in yellow is shown the resulting cystine knot disulfide connectivity (C_I–C_{IV}, C_{II}–C_V, and C_{III}–C_{VI}). Below the structure are shown the amino acid sequence and disulfide connectivity of kalata B1. The possible length (in amino acids) of the intercysteine loops, comprising all currently known cyclotides (according to Ireland et al., 2010), is indicated by the numbers (n). A wide variety of amino acid substitutions can be tolerated by the intercystine loops and they are an indicator of the combinatorial diversity of the cyclotide scaffold. The figure was adopted from Gründemann et al., (2012)

In the literature two classes of cyclotide subfamilies have been described – Möbius and bracelet cyclotides (Daly et al., 2009). The difference is in the presence or absence of a cis-Pro peptide bond in loop 5. Möbius cyclotides, like kalata B1, contain such a structure which induces a local 180° twist in the peptide angle bond (Ireland et al., 2010). NMR α-H analysis showed that there was no significant difference in the three-dimensional structure when comparing wild type kalata B1 and kalata B1 T20K mutant (Gründemann et al., 2013). The mutation was located on the opposite side of the peptide surface and the exchange of threonine to lysine had little effect on the hydrophobic properties and area of the cyclotide (Gründemann et al., 2013).

Cyclotides have a hydrophobic surface which is the reason for their late elution time on reversed-phase chromatography (Daly et al., 1999). Their size is

between 28 and 37 amino acids which correspond to a mass in the range of 2500 - 4000 Da (Daly et al., 1999). Additionally, they are interesting for the pharmaceutical industry due to their stability and bioactivity. Due to these properties cyclotides can be implemented as a scaffold for peptide based drugs which is the reason they are suitable for therapeutic agents (Wang et al., 2009).

1.2.3 Bioactivity of cyclotides

Many bioactive peptides are inappropriate as drugs, because they have reduced bioavailability and stability under physiological conditions. However, cyclotides have a great pharmaceutical potential due to their stability in plasma and against gastrointestinal proteases (Colgrave and Craik, 2004; Colgrave et al., 2005). Due to the presence of hydrophobic patches (Clark et al., 2006) and because of their retained activity upon oral administration as tea in humans, cyclotides are promising tools for the development of novel drugs (Gran, 1970).

The main aim of these bioactive peptides within the plant is to protect it from different pathogens, but also to participate in a variety of physiological processes and signaling (Farrokhi et al., 2008). Due to the previously investigated uterotonic activity, cyclotides got interesting for scientists. Further research determined many others biological activities, including insecticidal (Barbeta et al., 2008; Gruber et al., 2007), antimicrobial (Tam et al., 1999), antifungal (Tam et al., 1999), anticancer (Lindholm et al., 2002; Görranson et al., 2004; Gerlach et al., 2010) nematodical (Colgrave et al., 2008; Colgrave et al., 2009), antifouling (Görranson et al., 2004), molluscicidal (Plan et al., 2008), anthelmintic (Colgrave et al., 2008), neurotensinantagonism (Whiterup et al., 1994), haemolytic (Ireland, 2006) and anti-HIV (Ireland et al., 2008) activity. Furthermore, cyclotides showed cytotoxicity to lymphoma cell lines which is a main drawback when using this peptides in higher concentration to treat diseases (Svangard et al., 2004; Lindholm et al., 2002). The mechanism of action of the different bioactivities of cyclotides is still unknown. However, it is evident that the cyclotides interact with the cell membrane and are internalized

into the cell (Wang et al., 2012). Furthermore, recent research with one of the most abundant cyclotides from *Oldenlandia affinis* – kalata B1, determined antiproliferative function of this peptide in activated primary human lymphocytes (Gründemann et al., 2012). This immunosuppressive function, combined with their stability can be used for treatment of autoimmune diseases (Gründemann et al., 2012).

1.2.4 Immunosuppressive properties of cyclotides

The body's immune system protects the organism from different diseases. However, failures in the regulation and activation of T-cells or B-cells, or both can cause an over–reactivity and this can result in autoimmune diseases as rheumatoid arthritis, Crohn's disease or multiple sclerosis (Gründemann et al., 2012; Thell et al., 2013). Autoimmune conditions are individually rare, but still 5% of the population in Western countries is affected (Sinha et al., 1990; Jacobson et al., 1997). There are different reasons for those autoreactivity. Besides genetic susceptibility and the environment, main roles for the autoimmune diseases play gender, tissue injury and defects of lymphocyte development (Davidson and Diamond, 2001).

An option for treatment of these autoimmune conditions is immunosuppression. In this way the activation or efficiency of the immune system is reduced which can be implemented through action on the proliferation of T-lymphocytes by blocking the cell cycle progression of these cells (Macian, 2005). The progress of autoimmune diseases could be decreased through the implementation of drugs like cyclosporine, rapamycin or tacrolimus (Matsuda and Koyasu, 2000). Regularly implemented by organ transplantation and to prevent allograft rejections is cyclosporine which is a cyclic nonribosomal depsipeptide of fungal origin (Thell et al., 2013). In spite of the fact that it has severe side effects (De Mattos et al., 2000) it is a clinically used immunosuppressive drug (Thell et al., 2013). The mechanism of action of this peptide is the repression of IL-2 dependent T-cell proliferation through inhibition of NFAT dephosphorylation and

subsequent activation. Additionally, it interferes with p38 and JNK signaling cascades (Getts et al., 2011; Matsuda and Koyasu, 2000).

Moreover, traditional and alternative herbal treatments have yet not proven, but promising efficacy as immunosuppressive drugs (Reuter et al., 2010). Recent research reported that a mutant from the cyclotide kalata B1, where the threonine at position twenty is exchanged with a lysine (T20K mutant) has an antiproliferative effect on lymphocytes (Gründemann et al., 2012). Although the main mechanism of action is still unclear, the cyclotide [T20K] kalata B1 suppresses the proliferation of human T-cells (Gründemann et al., 2012). Cytokine signaling analysis with this peptide demonstrated that treatment of activated T-lymphocytes with this compound decreased the expression of IL-2 surface receptor (CD25) as well as IL-2 cytokine secretion and IL-2 gene expression (Gründemann et al., 2013). This is evidence that cyclotides interfere with T-cells and inhibit the proliferation of immune competent cells through inhibiting IL-2 biology at more than one site. Additionally, the production of IFN–γ and TNF–α was also reduced (Gründemann et al., 2013). Although the exact target of [T20K] kalata B1 remains unknown, this novel cyclotide could be implemented in non-cytotoxic concentration as potential therapeutic drug against immunosuppressive diseases (Gründemann et al., 2012). To perform its biological activity, the cyclotide should firstly reach its intracellular target. This ability to penetrate into living cells categorizes it as a cell penetrating peptide.

1.3 Cell penetrating peptides

Cell penetrating peptides are short proteins which have the ability to cross through cellular membranes of living cells and this makes them a promising tool for drug delivery applications. It was shown that kalata B1 and MCoTI-II have the ability to penetrate into living cells (Greenwood et al, 2007; Cascales et al., 2011). The molecular mechanism of cellular uptake for MCoTI-II was suggested to be via macropinocytosis (Greenwood et al., 2007). However kalata B1 interacts directly with the membrane and targets phosphatidylethanolamine

phospholipids which leads to membrane bending and formation of vesicles (Cascales et al., 2011).

Cascales and co-workers constituted a new family of cell penetrating peptides – cyclic cell penetrating peptides which are advantageous due to their extraordinary stability and because of their increased bioavailability which makes them essential for the field of drug delivery.

1.4 Characterization of peptide-membrane interaction

Living cells are protected from the surrounding environment with cell membranes so that this efficient barrier prevents the entry of extracellular macromolecules (Madani et al., 2011). However, in the last years there has been evidence that some cyclotides interact with the cell membrane and possess cell penetrating properties (Geenwood et al., 2007; Contreras et al., 2011; Cascales et al., 2011). They share a common mechanism of action concerning the targeting of biological membranes (Simonsen et al., 2008). Greenwood et al., discovered the first cyclotide (MCoTI-II) which is able to enter mammalian cells, however recent studies proposed that kalata B1 (Cascales et al., 2011) and MCoTI-I (Contreras et al., 2011) are able to pass through cell membranes, too. Previous research suggested that membrane interaction is involved in the biological activity of cyclotides. Besides NMR analysis (Shenkarev et al., 2006; Shenkarev et al., 2008) and plasmon resonance experiments (Kamimori et al., 2005), electrophysiological studies (Huang et al., 2009) and a Lys-scan (Huang et al., 2010) of kalata B1 approved its interaction with cellular membranes.

The interaction between cellular membrane and cyclotides is enhanced when the lipid bilayers consist of phospholipids, containing phosphatidylethanolamine headgroups (Henriques and Craik, 2012). The lipid composition is playing a main role for the amount of cyclotides bounded to the cell membrane and for their activity. Additionally, cyclotides with a positive net charge have higher activity of interaction with cellular membranes than those that are neutral or

negatively charged (Svangard et al., 2004; Ireland et al., 2008). Moreover, the majority of cyclotides have a cluster of surface exposed hydrophobic amino acids which integrity appears to be essential for their biological activities (Ireland et al., 2008; Svangard et al., 2007). Through these nonspecific hydrophobic peptide-lipid interactions the cyclotides can bind the cell membrane. Additionally, it might be that the ability of cyclotides to target and disrupt lipid bilayers correlates with their biological function (Henriques and Craik, 2012).

Moreover, it was demonstrated that the orientation of the cyclotides on the cell membrane or in the cell is similar (Shenkarev et al., 2006; Shenkarev et al., 2008). It is supposed that the cysteine knot is not responsible for the membrane binding interactions, although it provides a core framework where the hydrophobic patch regulates the membrane interactions (Daly et al., 2009). Previous NMR analysis showed that kalata B1 binds dodecylphosphocholine micelles mainly via this surface-exposed hydrophobic patch (Shenkarev et al., 2006). This interaction may be essential for the ability of cyclotides to target and disrupt lipid bilayers.

Moreover, Sando et al. showed that the peptide – membrane correlation is independent of a receptor and is due to hydrophobic interactions. Additionally, he defined the importance of phosphatidylethanolamine headgroups for the membrane binding of kalata B1. This interaction promotes outward movement of PE phospholipids so that more PE headgroups are exposed in outer leafet which promotes the binding of more cyclotides to the lipid bilayer. Furthermore, the affinity of the cyclotide to the cellular membrane increased, if cholesterol and sphingomyelin were available and if the fluidity of the membrane was low. This is evidence that the membrane consistency could affect the binding of kalata B1 (Henriques and Craik, 2012). The importance of membrane selectivity and the relevance of PE headgroups were supported by studies where higher amount of peptide was binding to nitrocellulose membranes which were containing phospholipids with a range of PE head groups (Cascales et al., 2011). Moreover, the membrane composition is essential for the lytic activity of cyclotides (Figure 1-2). After the attachment to the cell membrane and insertion in the bilayer core, a pore formation mechanism is being induced and in this

way cyclotides cause the destruction of the membrane (Henriques and Craik, 2012).

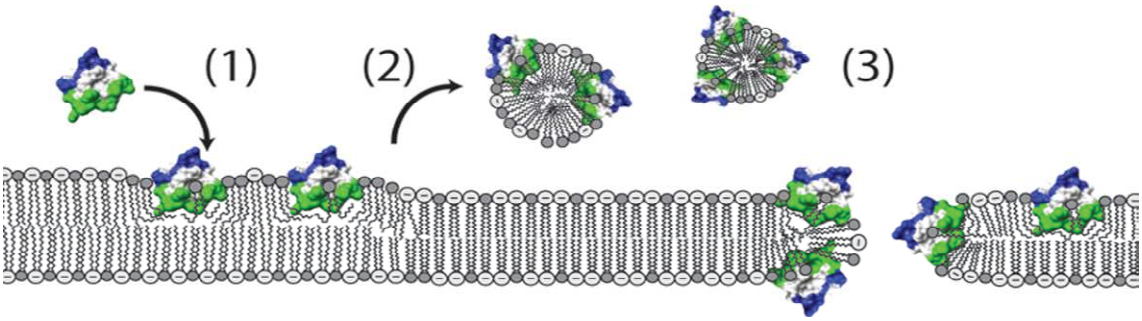

Figure 1-2: Proposed lytic mechanism of the cyclotide cycloviolacin O2 on a phosphatidylethanolamine/phosphatidylglycerol membrane. (1) Cyclotide adsorption driven by hydrophobic patch (green), cationic residues (blue), and PE affinity, results in demixing of PE and cyclotide (by PE affinity and negative curvature contribution). (2) Membrane thinning and increased positive curvature stress are the results from the depletion of PE lipids from the membrane by micellization. (3) Membrane perforations, resulting in leakage, are being forced when a higher local cyclotide concentration threshold is reached. The figure was adopted from Burman et al., (2014).

To apply this membrane disrupting activity, cyclotides must have affinity to the cellular membrane. When e threshold concentration is achieved the cyclotides induce pore-formation and cause membrane disruption (Henriques and Craik, 2012).

Different models of these mechanisms have been suggested. One mode of action is the specific pore formation or more general stress generated perforations. This process is characterized by the generation of “barrel-stave” or “toroidal” pores with a diameter of 4.1 – 4.7 nm (Huang et al., 2009; Wang et al., 2012). These features are related to the bioactivity of cyclotides to disrupt membranes and to interact with the intracellular target. Their activity is involved in the depletion of membrane lipids due to the solubilization of cell membranes by the peptide (Wang et al., 2012). Because of the positive membrane curvature, induced by the binding of kalata B1, the lipids have been extracted from the membrane surface to the space inside of the kalata B1 cluster (Nawae et al., 2014). The high local concentration of cyclotides and the lipid demixing

which is the result of membrane thinning and curvature stress are promoting the formation of pores and cleavage lined by cyclotides (Figure 1-2).

1.5 Molecular mechanism of cellular uptake

Although, cell-penetrating peptides have common properties, they differ in the internalization mechanism. The cell entry routes can be divided in energy driven (endocytosis) or energy independent (direct penetration) (D'Souza et al., 2014). Endocytosis seem to be the cell entry pathway for most peptides (Conner and Schmidt, 2003; Amand et al., 2008), however some of them are internalized through translocation involving direct interaction with the cellular membrane and direct penetration (Henriques et al., 2005). Additionally some peptides are using both mechanism of peptide internalization (Boisseau et al., 2006; Mano et al., 2006).

The cell penetrating peptides can bind specific, through a receptor, or non-specific, adsorptive, for the endocytotic internalization of the peptides (Conner and Schmidt, 2003). The non-specific fluid endocytosis is a process with low efficiency that involves fluid uptake and is not specifically influenced by physicochemical properties of the peptide.

Previous research approved that MCoTI-I and MCoTI–II, which have sequence similarity, are internalized by an energy dependent pathway and they cannot pass through the membrane implementing direct penetration (Greenwood et al., 2007; Cascales et al., 2011; Contreras et al., 2011). Moreover, the positive patch at the surface of MCoTI-II is important for its internalization. A main role for the endocytic process is playing the interaction of basic residues in MCoTI-II with negatively charged phosphoinositides on the cell membrane (Greenwood et al., 2007). However, kalata B1 has a different mechanism of interaction with the cellular membrane. For its internalization it should bind to lipid components and its hydrophobic patch should be transferred into the cell membrane (Greenwood et al., 2007).

1.5.1 Membrane permeable peptides (direct penetration)

The direct penetration of peptides is an energy-independent way for transporting them through the cellular membrane (Madani et al., 2011). The first step of this process is the interaction between the positively charged cell penetrating peptide and the negatively charged components of the cellular membrane such as heparin sulphate or the phospholipid bilayer. Previous research described the process of direct penetration as pore formation (Matsuzaki et al., 1996), inverted micelle formation (Derossi et al., 1996), the carpet-like model (Pouny et al., 1992) and the membrane thinning model (Lee et al., 2005). The interaction between the peptide and the cellular membrane is dependent on the peptide concentration, peptide sequence and lipid concentration (Madani et al., 2011).

1.5.2 Endocytic uptake of peptides

Endocytosis is an energy dependent process which consists of several pathways (Madani et al., 2011). One of them is phagocytosis which includes cellular uptake of large particles. Another one is pinocytosis which is identified as macropinocytose, separated in clathrin and/or caveolin dependent and independent uptake (Jones, 2007; Major and Pagano, 2007). Macropinocytosis is characterized as a folding of the outer surface of the cell membrane, resulting in the formation of vesicles which are surrounded by membrane, similar to the cell membrane. Additionally, for the invagination of the membrane, a protein called dynamin is required (Madani et al., 2011). For the receptor dependent endocytosis clathrin and calveolin are required for membrane curvature and for the support of the formation of vesicles after binding of the ligand to the extracellular receptor (Madani et al., 2011).

Interestingly, mainly hydrophilic macromolecules are entering the cells through endocytosis. This involves absorption to the cell membrane, followed by an

energy-dependent formation of a vesicle (Murkherjee et al., 1997). In this way molecules can be delivered to the cytoplasmic compartments. Additionally, low temperature treatment arrests all energy-dependent movements across the membrane (Kaplan et al., 2005).

1.5.3 Direct translocation through biological membranes

It was indicated recently that the internalization mechanism of arginine-rich peptides differ on several conditions – peptide sequence, concentration, cell type and culture medium and that endocytosis may not be the sole uptake mechanism of arginine rich peptides (Durchardt etal., 2007; Fretz et al., 2007; Kosuge et al., 2008). Due to special formations on the cellular membrane, which are called “particle-like”, the peptide was able to diffuse through the cellular membrane (Hirose et al., 2012). Because of the attachment of the peptides to hydrophobic cargo molecules, structural changes in the membrane have been induced and the peptides were allowed to penetrate through the cell membrane which can be implemented as a novel drug delivery system for arginine-rich peptides (Hirose et al., 2012).

1.5.4 Factors, affecting cellular uptake

There are some factors, playing an important role for the cellular uptake. One of the most important aspects is the positive charge of the peptide. Arginine-rich peptides are more favorable for delivery and for the cell penetrating activity of the peptide (Wender et al., 2000; Thoren et al., 2003). On the other hand, the conformation and length of the sequence are playing an essential role for the cellular uptake. The hydrophobic alpha helical structures are beneficial (Mitschell et al., 2000; Futaki et al., 2001). Additionally, the presence of the cargo could also alter the uptake pathway. Moreover, the experimental conditions like implemented peptide concentration, temperature, incubation type

and cell type may have an impact on the peptide entry (Madani et al., 2011). However the labeling of the peptide may also influence the intracellular distribution, the cytotoxicity and the molecular mechanism of peptide uptake (Fisher et al., 2002; Lundberg et al., 2007).

1.5.5 Methods to study molecular mechanism of uptake

A common way to measure the uptake of peptides is through coupling them to a fluorophore and measuring the fluorescence of the treated cells. In this way the localization and the amount of peptide could be defined. However uptake does not always correlate with bioavailability (Madani et al., 2011). Additionally, some cationic cell penetrating peptides are known to bind to the membrane and this could inhibit the fluorescence analysis as it is complicated to differentiate between surface bound and internalized peptide. A possibility to solve this problem is to quench the fluorescence (Madani et al., 2011).

Fluorescent-assisted cell sorting (FACS) is a method to measure the uptake of fluorescently labeled peptide as cells are sorted based on their fluorescent intensity. A drawback is that this method cannot differentiate between surface bound and internalized peptide (Madani et al., 2011).

However, the internalized peptide could be defined using fluorescent or confocal microscopy (Madani et al., 2011). Implementing these methods, it could be examined if the peptide – membrane interaction is extracellular or if the peptide is located in the cell (Madani et al., 2011).

1.6 T-Cells and Jurkats

T–cells are a type of white blood cells and are an important part of the cell mediated immunity. They form together with the B–cells the adaptive immunity. Moreover, T-lymphocytes originate from haematopoietic stem cells and are

formed in the bone marrow from where they migrate to the thymus where they mature (Alberts et al., 2002). During this time they are positively and negatively selected and they built MHC receptors on their surface which are known under the name T–cell receptor (TCR). This is a feature, which distinguishes them from natural killer cells (NK) and B–cells (Alberts et al., 2002).

The antigens should be presented to T-cells to initiate an adaptive immune response. The cells that do this efficiently are dendritic cells or macrophages which are cells of the innate immune system. They play the role of antigen-presenting cells (APC), which then activate the T-cells to respond to the antigens. As presented in Figure 1-3 some of the T-cells migrate to the site of infection, expand in number and size and help macrophages to destroy the invaders. Other T-lymphocytes remain in the lymphoidal organ and help B-cells to cope with the antigens. Some pathogenic antigens can have co-stimulative action and further enhance the proliferation (Alberts et al., 2002).

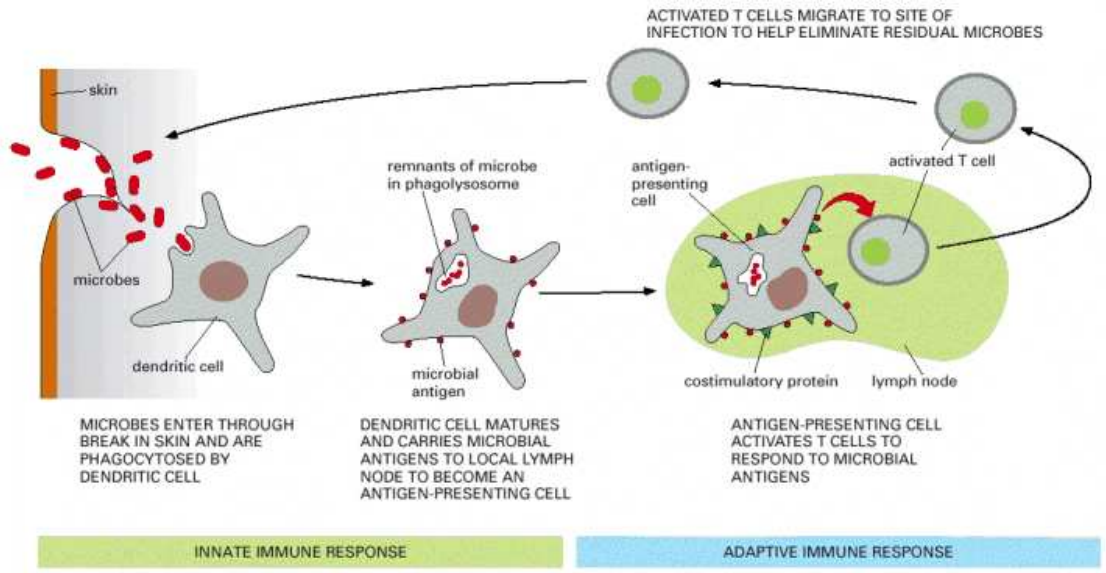

Figure 1-3: Interplay of the innate and adaptive immune systems. Invading microbes or their products at the site of infection are being ingested by specialized phagocytic cells of the innate immune system, including macrophages (not shown) and dendritic cells. After the maturation of dendritic cells they migrate in lymphatic vessels to a nearby lymph node, where they play a role as antigen-presenting cells. T-cells are being activated by antigen-presenting cells to respond to the microbial antigens that are displayed on the presenting cells' surface. Special proteins, called costimulatory molecules, are located on the surface of antigen-presenting cells and this feature helps the activation of the T-cells. Some of the activated T-cells then migrate to the site of infection where they either play a role in the activation of macrophages or they kill infected cells, thereby helping to eliminate the microbes**.** The figure was adopted from Alberts et al., (2002)

T-cell activation leads to different signaling cascades. T-lymphocytes have a major role in autoimmune disease and progression and this is the reason that they are target for investigation of the pharmaceutical industry (Yin et al., 2012). Recent research examined that plant cyclotides have anti-proliferative function (Gründemann et al., 2013).

Gründemann and co-workers showed that a mutant from the cyclotide kalata B1 where the threonine at position twenty is exchanged with a lysine (T20K) restrained the proliferation of T-cells through inhibiting the expression of IL-2 cell surface marker, the IL-2 cytokine secretion and IL-2 gene-expression. Additionally, the production of IFN–γ and TNF–α cytokines was reduced.

During my master thesis, I used as an *in vitro* model system mainly Jurkat T-cells. This is a transformed leukemic cell line which was obtained from John Hansen at the Fred Hutchinson Cancer Research Center, Seattle, USA. It was examined that Jurkat cells were producer of IL-2 after stimulation (Martin et al., 1981). For the maximal production of IL-2 two synergistic signals were required. The requirements were fulfilled as the TCR was ligated with CD3 antibody and the second signal was delivered by phorbol myristate acetate (PMA) (Weiss et al., 1984). Moreover, Jurkat cells were shown to be defective in the expression of two lipid phosphatases when comparing them with untransformed T-lymphocytes. The two enzymes are PTEN (phosphatase and tensin homologue) and SHIP (SH2-domain-containing inositol polyphosphate 5' phosphatase) (Wang et al., 2000; Shan et al., 2000). Moreover, the impact of these mutations cannot be estimated, because a lot of signaling pathways are still poorly understood (Costello et al., 2002). Although Jurkat cell line has some limitations and a lot of molecular pathways are still not examined, this cell line is a good *in-vitro* model system for the examination of T-cell development and function (Abraham and Weiss, 2004).

2. Aims of this study

Cyclotides are a class of plant-derived peptides containing three highly conserved disulfide bonds and a head–to–tail cyclic backbone, which form together the cyclic cystine knot (CCK). They possess a variety of biological activities, including antitumor, antimicrobial and insecticidal activities (Tam et al., 1999; Gruber et al., 2007). Recently, it was found that they have immunosuppressive activity and that cyclotides can enter cells; hence cyclotides may be useful for treatment of autoimmune diseases (Gründemann et al., 2012, 2013).

The aims of this Master's thesis project will be (i) to confirm that immunosuppressive cyclotides can enter their target cell (Jurkat cells and CD3 isolated primary T-lymphocytes), (ii) to characterize the pathway of peptide import and (iii) to define the cell viability. To enable the visualization of T20K, it will be fluorescently labeled and the modified peptide will be purified and analyzed by HPLC and mass spectrometry, respectively. Furthermore, the concentration that could be used for cellular entry studies so that the peptide is not disrupting the cellular membranes and act in a pore-forming cytotoxic fashion will be determined. Cytotoxicity will be measured using optical observation of the number of propidium iodide stained cells; hence through counting of the cells with disrupted cell membrane. The time-, dose- and temperature-dependent uptake of the tagged cyclotide will be examined with confocal microscopy

3. Materials and instruments

3.1 Materials

• Acetonitrile Rotisolv HPLC Gradient Grade ≥ 99.95% (Carl Roth GmbH, Germany)

• Acetonitrile Rotisolv LC-MS Gradient Grade ≥ 99.95% (Carl Roth GmbH, Germany)

• α-cyano-4-hydroxycinamic-acid (Sigma – Aldrich, USA)

• Anti-human CD3-functional grade purified; clone OKT3 (eBioscience, California)

• Anti-human CD28-functional grade purified; clone CD28.2 (eBioscience, California)

• BD IMag™ anti-human CD3 Particles (BD Bioscience, USA)

• BD IMag™ buffer (BD Bioscience, USA)

• 5(6)–carboxyfluorescein-succinimidyl ester (Sigma - Aldrich, USA)

• CellMask Deep Red® plasma membrane stain (Life Technologies, USA)

• CellMask Orange® plasma membrane (Life Technologies, USA)

• Dimethyl sulfoxide (DMSO) (Sigma – Aldrich, USA)

• erythrocyte lysis buffer: per liter: 89.9 g NH_4Cl; 10.0 g $KHCO_3$; 370 mg tetrasodium EDTA; pH 7.3

• freezing medium: FBS + 10% DMSO

• Bis benzimide H 33342 trihydro – chloride for fluorescence, ≥ 97.0% (Sigma Aldrich, USA)

• Ionomycin (Sigma Aldrich, USA)

• RPMI 1640 (Sigma Aldrich, USA)

- RPMI 1640 with L-Glutamine and without phenolred (Sigma Aldrich, USA)
- Penicillin/streptomycin (Sigma Aldrich, USA)
- Phorbol 12–myristate 13–acetate; ≥ 99% (Sigma Aldrich, USA)
- Propidium iodide; ≥ 94% (Sigma Aldrich, USA)
- Fetal bovine serum (Sigma Aldrich, USA)
- Solvent A: ddH_2O / 0.1% TFA
- Solvent B: acetonitrile / ddH_2O / TFA; 90/10/0.08 (v/v/v)
- Trifluoroacetic acid (Sigma Aldrich, USA)
- ZipTip (Merck Millipore, Germany)

3.2 Instruments

- AB 4800Sciex MALDI TOF/TOF analyzer (Biomarker and Omics, USA)
- Centrifuge Sigma 1-14K (Sigma, Germany)
- Centrifuge Heraeus Sepatech
- Chromeleon software 6.8
- Counting Slides, dual chamber (Bio-Rad laboratories)
- Data Explorer Software
- Fiji (just ImageJ)
- freeze dryer, Christ alpha 2-4 LD plus
- HPLC, Dionex UltiMate 3000
- Mr. Frosty (isopropanol-based freezing container) (Thermo Scientific, USA)
- laminar flow (Thermo Scientific Hepa Safe)
- LSM 510 software
- MACS Column (Miltenyi Biotec, Germany)

• MACS Separator (Miltenyi Biotec, Germany)

• Microscope cover glasses (16 mm) (Marienfield, Germany)

• Microscope cover glasses (24 mm) (Thermo Scientific, USA)

• Microscope slides

• Nikon Eclipse Ti A1 inverted microscope system

• Nikon TMS microscope

• NIS-Elements Imaging Software

• Ultrasonic cleaner

• Zeiss 510 Laser Scanning Microscope

Table 1 summarizes the HPLC columns that were used during the purification and analytical examination of T20K-CF.

Table 1: List of HPLC columns

Column	Full name, column dimensions, particle and pore size
semipreparative column	Kromasil, RP C_{18} , 250 x 10.0 mm ID 5 μm particle size
analytical column	Kinetex 2.6u, C_{18}, 100A, 150 x 3 mm

4. Methods

This section represents a detailed description of experimental methods, performed during this master thesis. Firstly, synthesis, purification and quality control of T20K-CF using methods as RP-HPLC, MALDI–TOF–MS and analytical HPLC has been described, followed by general representation of cell culture work. Finally, a detailed report on the cell preparations for microscopic observation and the conditions and settings for confocal microscopy will be given.

4.1 Fluorescent tagging of cyclotide T20K, purification and quality control of T20K-CF

4.1.1 Labeling of T20K using 5(6)–carboxyfluoresceine-succinimidyl ester

The [T20K] kalata B1 mutant - T20K was synthesized by Roland Hellinger, a PhD student in the group of Dr. Gruber. 2 mg of this peptide was dissolved in 100 mM hydrogencarbonate buffer of pH 8.8 to keep the non-protonated form of the amine group of the lysine. 5(6)-carboxyfluoresceine-succinimidyl ester have been dissolved in 200-300 µl DMSO immediately before starting of the reaction and the mixture has been briefly vortexed. The reactive dye was added in excess for the derivatization of the peptide (around 20x higher concentration). The reaction took place in the dark at room temperature and it lasted for 2 hours. After this incubation, the sample was stored at 4°C overnight. On the next day, a MALDI–TOF–MS analysis was performed to check if the peptide was quantitatively converted to the fluorescent probe. As the reaction contained DMSO, ZipTip™ was used to prepare the sample for MALDI–TOF–MS analysis. Firstly two µl of the sample were diluted 1:10 with buffer A. The Zip-Tip pipette tip was wetted with 10 µl of 100% acetonitrile and afterwards equilibrated 2

times with buffer A. This step was followed by 10 times aspiration and dispension of the sample. Afterwards the C_{18} material was washed with 10 µl of 5% MeOH in buffer A. Then the sample was eluted in 4 µl 80% acetonitrile. Finally, the sample was spotted onto a MALDI–plate. The settings and conditions which have been implemented are illustrated in Table 3. In case of not fully derivatized T20K, a ten time higher concentration of 5(6)-carboxyfluoresceine-succinimidyl ester, dissolved in 200 µl DMSO, was added to the peptide. The sample was vortexed and incubated for 3 more hours at room temperature. For the termination of the reaction, a buffer of H_2O/AcN/TFA 80/20/0.1 (v/v/v) was used. The sample was centrifuged for 20 minutes and 1000 rpm. The supernatant was collected in a new tube and the pellet was resuspended in 2-3 ml of the same buffer. This procedure was repeated a couple of times.

4.1.2 Semi-preparative purification of T20K-CF

For the purification of T20K-CF a semi-preparative Kromasil, RP C_{18} , 250 x 10.0 mm ID 5 µm particle size column was used. The column and the loading device were washed with buffer B and with buffer A and calibrated with a buffer of H_2O/AcN/TFA 80/20/0.1 (v/v/v) before the sample was loaded. The purification of the labeled peptides was done by reversed-phase HPLC and the dissolved sample was loaded to the semi-preparative HPLC column. The used HPLC program is listed in Table 2.

The purification was accomplished by a flow of 3 ml/min for 62min. The fractions have been collected every 30 sec from 25 min to 55 min.

Table 2: Gradient setup for the semi-preparative HPLC of T20K-CF

Retention time (min)	Flow (ml/min)	% B
0	3	5
3	3	5
25	3	35
55	3	50
56	3	80
57	3	80
58	3	5
62	3	5
Fraction collection by time, every 30 sec. from 25 min to 55 min		

The absorbance of the eluting peptides was measured at 280 nm and 490 nm (excitation maximum of the dye) wavelength and were analyzed with Chromeleon software 6.8. After the completion of the HPLC program, every fraction was checked via MALDI–TOF–MS for the containment of T20K-CF. MS experiments were performed, using α-cyano-4-hydroxycinamic-acid matrix at a concentration of 5 mg/ml in H_2O/AcN/TFA 50/50/0.1 (v/v/v). To determine the presence of the target peptide, 0.5 µl of the sample were mixed with 3 µl α-cyano-4-hydroxycinamic-acid (CHCA) and 0.5 µl of that mixture was spotted on a MALDI-plate and analyzed via MALDI–TOF–MS. The analysis was accomplished in reflector positive ion mode acquiring 3000 total shots per spectrum with a laser intensity of 4200. All data was processed, using Data Explorer Software. A summary of the MALDI program and the conditions are listed in Table 3.

Table 3: MALDI–TOF–MS set up

MALDI–MS conditions	
Operating mode	MS reflector positive
Mass range (Da)	2600 - 3600
Focus mass	3276
Shot/sub - spectrum	60
Total shots/spectrum	3000
Laser intensity	4200
Detector voltage multiplier	0,90

The monoisotopic peak which is corresponding to the 5(6)-carboxyfluorescein-succinimidyl ester derivative was estimated to be 3275.49 Da. The mass gain is due to the derivatization. The monoisotopic mass correlating to T20K corresponds to 2917.19 Da (CyBase). In addition, the mass of the 5(6)-carboxyfluorescein-succinimidyl ester was 473.4 Da and the mass of *N*-hydroxysuccinimide was 115.1 Da, both defined by the manufacturer data sheet. After successful derivatization, the *N*-hydroxysuccinimide should be hydrolized and this is the reason that this mass is deducted from the mass of the 5(6)-carboxyfluorescein-succinimidyl ester, resulting in a final mass of 3275.49 Da.

The fractions, containing the estimated mass of T20K-CF were collected and lyophilized. Afterwards, the peptide was dissolved in sterile PBS. It was determined by analytical HPLC and MALDI–TOF–MS that the working solution was pure; hence that it was containing T20K-CF and no other peptides.

For the analytical HPLC a 1:5 dilution of the working solution with solvent A has been performed. 25 µl of it have been inserted on the analytical column. The program for the analytical HPLC and the conditions will be listed in Table 4.
The purity analysis has been accomplished by a flow of 0.3 ml/min for 66 min. The injected volume has been 25 µl.

Table 4: Gradient setup for the analytical HPLC

Retention time (min)	Flow (ml/min)	% B
0	0,300	5
1	0,300	5
56	0,300	60
58	0,300	100
60	0,300	100
61	0,300	5
66	0,300	5
Injection volume: 25 µl column oven: 30°C		

The absorbance of the working solution has been measured at 280 nm and 490 nm (excitation maximum of the dye) wavelength.

Additionally, the concentration of the working solution was defined, using a NanoDrop. Dilutions in the range of 1:5, 1:10 and 1:20 of the working solution with PBS were performed. The absorbance of the peptide was measured with a user pre-defined method at a wavelength of 280 nm and at a UV-VIS scan at wavelength of 280 nm and 490 nm (excitation maximum of the dye) in ultraviolet-visible spectral region. The molar absorbance values has been estimated to be ε_{280} = 15419 $mol^{-1}cm^{-1}$ and ε_{490} = 75000 $mol^{-1}cm^{-1}$. Using the Lambert-Beer law, the approximate concentration of the working solution was estimated.

4.2 Cell Culture methods

4.2.1 General handling of cells

Cell culture work was accomplished in a cell culture hood to keep cells free from contamination. The cells were cultured in RPMI 1640 medium supplemented

with 10% (v/v) fetal bovine serum and 100 U/ml penicillin and 100 U/ml streptomycin. To ensure good conditions for growth and proliferation, cells were stored in a petri dish or in a culture flask at 37°C and 5% CO_2. Every second day the cells were subcultured by removing of the medium, washing the cells with PBS and transferring them from a previous culture into fresh growth medium. To confirm the healthy status of the cells, they were inspected by microscope and eye every time before handling them so that any signs of possible contaminations could be detected before spreading around. To combat genetic instabilities, which can propagate with increasing of passage number, working stocks of Jurkat cells were prepared. The cells were transferred in freezing medium and placed in a cryo-tube which was placed in an isopropanol-based freezing container with a freeze rate of -1°C/minute at -80°C. After the cell freezing process, the cells were kept in a -80°C freezer.

4.2.2 Thawing cells from -80°C

For the cultivation and thawing of cells, the cryo-tube was defrosted at room temperature. The cell content of it was transferred in a 15 ml centrifuge tube with 10 ml of fresh medium. The mixture was centrifuged for 4 min at room temperature and 1000 rpm. The supernatant was discarded and the cells were resuspended in fresh medium and cultivated in a petri dish or culture flask at 37°C and 5% CO_2.

4.2.3 Handling of human T-cells and Jurkat cells

4.2.3.1 Isolation of peripheral blood mononuclear cells (PBMC)

Human PBMC were isolated from the blood of children donors, patients at St. Anna Children's Hospital for Children's Cancer Research (Medical University of

Vienna, Austria). For the isolation of the peripheral blood mononuclear cells, the blood was transferred to 50 ml falcon tubes and then centrifuged for 5 min at 4°C and 300 rcf. The supernatant was removed and the pellet was resuspended in 5 ml of erythrocyte lysis buffer. After an incubation time of 2 minutes, the reaction was stopped by the addition of RPMI 1640 medium, containing 10% fetal bovine serum. The cell suspension was combined in tubes and afterwards centrifuged at the same conditions. The pellet was resuspended in freezing medium and transferred into cryo-tubes. The cells were placed in an isopropanol-based freezing container with a freeze rate of -1°C/minute at -80°C. After the cell freezing process, the cells were kept in a -80°C freezer.

4.2.3.2 Isolation of T-lymphocytes

Purified T-cells were obtained by $CD3^+$ positive selection, using magnetic beats that have monoclonal antibody attached to their surface. The peripheral blood mononuclear cells (PBMC) were resuspended in 10 ml pre-cooled BD IMag™ buffer. The cell number was determined. The BD IMag™ anti-human CD3 Particles - DM were vortexed thoroughly and 50 µl of magnetic particles were added for every 10^7 total cells. The sample was mixed and incubated for 30 minutes at room temperature. Meanwhile, the magnetic separation system was build up in the cell culture hood. The cell separation magnet and the appropriate separation column were assembled. The column was prepared by rinsing with 3 ml of BD IMag™ buffer. Afterwards, the suspension was applied onto the column. The magnetically labeled T-cells retained on the magnetic field of the column. It was washed by adding 3 times 3 ml of BD IMag™ buffer, each time once the column reservoir was unfilled to remove the negative, unlabeled fraction. The column was removed from the separator with magnetic field and was placed on a 15 ml falcon tube. 5 ml of BD IMag™ buffer were pipetted onto the column to elute the magnetically retained $CD3^+$ cells as positively selected cell fraction. The isolated T-cells were centrifuged for 5 minutes at room temperature and 300 rcf. The pellet was resuspended in RPMI 1640 and was incubated in a petri dish at 37°C and 5% CO_2.

4.2.3.3 Activation of Jurkat cells

Around 8 x 10^5 Jurkat cells/ml were activated in two different ways. The first type of stimulation was using anti-human CD3 (clone OKT3) and anti-human CD28 (clone 28.2), each in a concentration of 100 ng/ml. Alternatively the cells were stimulated with PMA (50 ng/ml) and ionomycin (500 ng/ml). In both cases, the process of activation was done overnight at 37° C and 5% CO_2.

4.3 Internalization assay and confocal microscopy

4.3.1 Cell preparation for microscopic observation

For the internalization assay, 8 x 10^5 Jurkat cells were pelleted with centrifugation at room temperature for 4 min and 300 rcf. To avoid the effects of serum-containing growth factors that may induce morphological differences, they were resuspended in RPMI 1640 medium without fetal bovine serum and without phenolred, containing fluorescein labeled peptide T20K (T20K-CF) in a concentration between 1 µM and 10 µM. The cells were placed on a 3 cm petri dish and cultured at 37°C and 5% CO_2 for a time interval between 1 h and 48 h. Afterwards the cells were pipetted into a tube and were centrifuged for 4 minutes at room temperature and 300 rcf. The cells were resuspended in fresh medium, containing 10 µg/ml Hoechst, which is a fluorophore implemented to stain the cell nucleus. After incubation for 10 minutes at 37°C and 5% CO_2, the cells were pelleted by the same centrifugation conditions. To allow later the differentiation between cells with intact membrane and cells with disrupted one, the cells were incubated in fresh RPMI 1640 medium without phenolred and without serum, containing 1 µg/ml propidium iodide for 5 minutes at 37°C and 5% CO_2. Following the centrifugation step by the same conditions as previously mentioned, the cells were resuspended in 0.5 µg/ml CellMask Deep Red® plasma membrane stain to enable the visualization of the cell membrane. The

cells have been incubated for 5 minutes at 37°C and 5% $CO_{2.}$ After all this staining steps, the cells were again centrifuged and were washed with PBS. Before mounting of the cells into a microscopy chamber, they were against pelleted and resuspended in fresh PBS.

For the microscopic observation with Nikon eclipse Ti laser-scanning inverted microscope, the cells were placed onto a 24 mm cover slip, situated in an aluminum microscopic chamber.

However, for the microscopy with Zeiss LSM 510 inverted laser-canning microscope, the cells were placed onto a 16 mm cover slip, situated in an aluminum microscope slide. Additionally, the staining of the nucleus with Hoechst was skipped, because of the dismissal of appropriate laser for the excitation of this stain. At this microscope the initial studies for the internalization of T20K-CF have been performed. At the beginning, the cellular membrane was visualized with CellMask Orange® plasma membrane stain instead of CellMask Deep Red® plasma membrane stain. For this, the implemented concentration of cellular membrane stain was 0.25 µg/ml or 0.5 µg/ml and the incubation lasted for 5 minutes at 37°C and 5% CO_2. The next steps followed as previously described. As there was a spillover effect of CellMask Orange® plasma membrane stain in the green channel of the fluorescently labeled T20K peptide, for the next experiments the cellular membrane has been visualized with CellMask Deep Red® plasma membrane stain as it does not showed any spectral mixing properties in comparison to CellMask Orange® plasma membrane stain.

4.3.2 Settings and configurations for confocal microscopy

To investigate the internalization of T20K-CF in living cells, confocal images were acquired with a Nikon eclipse Ti laser-scanning inverted microscope and with a Zeiss LSM 510 Meta inverted laser-scanning microscope.

The optical sections with Nikon microscope were recorded with a 40x water objective. For the excitation of the four different stains, four different laser units were used. The excitation and emission spectra of all four fluorophores will be illustrated in Table 5. Additionally, it was shown which combinations of dyes (labeled with "+") could be used for the visualization of the peptide or for the visualization of the intracellular compartments. Due to inappropriate laser at Zeiss LSM 510, the staining with Hoechst has been skipped. Additionally, the combination of CellMask Orange® plasma membrane stain with propidium iodide or fluorescein was not advisable due to spillover effect of the fluorophores.

Table 5: **Excitation and emission wavelengths of the implemented fluorophores**

Dye	Excitation [nm]	Emission [nm]	Nikon Ti eclipse	LSM 510
Hoechst	350	461	+	No appropriate laser
Fluorescein	485	514	+	+
CellMask® Orange	554	567	Spillover with propidium iodide; spillover with florescein	Spillover with propidium iodide; spillover with florescein
Propidium iodide	535	617	+	+
CellMask® Deep Red	649	666	+	+

The nuclei were visualized, using Hoechst which is capable of permeabilising cell membranes of living cells. The dye was excited at 403.5 nm and the emission was detected with a 495 long pass filter at 425-475 nm. Imaging of the fluorescein- tagged peptide T20K-CF was performed by excitation at 488 nm and the fluorescein emission was collected with a 500 long pass filter at 500-550 nm. For the differentiation of cells with intact membrane and cells with disrupted one, propidium iodide stain was used and the imaging was presented

by excitation at 561.9 nm and detection of the emission with a 640 long pass filter at 570–620 nm. Additionally, the cell membrane was visualized with CellMask Deep Red® plasma membrane stain with an excitation wavelength of 641.9 and detection of the emission at 663-738 nm. The channel series were selected to be in direction 1→4 to reduce spectral mixing appearance of the fluorophores. For all acquisition settings, the first dichroic mirror was configured at 405/488/561/640. Additionally, Galvano was set as a scanner unit for all images. Moreover, the pinhole size was set to be 0.6 airy units. The scan settings were adjusted to linear, unidirectional scanning with a size of 512 x 512 pixel. Confocal microscopic analysis was performed using images, z-stacks and 3D projections. 23 confocal slices were presented for each sample prepared. The most cells were in the range 10-15 µm which means that acquisition of 23 slices allowed investigation of the cell by steps of 430-650 nm. The stacks of the images and the 3D projection were obtained using ImageJ software (NIH). All images were exported as tiff and were further analyzed using Fiji. The four channel photos were stacked to images and the brightness and contrast setting of every channel were separately adjusted. Finally, the four different channels were merged together and the image was saved in png format.

Live cell microscopy was performed additionally with a Zeiss LSM 510 inverted microscope using a 63x phase contrast plan apochromat oil objective. For all acquisition settings, the main beam splitter was HFT UV/488/543/633. The lasers used were an argon/2 laser 488 nm, a HeNe 594 nm laser and a HeNe 633 nm laser. The parameters specific for each fluorophore were: fluorescein labeled T20K, excited at 488 nm and detected with a 500-530 nm bandpass filter at 25% laser intensity; CellMask Orange® plama membrane stain excited with a wavelength of 543 nm, detected with 565-615 band pass filter at full laser intensity or CellMask Deep Red® plasma membrane stain excited at 633 nm and detected with a 650 nm longpass filter at full laser intensity. Additionally, multi track configuration was chosen so that the laser scans multiple channels sequentially, which reduces the probable spillover effect of the fluorophores. Moreover, the pinhole diameter was adjusted at 3.18 airy units. The detector gain and the amplifier offset were separately modified for each channel and each sample. In addition, 512 x 512 pixels were selected for each scan. To

obtain a better image, a line averaging of 4 was chosen. For the reduction of noise in the images, a scan speed of 6 was selected and a unidirectional scan direction was confirmed. The images were generated in 12bit format (4096 gray levels). For the scanning of regions of interest, the crop function was selected which is an optical zoom performed upon image acquisition. All images were exported a tiff and were further analyzed with Fiji as previously described.

4.4 Temperature dependent uptake of T20K-CF

Temperature dependent studies were examined at 37°C, at 4°C and at 4°C and following re-incubation at 37°C. All such uptake assays were performed with 10 µM T20K-CF in RPMI 1640 medium without serum and without phenolred.

The internalization study at 4°C was performed with Jurkat cells, pre-cooled for 30 minutes at 4°C and with pre-cooled staining solutions and PBS. The cells were then incubated for 1 h with 10 µM T20K-CF at 4°C and were washed once with PBS. Afterwards, the further staining procedures were performed as previously mentioned and at 37°C and 5% CO_2.

To enable the comparison between cells, incubated with T20K-CF at 4°C and cells, incubated with T20K-CF at 37°C, Jurkat cells were treated with the same concentration of peptide for the same interval of time, but with a following incubation at 37°C. The further staining procedures were performed as previously mentioned and at 37°C and 5% CO_2.

To examine if peptide uptake could be restored, Jurkat cells were incubated with 10 µM T20K-CF for 1 h at 4°C as previously described, followed by a re-incubation at 37°C.

5. Results

In this chapter the results from the experimental work will be presented. At the beginning, the purification and analysis of T20K-CF will be described, followed by dose, time and temperature dependent studies, conducted with confocal microscopy to determine and to characterize the internalization of T20K-CF.

5.1 Fluorescent tagging of cyclotide T20K, purification and quality control

One of the main aims of this master project was to analyze the internalization of the immunosuppressive peptide [T20K] kalataB1. For this study, the peptide was labeled with the fluorophore 5(6)–carboxyfluorescein, which enables microscopic observation of emission signals by the peptide distribution in the cell or on the cellular membrane. To perform this investigation, the procedure of chemical derivatization, described in section 4.1, was implemented. For the separation of the derivative from the reaction mixture semipreparative reversed-phase HPLC was applied (Figure 5-1). The proportion of solvent B gradually increased as described in Table 1 of section 4.1. During this process each of the bounded protein dissociated and appeared in the effluent. Two different wavelengths have been used to detect the eluted peptide. Figure 5-1 shows the absorbance at 280 nm (black) and at 490 nm (blue). Amino acids with aromatic ring (mainly tryptophan, but also phenylalanine and tyrosine) are the reason for the absorbance at 280 nm. Moreover, the second wavelength is the excitation maximum of fluorescein of the collected fractions from the T20K-CF purification.

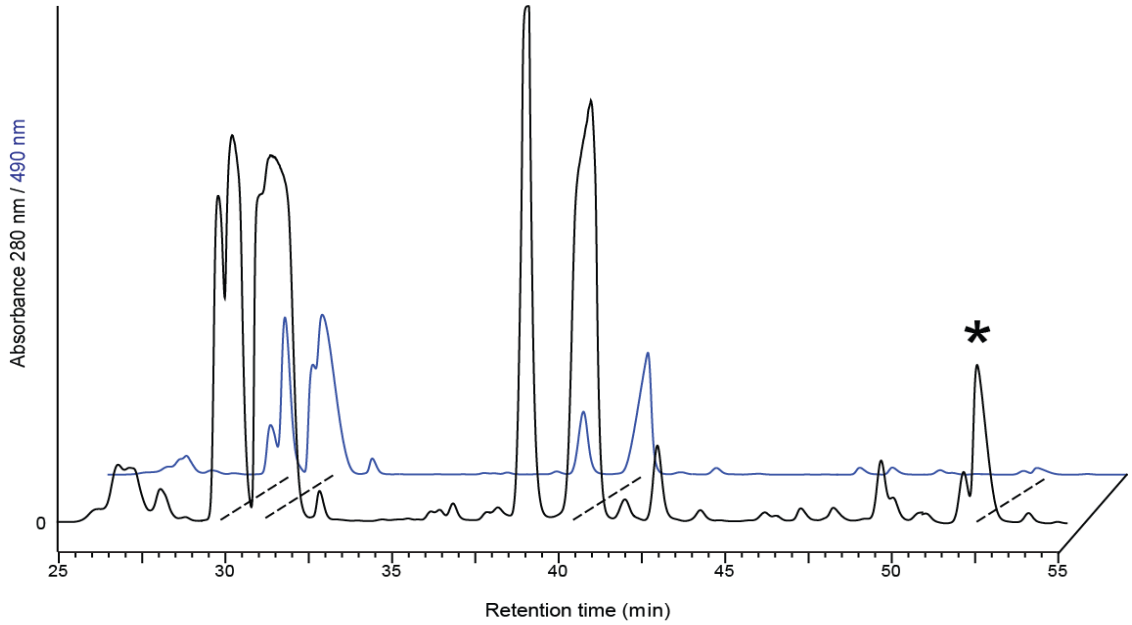

Figure 5-1: **Purification of fluorescein labeled T20K (T20K-CF) by reversed-phase HPLC.** Absorbance at 280 nm (black) and absorbance at 490 nm (blue); the labeled peak corresponds to the purified T20K-CF peptide. The purification was accomplished by a flow of 3 ml/min for 62 min with a Kromasil, RP C_{18}, 250 x 10.0 mm ID 5 µm particle size column. The fractions have been collected every 30 sec from 25 min to 55 min as described in section 4.1.

To identify the target peptide, the fractions were collected and further analyzed. The fluorescein labeled T20K is a less polar molecule and the elution of it was expected at longer retention time. This prediction was confirmed by MALDI–TOF–MS analysis of the collected fractions. It indicated the presence of peptide with the mass, corresponding to the estimated mass of 3275.49 Da for T20K-CF (Figure 5-2). The labeled peak at Figure 5-1 is those, which contained the target peptide.

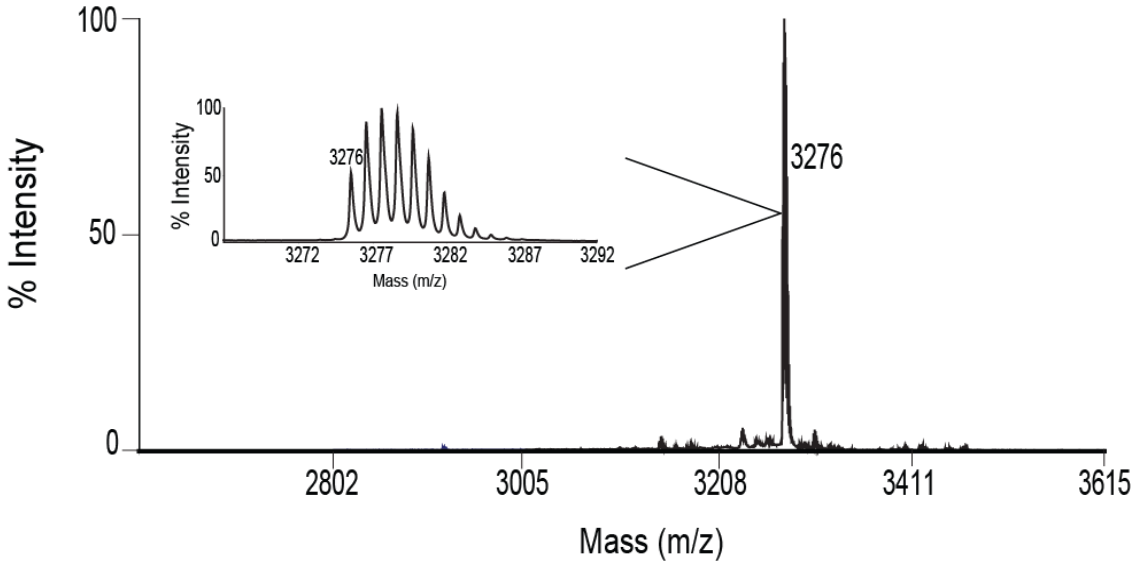

Figure 5-2: Mass spectrum of the purified T20K-CF. It indicated the isotopic mass of T20K-CF which was estimated to be 3275.49 kDa. To determine the presence of the target peptide, 0.5 µl of the sample were mixed with 3 µl α-cyano-4-hydroxicinamic-acid (CHCA) and 0.5 µl of that mixture was spotted on a MALDI-plate and analyzed via MALDI–TOF–MS with the configurations, described in 4.1.

The working solution was further analyzed, using analytical HPLC. This method was applied to approve the purity specification of the working solution and to quantitate the compounds which are present in the sample.

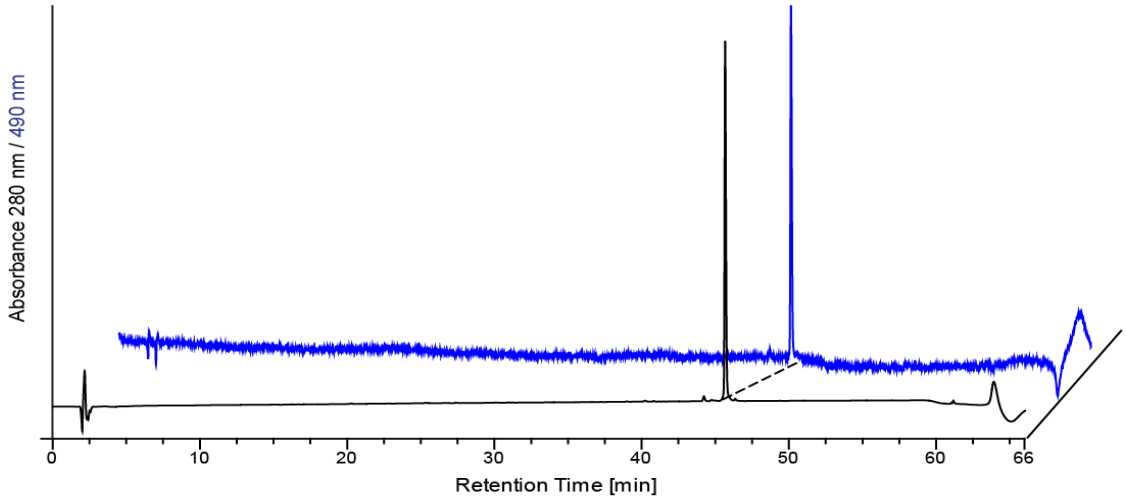

Figure 5-3: **Purity control of T20K-CF performed by analytical HPLC.** Absorbance at 280 nm (black) and absorbance at 490 nm (blue). A 1:5 dilution of the working solution with solvent A has been performed and 25 µl of it have been inserted on the analytical column. The purity analysis has been accomplished by a flow of 0.3 ml/min for 66 min using a Kinetex 2.6u, C_{18}, 100A, 150 x 3 mm column. The conditions and setups have been described in section 4.1.

Figure 5-3 shows just one peak, which guarantees high purity of the compound of interest. This conclusion was important, because a pure peptide, isolated from the peptide mixture, was desired for the further internalization studies of [T20K] kalataB1.

To summarize these results, the aim was to label the cyclotide T20K with the fluorophor 5(6)-carboxyfluorescein. Afterwards, T20K-CF has been purified implementing reversed-phase HPLC (Figure 5-1). Finally, quality control experiments for purity check have been provided. The results from the MALDI–TOF–MS (Figure 5-2) and the analytical HPLC (Figure 5-3) showed that T20K-CF was isolated from the reaction mixture and that further microscopic observations could be executed with the peptide solution.

5.2 Cell-based cyclotide localization

This study will examine the binding, internalization and distribution of the fluorescently labeled T20K peptide into mammalian cells. Gründemann et al. showed in his work, that [T20K] kalataB1 has immunosuppressive activity in vitro on activated human T-lymphocytes. Hence, one of the aims of this master thesis was to examine the localization of the peptide in-vitro within the human T–cell model system Jurkat cells, an immortal lymphoma cell line generally used to study T–lymphocytes (Abraham and Weiss, 2004). First of all, it has been analyzed if T20K-CF can enter within mammalian cells. Secondly, further investigations encompassed a dose, time and temperature depending study with the immunosuppressive peptide T20K.

5.2.1 Configurations for fluorescent and confocal microscopy

For this, initial microscopy study was executed with the methods of fluorescent and confocal microscopy to observe how the immunosuppressive peptide T20K interacts with mammalian cells. The distribution of the fluorescently labeled cyclotide was observed and it was examined that it interacts with the cellular membrane of Jurkat cells at lower concentrations and shorter incubation times. At longer incubation times and higher peptide concentrations it internalizes within the cells (data not shown). At the beginning, CellMask Orange® plasma membrane stain was used to visualize the cellular membrane.

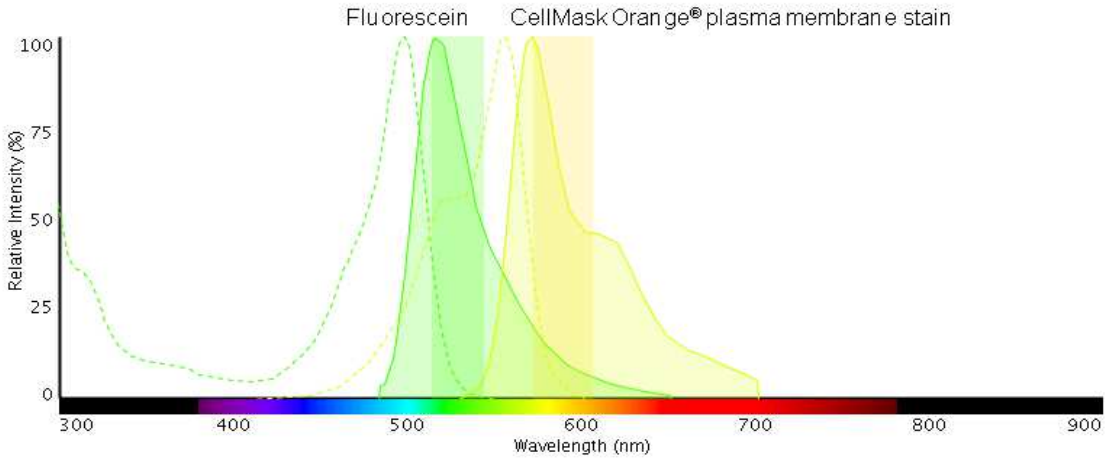

Figure 5-4: **Absorbance and emission spectrum of fluorescein and CellMask Orange® plasma membrane stain.** Additionally the fluorescence emission light filter settings implemented to record double stains using both fluorophores have been illustrated.

Because of spillover effects of the orange fluorophore in the green channel (Figure 5-4), further analysis and optimization was performed with a Zeiss LSM 510. Moreover, the spectral mixing obstacle was avoided by sequentially scanning in multichannels (Figure 5-5). It was shown that the fluorescently labeled peptide T20K penetrates through the cell membrane of anti-CD3 purified primary T-cells (Figure 5-6) and Jurkat cells (Figure 5-5).

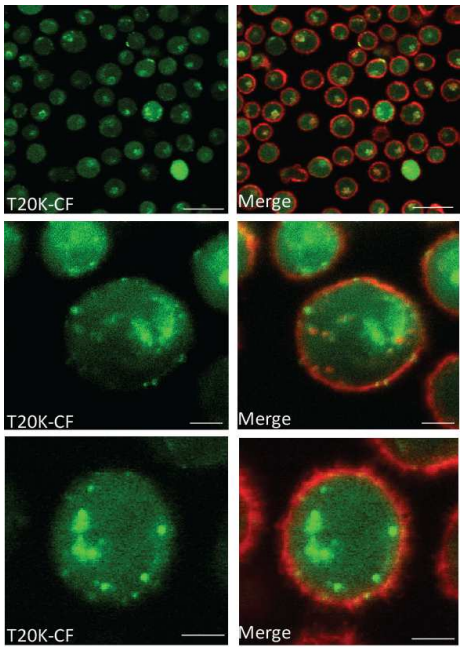

Figure 5-5: **Cellular uptake of T20K-CF in Jurkat cells.** The cells were incubated for 1 h at 37°C with 10 µM T20KCF and for 5 min at 37°C with 0.25 µg CellMask® Orange plasma membarne stain. After the staining procedure, a washing step with PBS has been performed. It was investigated, if T20K-CF internalized into the cell. To avoid the obstacle of spill over effect, it was sequentially scanned in multichannels; scale bar: 50 µm for the overview photo and 5 µm for the single cell photos.

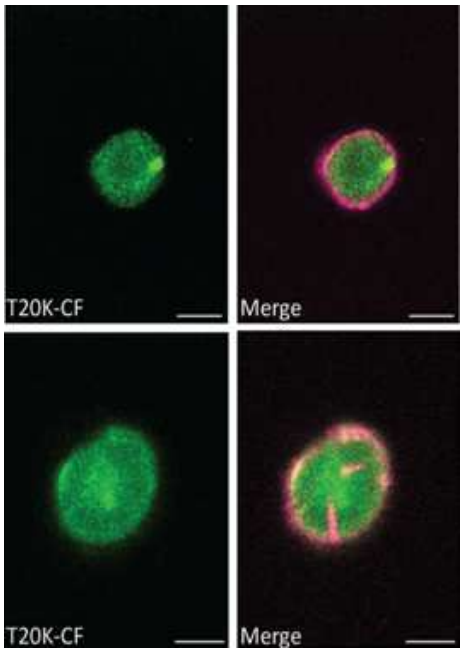

Figure 5-6: **Cellular uptake of T20K-CF in anti-CD3 isolated primary T-cells.** The cells have been incubated for 1 h at 37°C with 4 µM T20KCF and for 5 min at 37°C with 0.5 µg CellMask® Orange plasma membarne stain. It was investigated, if T20K-CF internalized into the cell. To avoid the obstacle of spill over effect, it was sequentially scanned in multichannels; scale bar: 5 µm.

Based on the previous experiments on peptide localization, CellMask Deep Red® plasma membrane stain provided better visualization, because of its far-red emission and due to the absence of spillover impact in the green channel (Figure 5-7).

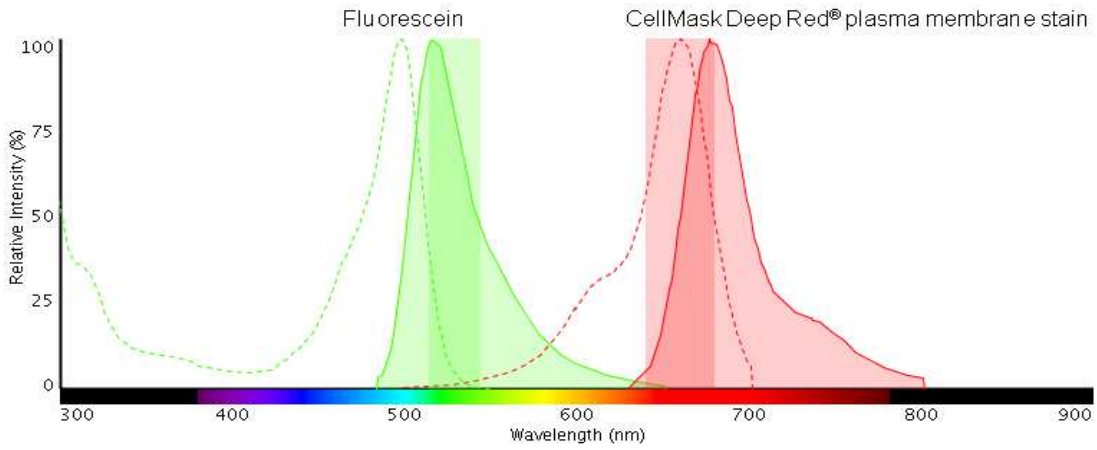

Figure 5-7: **Absorbance and emission spectrum of fluorescein and CellMask Deep Red® plasma membrane stain.** Additionally the fluorescence emission light filter settings implemented to record double stains using both fluorophores has been illustrated.

The analysis with Zeiss LSM 510 has been handicapped by the absence of appropriate laser for the excitation of the Hoechst nuclei stain. Due to the missing possibility to visualize the cell nucleus, no accurate intracellular localization of the peptide was possible. Hence, to overcome this problem, the measurements were performed on another confocal microscope – Nikon eclipse Ti, which was available to use at the campus facility.

5.2.2 Time-, dose- and temperature-dependent studies

The dose-, time- and temperature-dependent studies have been executed with living cells. Fixation of them may significantly affect the cellular distribution of the fluorescein labeled peptide (Richard et al., 2003; Nakase et al., 2007). Additionally, no fetal bovine serum was added to the RPMI medium, because

previous research has shown that it may cause differences in the morphology of cells (Meies et al., 2002; Nakase et al., 2004). Furthermore, for microscopic purpose, medium without phenolred was applied so that the red colour does not have any influence on the peptide and cell compartment visualization with confocal microscopy.

To investigate the internalization of T20K-CF a time and a dose dependent study was performed using concentrations of 1 µM, 4 µM and 10 µM T20K-CF for time periods of 1 h, 4 h, 24 h and 48 h. The green emission of the fluorescently labeled peptide was visualized with confocal microscopy as an optical imaging technique. The nuclei were illustrated using Hoechst, which freely permeates the membranes of all cells. Cells with disrupted membrane were differentiated from cells with intact outer membrane with propidium iodide stain. For the visualization of the cell membrane, CellMask Deep Red® plasma membrane stain was implemented. The four channel images were processed in Fiji and a merge photo of them was represented. For the further figures within this master thesis, the channel of the fluorescein labeled peptide and the merge photo will be presented, because the main aim was to define and to describe the localization of the peptide within the cell. Figure 5-8 shows an example of all four channels and the merge photo of the images

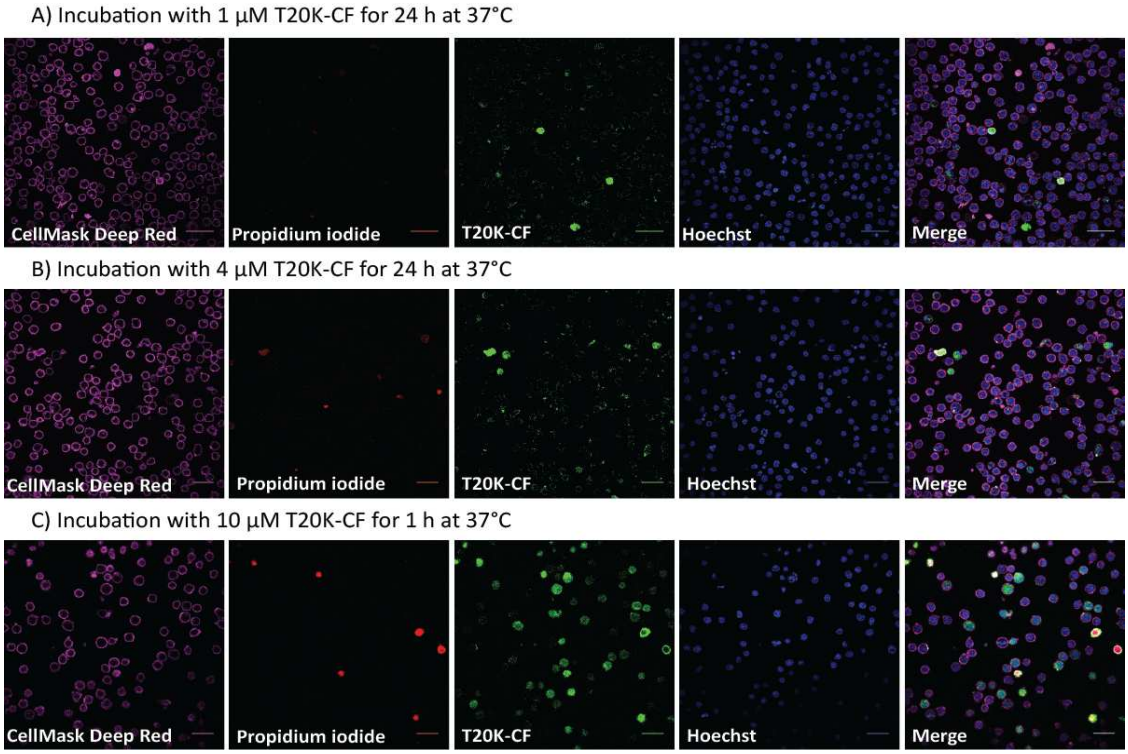

Figure 5-8: **Internalization of T20K-CF in Jurkat cells.** A) Incubation with 1 µM T20K-CF for 24 h at 37°C; B) Incubation with 4 µM T20K-CF for 24 h at 37°C; C) Incubation with 10 µM T20K-CF for 1 h at 37°C; The cellular membrane of Jurkat cells has been stained with 0.5 µg/ml CellMask Deep Red® plasma membrane stain for 5 min at 37°C. The cell nucleus has been visualized, implementing 10 µg/ml Hoechst 33342 for 10 min at 37°C. To allow the differentiation between cells with intact membrane and cells with disrupted one, the cells have been incubated for 5 min at 37°C with 1 µg/ml propidium iodide. Before the microscopic observation, the cells have been washed with PBS. At these concentrations most of the cells have internalized T20K-CF. The cell images of all four channels and a merge photos are illustrated; scale bar: 50 µm

Firstly it was examined by which concentration and at which time point T20K-CF distributes into most of the cells. Microscopic observation showed that at an incubation time of 1 h unstimulated Jurkat cells, treated with 10 µM peptide, have emission in the green channel (Figure 5-8C). However, this incubation time was not enough for the attachment of 1 µM or 4 µM peptide to the cells. For both concentrations binding of T20K-CF to all cells was observed at an incubation time of 24 h (Figure 5-8A and 5-8B). The difference in the fluorescence intensity from the T20K-CF treated cells in Figure 5-6A-B compared to figure 5-8C corresponds to the amount of surface adsorbed peptide.

Another observation from the overview confocal images, shown in Figure 5-8 was that the number of cells with disrupted cell membrane was rising with expanding of the incubation times and with increasing of the peptide concentration. This conclusion was made by observation of the propidium iodide stained cells in every sample. This stain is membrane impermeable and is excluded from viable cells. It can be used to identify the dead cells within a population of viable cells. The percentage of cells with disrupted membrane has been calculated through counting of all cells for every image and identification of the number of dead cells through cell counting in the red channel. In spite of the fact that every incubation with the peptide was performed only once, at least three representative overview images in all four channels have been determined to present the results of cell viability after peptide treatment as illustrated in Figure 5-9.

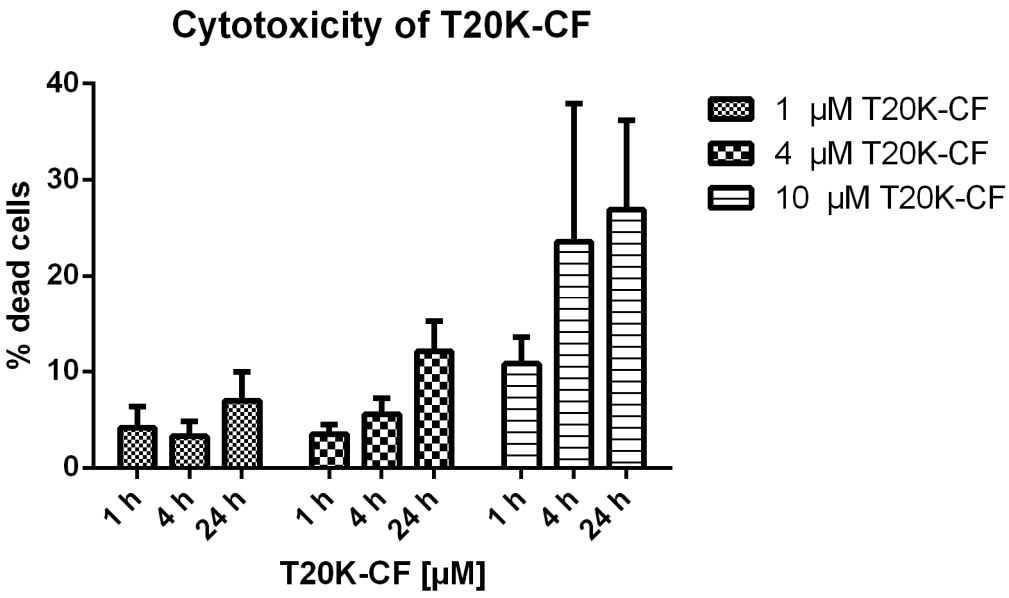

Figure 5-9: Cytotoxicity of T20K-CF on Jurkat cells. The impact of peptide concentration and incubation time on the cell viability was determined. For this expeiment 1 µM, 4 µM and 10 µM were incubated with T20K-CF for 1 h, 4 h and 24 h at 37°C. The number of dead cells has been assigned after counting of the propidium iodide stained cells. In this way those with disrupted cellular membrane have been defined. Data represents the average (±SD) of three different images of the same experiment.

Incubation times between 1 h to 4 h with 1 µM to 4 µM T20K-CF were determined to be non-cytotoxic. The dead rate was calculated to be 6%. Higher cytotoxicity has been examined by incubation with the same peptide concentration for 24 h. Furthermore, at incubation for 24 h at 37°C 10% of the cells, treated with 4 µM T20K-CF were dead. Additionally, 7% of the cells, incubated with 1 µM peptide were with disrupted cell membrane. The highest cytotoxicity has been observed by an incubation of 48 h with 4 µM T20K-CF, at which all of the cells were dead. In the case of 10 µM peptide concentration, the cytotoxicity at an incubation point of 1 h was twice higher in comparison to the incubations with 1 µM and 4 µM T20K-CF for the same time point. Additionally, much higher cells with disrupted membrane were counted at incubation for 4 h with the same peptide concentration. Surprisingly, not all cells were stained with propidium iodide after incubation for 24 h with 10 µM T20K-CF. The mean percentage of dead cells in this case was estimated to be 27%.

Moreover, the dependence of the peptide concentration on the peptide uptake was examined with confocal microscopy. For this purpose a 23 frame z-stack was performed and 3 different frames of living and representative cells were introduced in Figure 5-10.

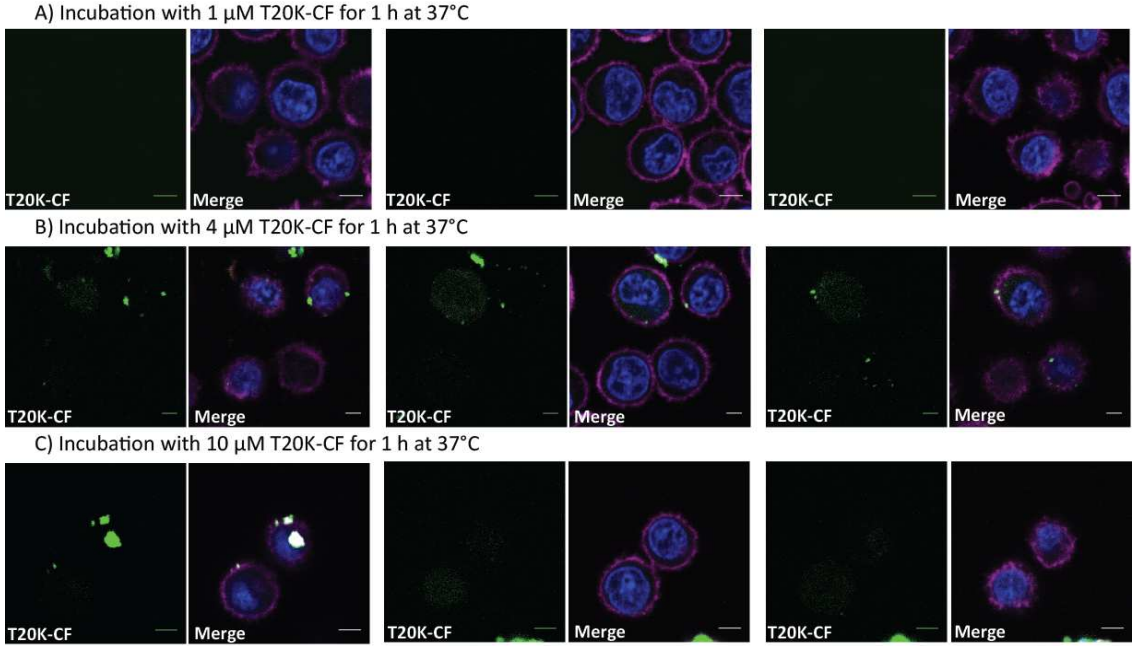

Figure 5-10: Concentration dependence of T20K-CF on the cellular uptake by an incubation for 1 h at 37°C. Confocal microscopy analysis of living unstimulated Jurkat cells incubated with concentrations of 1 µM (A), 4 µM (B) and 10 µM (C) T20K-CF for 1 h at 37°C; The cellular membrane of Jurkat cells has been stained with 0.5 µg/ml CellMask Deep Red® plasma membrane stain for 5 min at 37°C. The cell nucleus has been visualized, implementing 10 µg/ml Hoechst 33342 for 10 min at 37°C. To allow the differentiation between cells with intact membrane and cells with disrupted one, the cells have been incubated for 5 min at 37°C with 1 µg/ml propidium iodide. Before the microscopic observation, they have been washed with PBS. At a concentration of 1 µM T20K-CF there was no fluorescence on the cell membrane or within the cells. Incubations with four times higher and ten time higher concentration showed attachment of T20K-CF to the cell membrane and penetration of the peptide within the cells; scale bar: 5 µm

At incubation point for 1 h, at a concentration of 1 µM T20K-CF there was no significant fluorescence on the cell membrane or within the cells (Figure 5-10A). By an incubation with four times higher concentration of peptide for the same time, weak fluorescence of cells was microscopically observed, however the fluorescently labeled peptide did not bound or internalized to all of the cells (Figure 5-10B). At this concentration the peptide attached at some locations on the cell membrane and penetration in the cells was detected. The amount of bounded peptide to the cell membrane increased as the applied peptide concentration rose. This is the reason why at incubation with 10 µM T20K-CF for the same incubation time, fluorescence intensity within all cells was examined (Figure 5-10C). In the case of lower concentrations of T20K-CF this observation was made at incubations for 24 h (Figure 5-12A and 5-12B). At incubation time for 4 h, more peptide was attached to the cell membrane

(Figure 5-11B and 5-11C). However, at a concentration of 1 µM T20K-CF, no attachment of the peptide was observed (Figure 5-11A). A lot of cells with four times higher concentration of the peptide showed fluorescence intensity (Figure 5-11B).

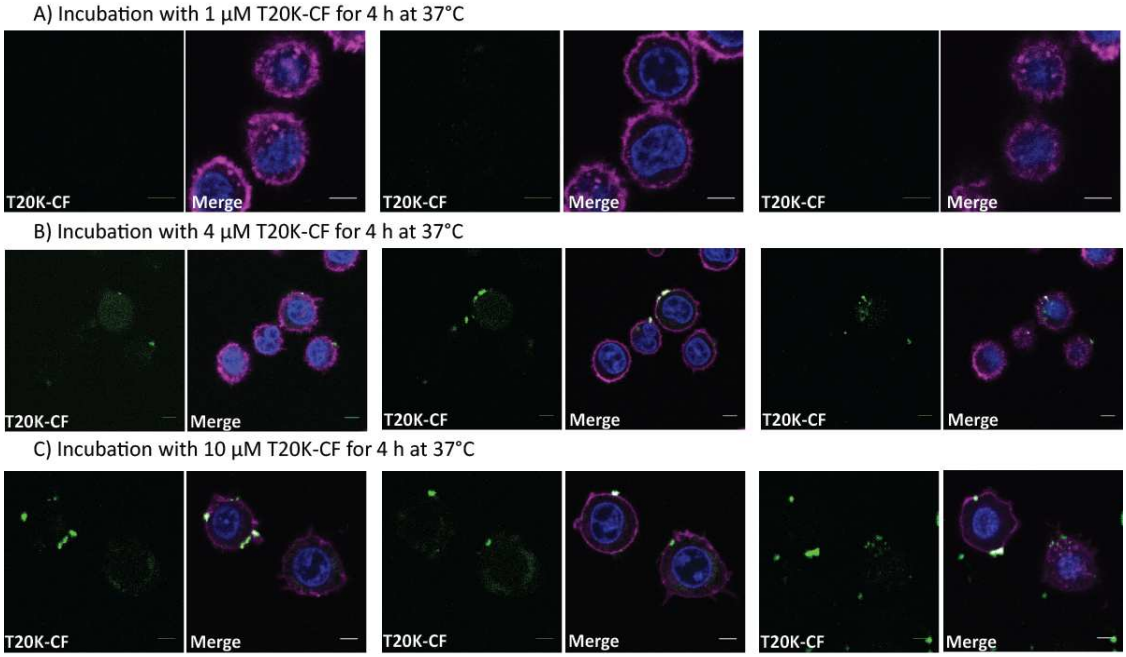

Figure 5-11: **Concentration dependence of T20K-CF on the cellular uptake by an incubation for 4 h at 37°C.** Confocal microscopy analysis of living unstimulated Jurkat cells incubated with concentrations of 1 µM (A), 4 µM (B) and 10 µM (C) T20K-CF for 4 h at 37°C; The cellular membrane of Jurkat cells has been stained with 0.5 µg/ml CellMask Deep Red® plasma membrane stain for 5 min at 37°C. The cell nucleus has been visualized, implementing 10 µg/ml Hoechst 33342 for 10 min at 37°C. To allow the differentiation between cells with intact membrane and cells with disrupted one, the cells have been incubated for 5 min at 37°C with 1 µg/ml propidium iodide. Before the microscopic observation, they have been washed with PBS. At a concentration of 1 µM T20K-CF there was no fluorescence on the cell membrane or within the cells. Incubations with four times higher and ten time higher concentration showed attachment of T20K-CF to the cell membrane and penetration of the peptide within the cells. The amount of peptide which was interacting with the unstimulated Jurkat cells increased with prolonging of the incubation time; scale bar: 5 µm

Treatment of the cells for longer incubation time of 24 h induced more attachment of the peptide to the cell membrane and more distribution of T20K-CF in the cytosol of the cells (Figure 5-12). Additionally, at incubation with 1 µM T20K-CF attachment of the peptide on single locations to the cell membrane was observed (Figure 5-12A). At higher concentrations, it was visualized not just on single positions on the cell membrane, but on many spots on it. The

peptide was reported to translocate through the cell membrane by a treatment of the cells for 24 h with 4 µM T20K-CF (Figure 5-12B). In this case, the peptide appeared as fluorescent vesicles emerging from the intracellular side of the plasma membrane. However, the mechanism of uptake of T20K-CF is still unknown, although it penetrated through the cell membrane.

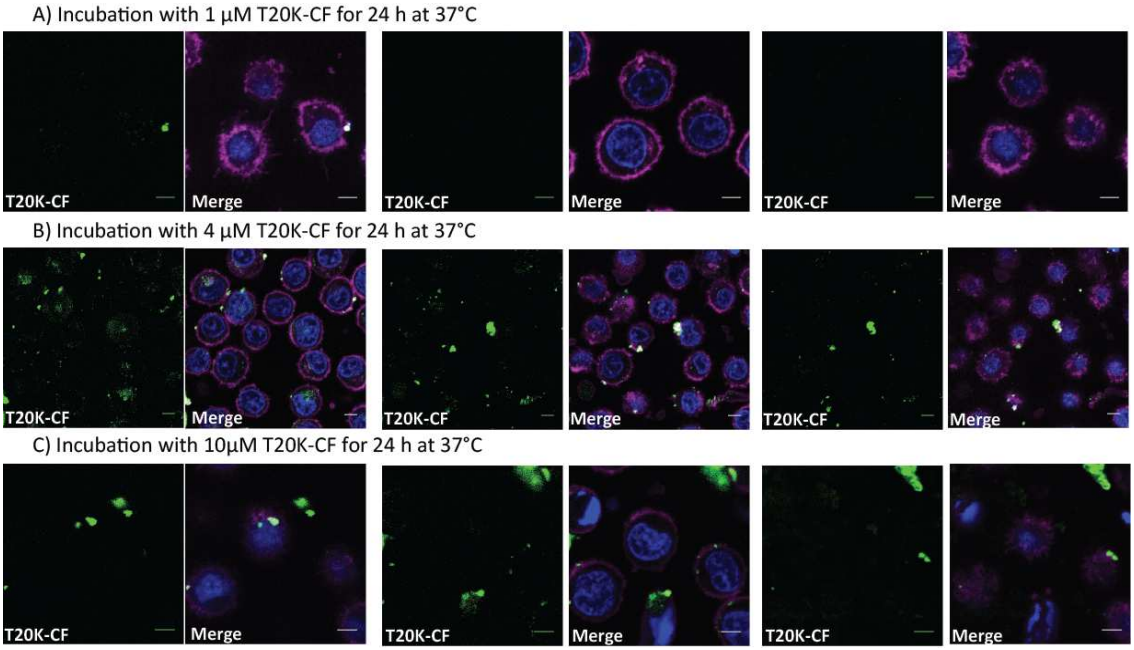

Figure 5-12: **Concentration dependence of T20K-CF on the cellular uptake by an incubation for 24 h at 37°C.** Confocal microscopy analysis of living unstimulated Jurkat cells incubated with concentrations of 1 µM (A), 4 µM (B) and 10 µM (C) T20K-CF for 24 h at 37°C; The cellular membrane of Jurkat cells has been stained with 0.5 µg/ml CellMask Deep Red® plasma membrane stain for 5 min at 37°C. The cell nucleus has been visualized, implementing 10 µg/ml Hoechst 33342 for 10 min at 37°C. To allow the differentiation between cells with intact membrane and cells with disrupted one, the cells have been incubated for 5 min at 37°C with 1 µg/ml propidium iodide. Before the microscopic observation, they have been washed with PBS. At a concentration of 1 µM T20K-CF the peptide bounded on the cell membrane of most of the unstimulate Jurkat cells. Incubation with four time higher concentration and ten time higher concentration showed attachment of T20K-CF to the cell membrane and penetration of the peptide within the cell. The amount of peptide which was interacting with the unstimulated Jurkat cells increased with prolonging of the incubation time; scale bar: 5 µm

Another observation about the cellular uptake of T20K-CF in Jurkat cells within the dose dependent study is shown in Figure 5-13. The number of unstained cells is decreasing with prolonged incubation times and with increasing peptide concentrations. Over 90% of the unstimulated Jurkat cells, treated for 1 h or 4 h with 1 µM or 4 µM T20K-CF occur to have no or low interaction with the

fluorescently labeled immunosuppressive peptide T20K. Furthermore, all of the cells at all examined time courses, incubated with 10 µM T20K-CF occurred to be fluorescently stained. Additionally within all concentrations and time courses, the number of intensely stained cells increased. At lower concentration and at short incubation times, only 1% of the cells appeared to be intensely fluorescein stained. Furthermore, 40% of the cells treated for 4 h with a concentration of 10 µM T20K-CF appeared to be intensely stained. Hence, high amounts of the peptide bound to the cells or internalized into the cytosol.

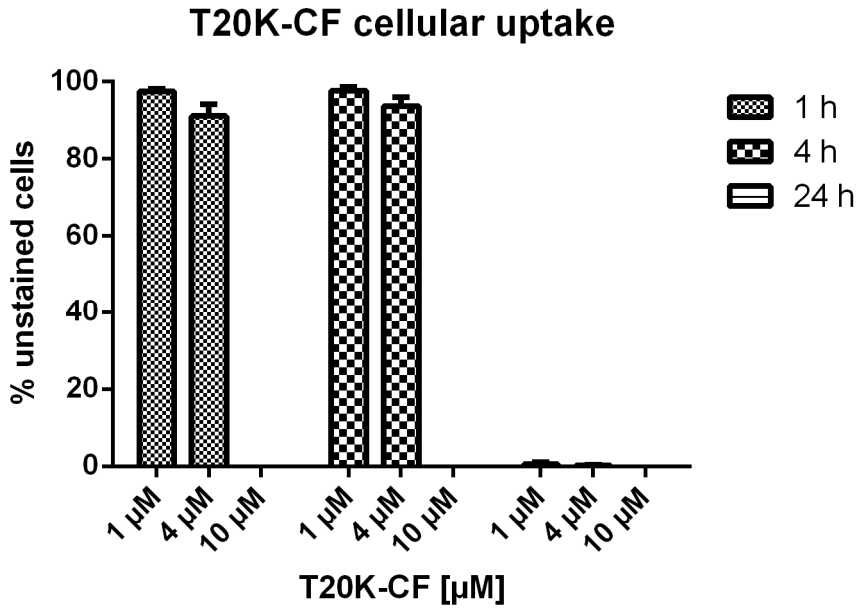

Figure 5-13: Semi-quantitative analysis of T20K-CF cellular uptake. Unstimulated Jurkat cells have been treated with 1 µM, 4 µM and 10 µM T20K-CF for incubation times of 1 h, 4 h and 24 h at 37°C. The percent of unstained cells has been estimated through optical observation and counting of the cells which have not shown any interaction with T20K-CF. Data represents the average (±SD) of three different images of the same experiment.

To gain some more information on the kinetics of the internalization, the time course of peptide attachment and penetration was examined. A concentration of 4 µM T20K-CF was chosen, because it appeared that most of the cells are with intact membrane and the action of peptide attachment and penetration could be examined. The activity of the compound was investigated for 1 h, 4 h, 24 h and

48 h at 37°C. The representative confocal images of unstimulated Jurkat cells are shown in Figure 5-14.

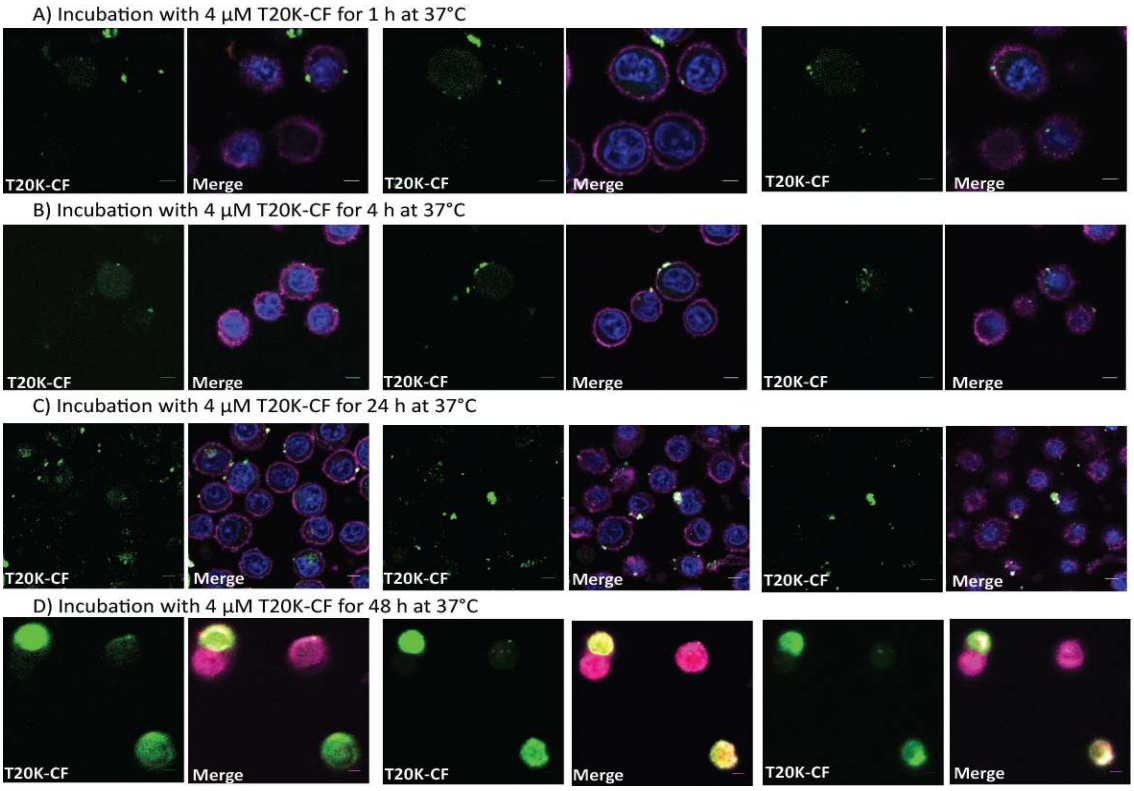

Figure 5-14: **Time course of the cellular uptake of T20K-CF at 4 µM.** Confocal microscopy observation of the peptide uptake for incubation times of 1 h (A), 4 h (B)**,** 24 h (C) and 48 h (D); The cellular membrane of Jurkat cells has been stained with 0.5 µg/ml CellMask Deep Red® plasma membrane stain for 5 min at 37°C. The cell nucleus has been visualized, implementing 10 µg/ml Hoechst 33342 for 10 min at 37°C. To allow the differentiation between cells with intact membrane and cells with disrupted one, the cells have been incubated for 5 min at 37°C with 1 µg/ml propidium iodide. Before the microscopic observation, the cells have been washed with PBS. Before the microscopic observation, the cells have been washed with PBS. Incubation with 4 µM T20K-CF showed attachment of T20K-CF to the cell membrane and penetration of the peptide to the unstimulated Jurkat cells within the whole time coarse. The amount of peptide which was interacting with the unstimulated Jurkat cells increased with prolonging of the incubation time. The number of cells with disrupted cell membrane rose; scale bar: 5 µm

The amount of attached peptide to the cell membrane or internalized T20K-CF increased as the applied time of incubation roused. Treatment, using incubation time of 48 h induced cytotoxicity and the cells appeared to be completely stained in all four channels (Figure 5-14D). No estimation of the peptide localization at this incubation time was possible.

Additionally, an optical observation of the effect of 4 μM T20K-CF during the time dependent course was performed (Figure 5-15). Within incubation times for 1 h and 4 h, most of the cells, 91% and 94% respectively, appeared to be unstained; hence, they did not show interaction with T20K-CF. However, at longer time course – for 24 h and 48 h, all cells have attached or internalized the fluorescently labeled peptide. Additionally, the presence of intensely stained Jurkat cells increased within the kinetics study. At a time course of 1 h, just 1% of the cells displayed intense fluorescein emission; however the amount has risen to 42% at the highest examined incubation time of 48 h. However, the optical observation determined that not all intensely stained cells are propidium iodide positive. Additionally, 8 % of the unstimulated Jurkat cells occurred to be weakly stained at incubation of 1 h and 4 h, treated with 4 μM peptide. The number of these cells increased to 77% at an incubation for 24 h, however this tendency decreased at a treatment for 48 h. Nevertheless, the number of intensely stained cells which showed membrane binding or internalization of higher amounts of T20K-CF roused within this time course, which correlated with the observation that peptide attachment or internalization increased with prolonging of incubation times and enhancement of the peptide concentration.

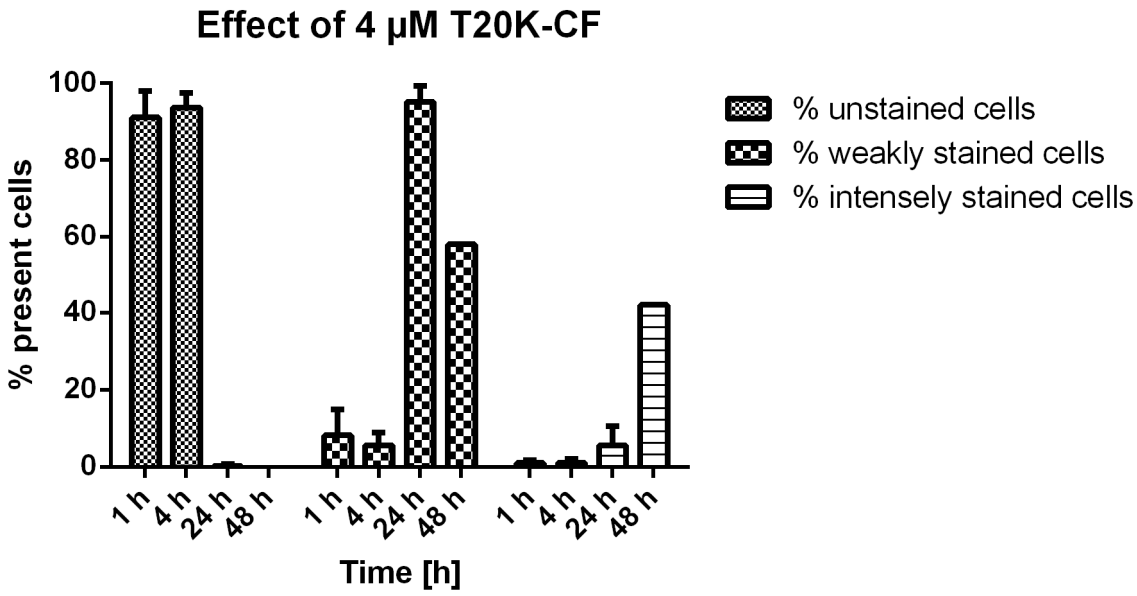

Figure 5-15: **Semi-quantitative assessment of T20K-CF cellular uptake using a time course.** Unstimulated Jurkat cells have been treated with 4 µM T20K-CF for 1 h, 4 h, 24 h and 48 h at 37° C. It was observed that the number of unstained cells, hence those which do not show interaction with T20K-CF, decreased with prolonging of the incubation time. Moreover, with increasing of the time course, more cells appeared to attach or to internalize T20K-CF, because the number of weakly or intensely stained cells increased. With prolonging of the incubation time, the amount of cells, which binded or internalized higher quantity of the peptide, hence the intensely stained ones, increased. Data represents the average (±SD) of three different images of the same experiment.

Next, a comparison between stimulated and unstimulated Jurkat cells was performed using confocal microscopy. Two different methods for activation of Jurkat cells were examined – stimulation with CD3 / CD28 and stimulation with PMA / Ionomycin (see also 4.2.3). Both activations types were performed overnight. Afterwards, the stimulated cells were treated with 4 µM T20K-CF for 4 h at 37°C as previously described. To enable the comparison study, the same peptide concentration and the same incubation time as by the stimulated cells was implemented to present images of the unstimulated Jurkat cells (Figure 5-16).

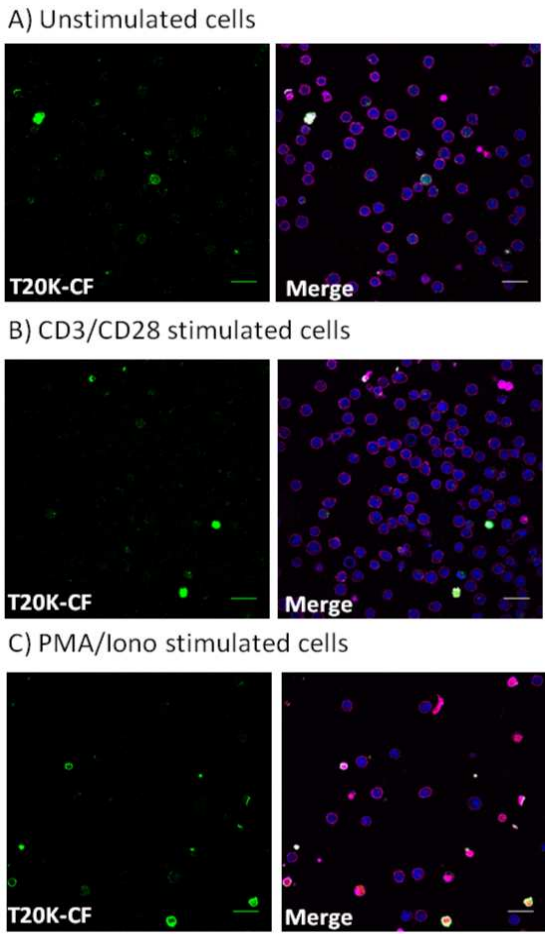

Figure 5-16: **Analysis of the cellular uptake of T20K-CF into stimulated and unstimulated Jurkat cells.** Comparison between unstimulated (A), CD3 / CD28 (B) stimulated and PMA / ionomycin (C) stimulated Jurkat cells. The cells have been treated with 4 µM T20K-CF for 4 h at 37°C. The cellular membrane of Jurkat cells has been stained with 0.5 µg/ml CellMask Deep Red® plasma membrane stain for 5 min at 37°C. The cell nucleus has been visualized, implementing 10 µg/ml Hoechst 33342 for 10 min at 37°C. To allow the differentiation between cells with intact membrane and cells with disrupted one, the cells have been incubated for 5 min at 37°C with 1 µg/ml propidium iodide. Before the microscopic observation, the cells have been washed with PBS. No difference in the cell morphology or in the amount of internalized peptide has been observed; scale bar: 50 µm

According to Figure 5-16, some of the cells exhibited attachment of the peptide to the cell membrane or internalization of it within the cytosol. It was expected that the stimulated Jurkat cells appear bigger than the unstimulated due to the release of Ca^{2+} from internal cell stores which leads to the activation of the Ca^{2+} release-activated Ca^{2+} channel (CRAC) which open through the activation and increases thereby the level of Ca^{2+} in the cytosol (Feske et al., 2012). Nevertheless, when comparing the images with unstimulated (Figure 5-16A), CD3 / CD28 stimulated (Figure 5-16B) and PMA / Ionomycin stimulated (Figure

5-16C) Jurkat cells, no difference in the size, morphology or internalization of the immunosuppressive peptide was observed.

Next, it was examined whether the interaction of the peptide with the cell membrane is temperature dependent. The results of this study are shown in Figure 5-17, 5-18 and 5-19.

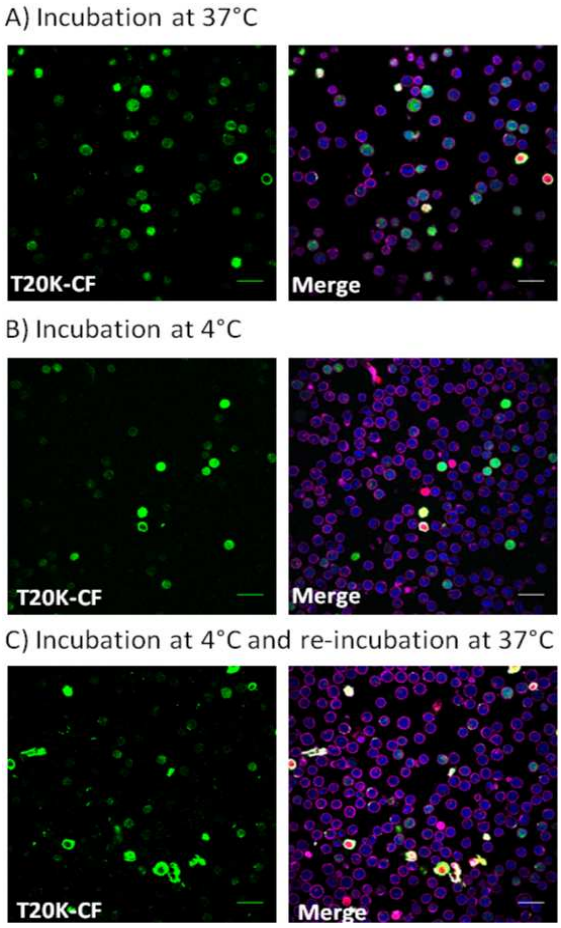

Figure 5-17: **Temperature dependence of the T20K-CF cellular uptake in overview images.** Overview Photos in green channel and merge photo; incubation with 10 µM T20K-CF for (A) 1 h at 37° C, (B) 1 h at 4° C and (C) 1h at 4° C and re-incubation for 1 h at 37° C; The cellular membrane of Jurkat cells has been stained with 0.5 µg/ml CellMask Deep Red® plasma membrane stain for 5 min at 37°C. The cell nucleus has been visualized, implementing 10 µg/ml Hoechst 33342 for 10 min at 37°C. To allow the differentiation between cells with intact membrane and cells with disrupted one, the cells have been incubated for 5 min at 37°C with 1 µg/ml propidium iodide. Before the microscopic observation, the cells have been washed with PBS. There was low distribution of T20K-CF in the cell membrane and within the cells at 4°C. Moreover, not only by incubation at 37°C, but also by re-incubation at 37°C after treatment at 4°C the cells attached the peptide on the cell membrane or internalized it within the cells; scale bar: 50 µm

At 4°C the active mechanisms for peptide attachment or internalization are suppressed. However, as presented in Figure 5-17B, the attachment of the peptide to the cell membrane could not be completely inhibited. There was weak fluorescence in cells having intact membranes.

Significantly reduced interaction of the peptide with the cell was observed at 4°C (Figure 5-18B) when comparing the peptide binding and internalization with cells, treated with the same concentration and for the same time course, but incubated at 37°C (Figure 5-18A) .

Based on the previous study of cyclotide internalization into mammalian cells (Greenwood et al., 2007), a re-incubation at 37°C was performed, following the treatment at 4°C. The peptide interaction with the cell membrane of Jurkat cells was restored during this experiment (Figure 5-17C, Figure 5-18C and Figure 5-19C). These observations suggested that the peptide is internalized in a temperature dependent manner possibly via physical interaction. Hence, the uptake pathway seems to be energy–dependent, because of the significantly reduced amount of internalized peptide at 4°C. At this temperature all energy-dependent uptake pathways are inhibited. However, there was low internalization, which suggests that the pathway of peptide uptake could be a combination of energy-dependent and energy-independent pathways.

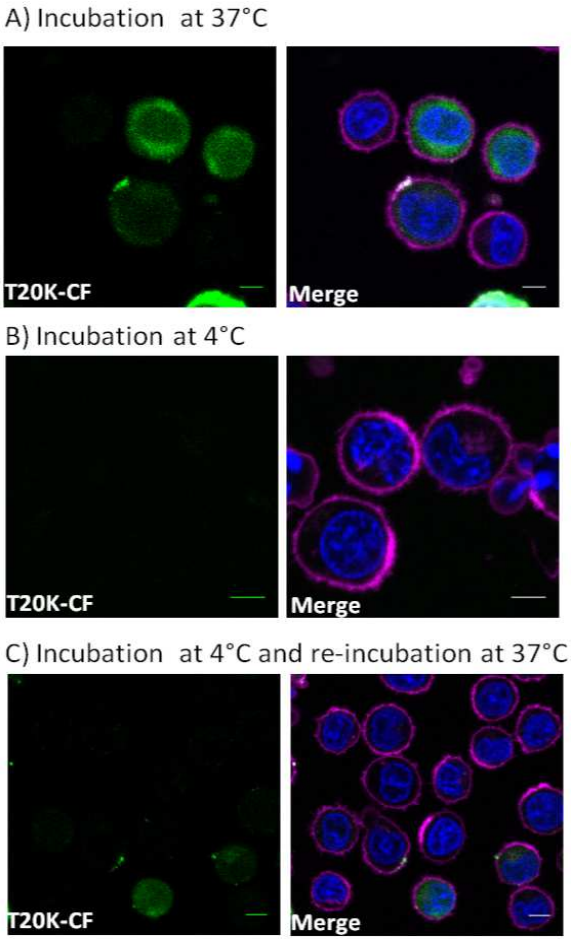

Figure 5-18: Temperature dependence of the T20K-CF cellular uptake. Confocal images of the temperature dependent analysis with 10 µM T20K-CF incubated for 1 h at 37° C (A), for 1 h at 4° C (B) and for 1h at 4° C and re-incubation for 1 h at 37° C (C). The cellular membrane of Jurkat cells has been stained with 0.5 µg/ml CellMask Deep Red® plasma membrane stain for 5 min at 37°C. The cell nucleus has been visualized, implementing 10 µg/ml Hoechst 33342 for 10 min at 37°C. To allow the differentiation between cells with intact membrane and cells with disrupted one, the cells have been incubated for 5 min at 37°C with 1 µg/ml propidium iodide. Before the microscopic observation, the cells have been washed with PBS. There was low distribution of T20K-CF in the cell membrane and within the cells at 4°C. Moreover, not only by incubation at 37°C, but also by re-incubation at 37°C after treatment at 4°C the cells attached the peptide on the cell membrane or internalized it within the cells; scale bar: 5 µm

Additionally, the temperature dependent study was performed with 3D images. In this way a profiling of the surface of the cells was performed (Figure 5-19).

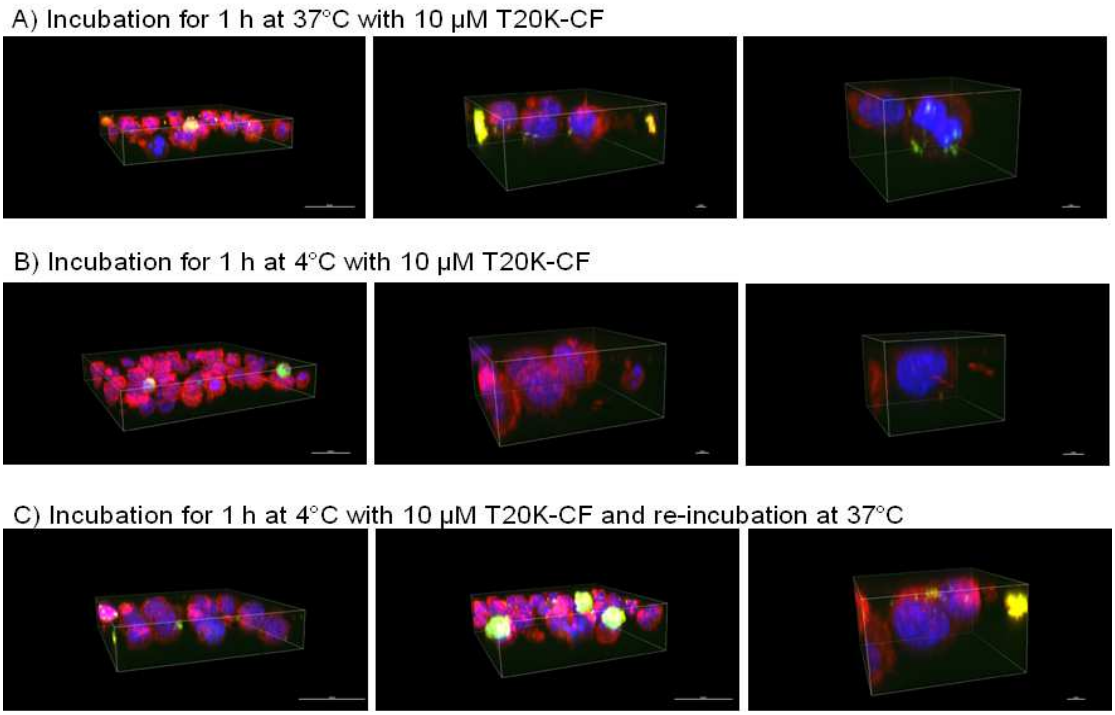

Figure 5-19: Temperature dependence of the T20K-CF cellular uptake in 3D images. Confocal images of the temperature dependent analysis with 10 µM T20K-CF incubated for 1 h at 37°C (A), for 1 h at 4°C (B) and for 1h at 4°C and re-incubation for 1 h at 37°C (C). The cellular membrane of Jurkat cells has been stained with 0.5 µg/ml CellMask Deep Red® plasma membrane stain for 5 min at 37°C. The cell nucleus has been visualized, implementing 10 µg/ml Hoechst 33342 for 10 min at 37°C. To allow the differentiation between cells with intact membrane and cells with disrupted one, the cells have been incubated for 5 min at 37°C with 1 µg/ml propidium iodide. Before the microscopic observation, the cells have been washed with PBS. A 23 frames z-stack through the cell from the top to the bottom has been performed and the 3D images were generated automatically.

In Figure 5-20 the appearance of stained cells by treatment for 1 h with 10 µM T20K-CF is demonstrated. As previously mentioned the peptide internalization was not completely inhibited when incubating the cells for 1 h at 4°C. Around 15% of the unstimulated Jurkat cells appeared to have bounded or internalized the peptide. In comparison, when incubating the cells with the same peptide concentration and for the same time but at 37°C, it was observed that all of the cells internalized weakly or intensely T20K-CF. Surprisingly, when the cells were re-incubated at 37°C after treatment at 4°C, half of them were able to interact with the immunosuppressive peptide.

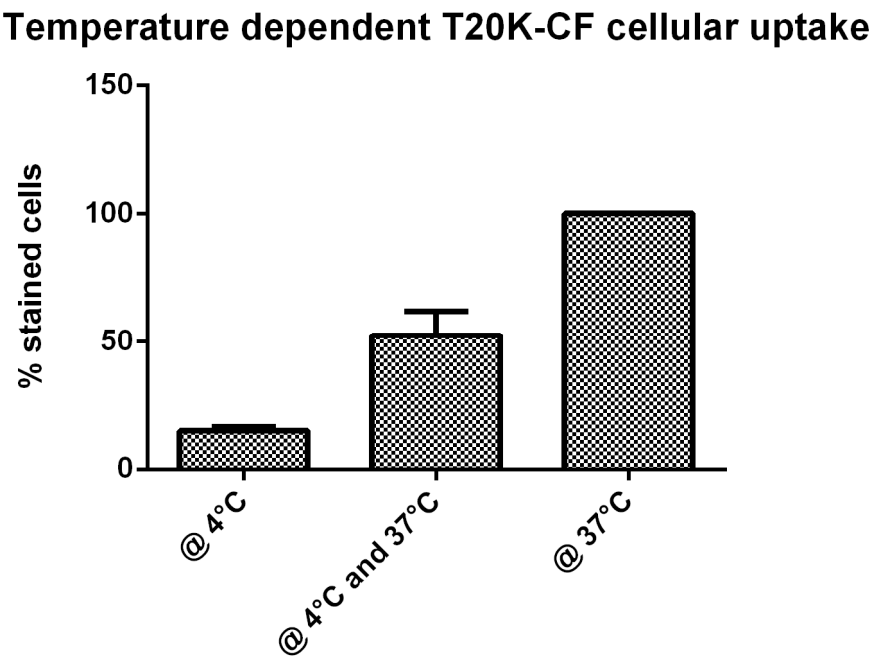

Figure 5-20: Semi-quantitative assessment of the temperature dependent T20K-CF cellular uptake. Unstimulate Jurkat cells have been treated for 1 h with 10 µM T20K-CF at 4°C, at 37°C and at 4°C and then following re-incubation for 1 h at 37°C. Through microscopic observation and counting of the cells which internalized T20K-CF, the percent of the stained cells has been estimated. It was observed that the peptide binding and internalization was not completely inhibited at 4°C. Moreover, by incubation of the cells at 37°C, all of them had interaction with T20K-CF. Additionally after treatment at 4°C and then re-incubation at 37°C, the half of the unstimulated Jurkat cells internalized the immunosuppressive peptide. Data represents the average (±SD) of three different images of the same experiment.

6. Discussion

Cyclotides exhibit numerous biological activities and many of them are due to interactions with the cellular membrane or intracellular targets. One property of cyclotides is cytotoxicity against mammalian tumor cells (Lindholm et al., 2002), nematodes (Colgrave et al., 2008), insect epithelial cells (Barbeta et al., 2008), bacteria (Tam et al., 1999; Pränting et al., 2010) and fungi (Tam et al., 1999). Additionally cyclotides have insecticidal (Barbeta et al., 2008; Gruber et al., 2007), antimicrobial (Tam et al., 1999), antifungal (Tam et al., 1999) and anticancer (Lindholm et al., 2002; Görranson et al., 2004; Gerlach et al., 2010) properties. To perform all of these activities cyclotides should have an affinity to cellular membranes (Burman et al., 2014). In this work the interaction of [T20K] kalata B1 and Jurkat/T-cells was investigated to assess a time-, dose- and temperature-dependent effects of their ability to penetrate cells.

The first step of this study was the derivatization and purification of fluorescent labeled peptides. Previously, the structure of kalata B1 was characterized and it showed a hydrophobic face which was located around residue Glu7 (Figure 6-1). This region was described as bioactive face of the peptide, since disruption of its physical or chemical properties by mutation of amino acids to lysine or alanine to loss of function and activity leaded (Huang et al., 2010). Another structural property of the native kalata B1 peptide is the surface exposed hydrophobic patch which was formed by Leu2, Pro3, Val4, Val10, Trp23, Pro24 and Val25 (Figure 6-1) (Henriques and Craik, 2012).

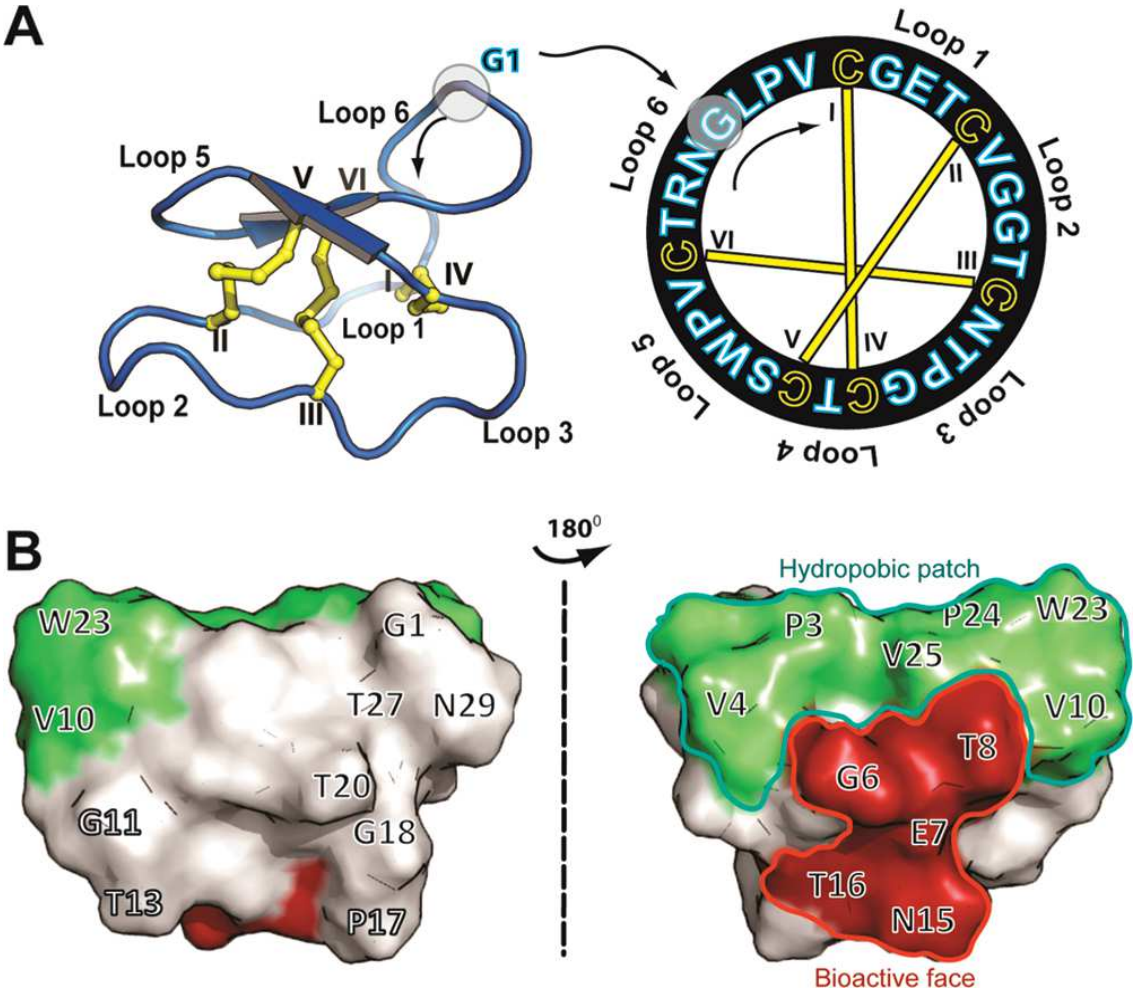

Figure 6-1: **Structure of kalata B1.** (A) Three-dimensional structure (PDB ID: 1nb1) and sequence of kalata B1 (kB1). The cyclic backbone and the six conserved Cys form a cyclic cystine knot which is typical for cyclotides and respectively for kalata B1. The backbone segments between Cys residues are termed loops. In yellow are shown disulfide bonds, the Cys are labeled I−VI, and the six loops are identified. The direction of the peptide chain N−C is indicated by the black arrow. The position of Gly1 is indicated in the structure; this residue is ligated to Asn29 during the biosynthesis of the circular backbone. (B) In two views showing the bioactive face, identified from an Ala scan62 (in red), and the hydrophobic patch (in green) is represented the surface of kB1. The molecule in the left view has the same orientation as the three-dimensional structure represented in panel A). On the same side of the molecule are localized the bioactive face and hydrophobic patch, shown in the right view. The hemolytic and insecticidal activities of kB1 are inhibited when any of the residues in the hydrophobic patch or in the bioactive face are substituted with a Lys residue (Simonsen et al., 2008). The figure was adopted from Henriques et al., (2011).

The native kalata B1 peptide did not contain any Lys residues and therefore a Lys was introduced to allow labeling with 5(6)-carboxyfluorescein succinimidyl ester. As previously mentioned, [T20K] kalata B1 is a mutant of the cyclotide kalata B1, where the threonine at position 20 was exchanged with a lysine. The replaced residue was located on the opposite side of the peptide and was a part

of the amendable face (Huang et al., 2010; Simonsen et al., 2008). This mutant was chosen due to the similar structure, bioactivity and membrane–binding properties in comparison to native kalata B1 (Cascales et al., 2011). The mutation affects slightly the hydrophobic properties of the cyclotide surface. Most importantly, the anti-proliferative capacity on lymphocytes and isolated T-cells was not affected negatively by this mutation (Gründemann et al., 2012). No significant differences in the three dimensional folds of both peptides has been observed when comparing the results of NMR α-H chemical shifts using 2D NMR spectra studies (Gründemann et al., 2013).

For the observation of the interaction between the kalata B1 mutant T20K and living Jurkat or T-cells, the peptide was firstly derivatized with 5(6)-carboxyfluorescein-succinimidyl ester and then separated from the reaction mixture. For this reason the fluorescently tagged T20K was purified using reverse-phased HPLC. The structure of the peptide is characterized by a cyclic–cystine knot motif, which is located interior and hydrophobic side chains which move to the exterior of the peptide (Leta Aboye et al., 2008). Due to these properties the peptide eluted later from the RP-HPLC column by the purification (Figure 5-1). To confirm if the fluorescently labeled cyclotide T20K-CF was isolated from the peptide mixture, its purity and quality were determined by MALDI-TOF–MS (Figure 5-2) and analytical–HPLC (Figure 5-3).

The first set of microscopy experiments were designed to confirm that T20K-CF can interact with Jurkat T-cells and anti-CD3 isolated human T-lymphocytes and that this cyclotide is able to internalize into the cells (Figure 5-5 and Figure 5-6). The primary goal was to analyze, the interaction of T20K-CF with native human T–lymphocytes, which are essential regulators of the immune system, but since these cells are more difficult to grow and maintain under laboratory conditions, Jurkat T–cells were used as the main *in-vitro* model system. It was examined that the cells, incubated with 4 μM and 10 μM labeled T20K (T20K-CF), internalize the peptide within 1 h of exposure. This provides evidence that the fluorescent-tagged kalata B1 mutant is able to enter through the cellular membrane into the cells. Previous research by Greenwood et al. (2008) showed that the cyclotide [T16K] kalata B1 is not able to permeate through the cell membrane and formed clusters at the cell surface. They produced a mutant of

kalata B1 where the threonine at position 16 was exchanged with a lysine. In this way the lysine of [T16K] kalata B1 was conjugated to biotin and purified. The labeled mutant was detected with streptavidin-FITC conjugate. The distribution was observed in fixed cells. Later Cascales and co-workers demonstrated using improved methodology that the kalata B1 peptide T20K can enter living, unfixed cells. They implemented Alexa488 for the detection of the peptide distribution which is brighter and more stable than FITC (Panchuk-Voloshina et al., 1999). This is the reason why during the experiments for my master thesis I followed the distribution of fluorescently tagged T20K (T20K-CF) in living, unfixed cells. This method has been chosen because a mild fixation with formaldehyde could drastically change the localization of the peptide (Richard et al., 2003). To enable the microscopic observation 5(6)-carboxyfluorescein succinimidyl ester was implemented which binds to the lysine in the structure of T20K.

Next I performed a dose-dependent study with concentrations between 1 μM and 10 μM T20K-CF. It was examined that at concentration 1 μM and 4 μM a treatment for 24 h with the peptide was necessary so that the peptide distributes within all of the cells (Figure 5-8). However, by a concentration of 10 μM T20K-CF this observation was made for 1 h of treatment (Figure 5-8). This was the first sign that T20K-CF interacts with Jurkat cells in a dose-dependent manner. When the cells were treated with concentration of 1 μM there was really weak interaction between the peptide and the cells (Figure 5-10 and 5-11). At a time point of 24 h most of the cells internalized the peptide, however the distribution of it in the cells was low (Figure 5-12). With increasing of the peptide concentration, more cells bounded the peptide on the cellular membrane or internalized it within the cells. By a treatment of the cells with 4 μM T20K-CF there was internalization of the peptide from the first hour (Figure 5-10). However, at this concentration incubation for 24 h was demanded for the internalization of the peptide of all cells (Figure 5-12). Moreover, all of the cells treated with 10 μM T20K-CF showed interaction with the peptide from the first hour of incubation (Figure 5-10, 5-11 and 5-12). These microscopic observations are evidence that the peptide concentration plays an important role for the activity and internalization of the peptide. This conclusion is in

agreement with the study of Nakase et al. who examined that the peptide concentration and cell line as *in-vitro* model system are playing an essential role for the cyclotide–cell interactions. The mechanism of action depends on the background of the implemented cell line. Membranes of eukaryotic cells are a barrier for the access of hydrophilic molecules to their intracellular targets (D'Souza et al., 2014). The plasma membrane consists of the following lipid composition: phosphatidylcholine (PC), phosphatidylethanolamine (PE), phosphatidylserine (PS), sphingomyelin and cholesterol (Fridriksson et al., 1999; Scott, 1976). Tumor cell membranes are characterized by a decrease in cholesterol due to rapid cell division (Hendrik and Michalak, 2003). They have higher negative charge density because they consist of three to seven times more phosphatidylserine (PS), located on the outer leaflet of the cellular membrane (Utsugi et al., 1991). These properties of tumor cell membranes are important for the study of the interaction between T20K-CF and the lipid bilayer of Jurkat cells. This *in vitro* model system is an immortalized cell line of leukemic cells which has the characterizations of tumor cells previously described. Moreover, for the binding of the cyclotide to the cellular membrane and for the internalization into the cytosol, the peptide structure is playing a crucial role. The cooperation between positively charged residues of the cyclotide and negatively charged membrane head groups is the reason for the electrostatic interaction between the peptide and the cellular membranes (Brooks et al., 2005). This is the explanation why cyclotides containing more positively charged amino acids have been found to be more active. They have conserved affinity to phosphatidylethanolamine (PE) membrane lipids and this selectivity is closely linked with their biological activity (Henriques et al., 2012). Moreover, the structure of T20K-CF and the membrane properties of Jurkat cells are important for the peptide affinity, selectivity and binding to the lipid bilayer and the following cytosolic internalization.

The different subfamilies of cyclotides possess diverse mode of action. The cyclotides of the bracelet family have amphiphilic and frequently cationic properties. This enables the interaction with the anionic surface of the membrane and through hydrophobic and electrostatic forces the peptide could be adsorpt toward the lipid core (Strömstedt et al., 2010). The sequences of

some typical peptide of this subfamily are illustrated in Table 6. Moreover, the Möbius cyclotides benefit from the semi-conserved tryptophan next to the cis-Pro in loop 5 (Burman et al., 2014). In the case of bracelet subfamily it is situated in loop 2. Both loops are hydrophobic and create the patch directly associated with the membrane (Burman et al., 2014). The structure and position is illustrated in Figure 6-1. The aromatic amino acid tryptophan has affinity for the hydroxyl/carbonyl region of the membrane phospholipids (de Planque et al., 2003). This property enhance the affinity of the cyclotide to the cellular membrane and promoted the binding process. Additionally, the amphiphilic properties of the cyclotide are improved by forcing of hydrophobic residues to the surface of the molecule (Burman et al., 2014).

	loop 6		loop 1		loop 2		loop 3		4		loop 5		loop 6
Möbius		I		II		III		IV	V			VI	
kalata B1	G - L P V	C	G - - - E T	C	V G - G T	C	N T - - - P G	C	T	C	S W - P V	C	T R - - N
kalata B2	G - L P V	C	G - - - E T	C	F G - G T	C	N T - - - P G	C	S	C	T W - P I	C	T R - - D
kalata B7	G - L P V	C	G - - - E T	C	T L - G T	C	Y T - - - Q G	C	T	C	S W - P I	C	K R - - N
varv F	G - V P I	C	G - - - E T	C	T L - G T	C	Y T - - - A G	C	S	C	S W - P V	C	T R - - N
Bracelet													
cycloviolacin O1	G - I P -	C	A - - - E S	C	V Y - I P	C	T V T A L L G	C	S	C	S N - R V	C	Y - - - N
cycloviolacin O2	G - I P -	C	G - - - E S	C	V W - I P	C	I S S - A I G	C	S	C	K S - K V	C	Y R - - N
kalata B5	G - T P -	C	G - - - E S	C	V Y - I P	C	I S G - V I G	C	S	C	T D - K V	C	Y L - - N
kalata B8	G S V L N	C	G - - - E T	C	L L - G T	C	Y T - - - T G	C	T	C	N K Y R V	C	T K - - D
Trypsin Inhibitor													
MCoTI-I	G - - G V	C	P K I L Q R	C	R R D S D	C	P G - - - - A	C	I	C	R G N G Y	C	G S G S D
MCoTI-II	G - - G V	C	P K I L K K	C	R R D S D	C	P G - - - - A	C	I	C	R G N G Y	C	G S G S D

Figure 6-2: Sequences of selected natural cyclotides belonging to the Möbius, Bracelet, and Trypsin inhibitor subfamilies. The Figure was adopted from Henriques and Craik, 2011.

During the dose-dependent study it was examined that the prolonging of the incubation time and the increasing of the peptide concentration correlates with the increase of cytotoxic effects. However, kalata B1 and MCoTI-II were reported to cross the membrane at subtoxic concentrations (Greenwood et al., 2007; Contreras et al., 2011; Cascales et al., 2011). Determining non-cytotoxic concentrations of T20K-CF was important to know the concentration range to be used for internalization studies of the peptide and examining distribution in living cells by entering through intact membranes (Figure 5-9). Gründemann et al., claimed that no signs of cytotoxicity have been observed between

concentrations of 1.9 μM to 4.4 μM of T20K. The cytotoxic properties of a fluorescently tagged T20K were examined. It was suggested that the labeling resulted in a less-cytotoxic peptide (Hellinger, unpublished data). Previous research with cycloviolacin O2 proposed that leukemic lymphocytes have higher cytotoxicity to this cyclotide in comparison to normal lymphocytes (Lindholm et al., 2002). A reason for the difference could be the membrane composition because as previously mentioned tumor cell membranes have higher content of phosphatidylserine located on the outer leaflet of the membrane and decreased cholesterol content due to the rapid cell division (Utsugi et al., 1991). This membrane composition of cancer cells and normal cells could affect the affinity of the peptide to the cellular membrane and could adjust the lytic activity of the cyclotide (Burman et al., 2014). Through microscopic observation and semi-quantitative analysis by counting of cells it was examined that treatment for 1 to 4 h was not cytotoxic with concentrations between 1 μM and 4 μM T20K-CF (Figure 5-9). Higher cytotoxicity has been examined with prolonging of the incubation time and increasing of the concentration to 10 μM T20K-CF (Figure 5-9). This observation is in agreement with the above mentioned cytotoxicity experiment by Greenwood et al. The examination that higher concentration of cyclotides is required to induce cytotoxicity overlapped with other investigations which were done with cyclotides in plant products, consumed for medicinal purposes (Greenwood et al., 2007). Moreover, therapeutical drugs are normally implemented in a nanomolar range due to the toxic effects (Brooks et al., 2005). Therefore, cyclotides offer a better possibility in the drug development area, because they show lower cytotoxicity in comparison to standard therapeutic drugs.

Although most of the cells possessed intact cellular membrane, because they were negative for propidium iodide staining, there were several papers suggesting disruption of the cellular membrane by pore formation when treating cells with cyclotides (Henriques et al., 2011; Cascales et al., 2011; Burman et al., 2011, Sando et al., 2011; Wang et al., 2012). Prolonged incubation time and increased concentration, led to additional pores in the membrane and more molecules were capable of penetrating into the cell. Implementing patch clamp methods the pore formation activity of kalata B1 was shown (Huang et al.,

2009). This lytic peptide generated curvature stress and in this way membrane perforations were formed (Burman et al., 2014). The Möbius cyclotides associate with phosphatidylethanolamine membrane lipids and this affinity was important for the lytic activity (Burman et al., 2011; Henriques and Craik., 2011). Moreover, the membrane composition had a crucial role for the binding of the cyclotides, for the cell internalization and for the lytic action (Burman et al., 2014). Research on model membranes showed that the cholesterol content increased the lytic activity of kalata B1 (Huang et al., 2009). The bioactivity of it was dependent on the membrane lipid composition and membrane consistency (Henriques et al., 2011). These factors could be the explanation for the differences in the interaction between T20K-CF and Jurkat cells. As previously observed and illustrated in Figure 5-13, some cells appear weakly stained and others occur to be intensely stained. The cells are in different cell-cycle phase and some of them are more susceptible to the interaction with the fluorescently labeled T20K. The membrane properties could be the reason for the differences in the internalization by the different cells in the same sample. It is suggested that the cellular membrane plays an essential role in different bioactivities of cyclotides (Wang et al., 2012). Furthermore, the anti-HIV activity of the cyclotides is due to their ability to destroy the membrane of HIV particles (Henriques et al., 2011). Peptides with hydrophobic patches available insert into the membrane and induce cell death due to pore formation or fissures (Lindholm et al., 2002). This kind of action is typical for a lot of peptides with antimicrobial activity. Generally, the pore formation process has been described by Sando et al. in four different steps. At the beginning the cyclotide bound to the cellular membrane due to hydrophobic interactions and because of the presence of phosphoethanolamine headgroups. Afterwards, the peptide oligomerized. The following step described was the insertion into the hydrophobic core. The fourth and last step of the interaction was the formation of pores by the peptide which spanned the two layers of the membrane (Sando et al., 2011). However, it was difficult to compare lytic activity of cyclotides between different cell types (Wimley, 2010). The property of cyclotides to form pores might be in connection with their immunosuppressive characteristic. To resolve this further analysis and investigations are necessary.

Still the question remained why some cyclotides have the ability to penetrate into the cells and other bind to the cellular membrane. The structures of kalata B1 and MCoTI-II are similar because both peptides have a cyclic backbone and possess the same disulfide connectivity which leads to the same folding in the organization of the cyclotide. Moreover, the structure of MCoTI-II contains six basic residues and three acidic residues (Felizmenio-Quimio et al., 2001). The sequence of kalata B1 contains two charged residues Glu3 and Arg24 which are located on the opposite sights of the molecular surface (Saether et al., 1995). When comparing the structures of both cyclotides kalata B1 possess more hydrophobic residues than MCoTI-II which has more charged residues. This could be the explanation for the differences in the cellular uptake of both peptides. On the other hand, the exchange of threonine on position twenty to the positively charged lysine in kalata B1 mutant T20K leads to a more charged molecule than the native one. This circumstance has an effect on the differences in the binding and internalization of peptides. Greenwood et al. demonstrated the affinity of kalata B1 to the cell membrane of macrophages. The interaction of the cyclotide with membranes has been shown previously due to antimicrobial and hemolytic activity of the peptide (Tam et al., 1999). Additionally, kalata B1 has affinity to phosphatidylethanolamine bilayers which has been shown by surface plasmon resonance (Kamimori et al., 2005). Experiments with diphosphatidylcholine micelles demonstrated that the hydrophobic residues Trp19 – Val21 in loop 5 and Leu27 and Val29 in loop 6 of the sequence of kalata B1 are essential for the binding to the membrane and for the formation of clusters (Shenkarev et al., 2006). This effect is called “carpet effect” and it is followed by peptide penetration (Greenwood et al., 2007). A reason for preventing cellular penetration of kalata B1 is supposed to be the concentration and arrangement of the hydrophobic patch which inhibits the penetration of the peptide (Greenwood et al., 2007).

To examine the mode of action of T20K-CF with Jurkat cells, the kinetics of the peptide uptake has been observed (Figure 5-14). The cells were treated with 4 μM T20K-CF because previous experiments by Greenwood et al. have defined this concentration as non-cytotoxic. However, it appeared to lead to disruption of the cellular membrane and cell death with prolonging of the incubation time. It

was observed that the peptide interacts firstly with the cellular membrane without causing any disruption. The interaction between positively charged residues of T20K-CF and negatively charged membrane head groups is the reason for the affinity and for the binding process of the peptide to the cellular membrane (Brooks et al., 2005). The peptide has conserved affinity to phosphatidylethanolamine (PE) membrane lipids as previously mentioned (Henriques et al., 2012). After the binding process, the peptide was observed to penetrate into the cell. To confirm that the peptide reached its target in the cell, its activity could be tested. This was achieved for the linear carrier peptide Tat protein transduction domain (Frankel and Pabo, 1988; Green and Loewenstein, 1988). There was evidence for functional identification of a secondary target, other than the cellular membrane. The DNA was damaged at a concentration 100 times lower than the lytic concentration. However, at 10 times lower concentration then the lytic, no DNA damaging effect and no lytic effect have been determined (Yeshak et al., 2012).

Moreover, Gründemann et al. observed a dose-dependent anti-proliferative function of T20K on human T-cells. There were no changes or differences in the immunosuppressive function when comparing activated lymphocytes and purified T-cells which suggested that the immunosuppression by cyclotides is of direct origin (Gründemann et al., 2012). This property of this cyclic peptide is compound specific, stereospecific and is directly related to the biology of T-cells. The proliferation of T-lymphocytes is initiated by the ligation of antigens on the T-cell receptor which induces the initiation of a whole T-cell receptor signaling pathway (Alberts et al., 2002). During this process the autocrine growth factor IL-2 is expressed and this event promotes interaction of it with its surface receptor which is upregulated in activated T-cells (Malek, 2008). When comparing the immunosuppressive activity of T20K and an antiproliferative drug – cyclosporine A, both chemical compounds reduced the expression of IL-2 cell surface receptor and the endogenous expression of IL-2 (Gründemann et al., 2012; Thell et al., 2013). Both substances did not showed inhibition or delay in the calcium flux which has been triggered by stimulation of the cells with CD3 / CD28 or PMA / ionomycin (Gründemann et al., 2012). Calcium is involved in the T-cell receptor signaling and is an important messenger. Moreover, with the

observation that T20K has no effect on it, a downstream mechanism of action of immunosuppressive cyclotides has been proposed. Exposure of cells to the combination of calcium ionophore (ionomycin) and a phorbol ester (PMA) triggered activation response which induced the production of IL-2 and the cell cycle progression (Baxter and Hodgkin, 2002; Truneh et al., 1985). The Ca^{2+} ionophore and the TCR-ligand acted with phorbol ester and behaved as stimuli for Jurkat cells (Wiscocil, 1985). Moreover, CD28 is a molecule which plays a role of costimulator for the activation of T-lymphocytes. It is a glycoprotein presented mainly on T-cells and it enhances the transcription of IL-2 (Korecka et al., 2007). CD3 had a stimulatory role for human T-cells and induced subunit mediated signal transduction across the plasma membrane (Meuer et al., 1983). Additionally, the TCR stimulation caused increase in the intracellular free Ca^{2+}concentration and it functioned as a Ca^{2+}-mobilizing transmembrane receptor during T-cell activation (Abraham and Weiss, 2004). Due to the increased concentration of Ca^{2+} it was expected that there should be a morphological difference between stimulated and unstimulated Jurkat cells. However, when observing the microscopic results, no difference in the peptide – cell interaction, in the size or in the form of the cells was investigated (Figure 5-16). Gründemann et al., showed in his work that 1.8 μM T20K leads to 20% reduction of activated T-cells. The immunosuppressive effect of T20K could be explained with the inhibition of IL-2 due to its lymphokine pivotal role during the immune response (Gründemann et al., 2013).

Another important question was to determine how T20K was internalized into the cells after the binding to the cellular membrane. Henriques et al. classified kalata B1 as a new family cell penetrating peptides due to its property to enter the cell. For this process as previously mentioned the strong ionic interaction between the positively charged amino acid residues and the negatively charged plasma membrane are responsible. Despite some common properties by the cell penetrating peptides, the translocation mechanism is not the same for the different families (Figure 6-3) (Madani et al., 2011). The direct penetration is an energy independent pathway for peptide uptake (Madani et al., 2011). It was described as pore formation (Matsuzaki et al., 1996), inverted micelle formation (Derossi et al., 1996), the carpet-like model (Pouny et al., 1992) or membrane thinning model (Lee et al., 2005). Previous research with cyclotides by

Henriques and Craik suggested the pore-formation as one of the properties of kalata B1. After the targeting of the membrane and insertion in the bilayer core, the peptide was able to disrupt the membrane by a pore formation mechanism. Due to these observations, the direct penetration by pore formation mechanism is one possibility for peptide uptake in the case of the kalata B1 mutant T20K. Additionally, the diffuse cytosolic labeling became predominant at higher peptide concentrations. However, some cells treated with the peptide showed punctate structures in the cytoplasm (Figure 5-5). This observation suggested that endocytosis is another possible pathway of peptide uptake for T20K-CF. Additionally, the dose- and time-dependent studies confirmed this result, although there were rarely punctate endosome-like signals. This observation suggested that endocytosis could be the molecular pathway for peptide uptake. It consists of several pathways which are illustrated in Figure 4-2. Phagocytosis described the uptake of large particles. In comparison to it, the solute uptake has been enabled with pinocytosis (Madani et al., 2011). This process could be presented as macropinocytosis, which is dependent on the coat proteins clathrin and caveolin, and receptor-mediated endocytosis, which is independent on both coat proteins (Jones, 2007; Mayor and Pegano, 2007).

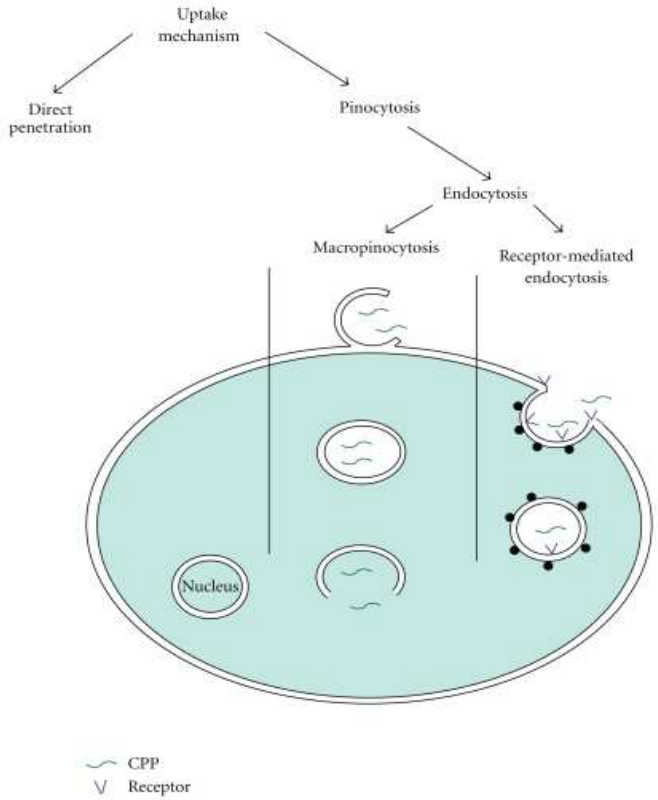

Figure 6-3: Scheme for different uptake pathways for CPPs. The figure was adopted from Madani et al. (2011).

Clathrin mediated and caveolin mediated endocytosis start with formation of concave structures of the plasma membrane. Their size in the case of clathrin was 120 nm and the invaginations in the case of caveolae were 60 nm (Nakase et al., 2004). Additionally, the molecular process of macropinocytosis was described with the formation of macropinosomes with a size greater than 1 μm (Conner and Schmid, 2003; Jones, 2007). This process is initiated by actin driven events, leading to membrane ruffling and protrusions that precede the formation of vesicles. When observing the endosomal structures in the cells, illustrated in Figure 5-5 it is obvious that they have a size of about 1 μm. This is a property which characterizes macropinocytosis, because the formed macropinosomes of this size are characteristic for this peptide uptake mechanism. Greenwood et al. reported that MCoTI-II, which is a cyclotide of the bracelet subfamily, is transported into the cell through a receptor independent non-specific mechanism - macropinocytosis. The peptide was encapsulated and located in macropinosomes (Conner and Schmid, 2003).

To investigate if endocytosis could be the peptide uptake pathway, some experiments at 4°C have been performed. At this temperature all of the energy-dependent uptake mechanisms are inhibited. As shown in Figures 5-17, 5-18 and 5-19 there was a clear inhibition of the peptide internalization by low temperature in comparison to cells, treated at the same way, but incubated at 37°C. The decreased internalization might result from either lower membrane fluidity and decrease in membrane dynamics or by inhibition of ATP-dependent process (Torcato et al., 2013). These results strongly supported the involvement of endocytosis as the major route for the internalization of T20K-CF. Greenwood et al. also suggested that the interaction of the cellular membrane and kalata B1 is temperature dependent and that at 4°C no binding could occur. Despite the prominence of endocytosis as an uptake mechanism, 15% of the cells internalized the peptide (Figure 5-20), suggesting that alternative internalization exists. However, by a re-incubation at 37°C following the treatment at 4°C, 50% of the cells took up the peptide. Due to the increase in the temperature, the energy-dependent pathways were activated again and this enabled the peptide penetration. However, as previously suggested due to the peptide uptake at 4°C, the internalization mechanism could neither be explained by adsorptive-mediated endocytosis nor by receptor-mediated endocytosis. The cellular uptake of cell penetrating peptides differ in the literature and range from endocytic (Mai et al., 2002; Vives, 2003) to a rapid and energy independent process (Mai et al., 2002). Cascales et al. made experiments with different subfamilies of cell penetrating cyclotides. Although there were structural similarities, the sequence of the peptides differed and this regulated the differing mode of cellular uptake. The interaction of the positively charged residues of MCoTI-II with phosphoinositides in the cellular membrane appeared to induce macropinocytosis as peptide uptake pathway (Cascales et al., 2011). On the other hand, kalata B1 interacts with phosphatidylethanolamine phospholipids and this leads to vesicle formation (Cascales et al., 2011). However, another peptide internalization pathway was shown for SFT-1 which can penetrate through the cell membrane without interaction with phospholipids and this is the reason that its mechanism of penetration appears to be different than the other mentioned above (Cascales et al., 2011). The cellular delivery of peptides mainly results from two different molecular pathways – direct plasma membrane

translocation and internalization by endocytosis (Durchardt et al., 2007; Lundin et al., 2008). Moreover, the extracellular concentration of the peptide, its sequence and the temperature are defining which pathway will take place for the peptide internalization (Alves et al., 2008; Alves et al., 2011; Jiao et al., 2009). Recent studies showed that direct penetration into the cytosol is also possible and this process is favored by hydrophobic groups of the peptides (Hirose et al., 2012). Some examples of cell penetrating peptides are HIV-Tat, penetratin, transportan and octaarginine which have the ability to enter cells via various mechanisms including endocytosis, membrane permeation or by combination of pathways (Madani et al., 2011). To sum up, there is evidence for energy-dependent and energy-independent pathways of uptake for T20K. This suggested that both mechanisms – endocytosis and direct penetration are involved in the peptide internalization.

The ability of T20K to penetrate into cells could be implemented for the transport of therapeutic peptides to their intracellular target. Through sequence changes in the scaffold of the cyclotide, it is possible to change its properties and capabilities. In this way the cyclotide framework could be adjusted for therapeutic usage and cellular compatibility. Experiments for diminishing of negative effects has been performed by Clark and co-workers as they decreased the hemolytic activity of kalata B1 by the replacement of three hydrophobic residues with polar and charged ones. Additionally, cell permeation of T20K-CF could be used as a template to introduce epitopes with defined biological activity through the cell membrane to the cell target. This could improve the pharmaceutical properties of linear peptides incorporated into the stable framework which otherwise are not capable of permeating through the lipid bilayer (Daly et al., 2009). In this way the bioactivity of the target peptide would be retained and its stability and bioavailability would be improved. Additionally, grafting bioactive peptides onto stable scaffolds would permit the increasing of the peptide size range to be implemented in the future. On the other side, some frameworks could be used for delivering of peptides to intracellular targets, based on their membrane permeability. Moreover, plant - derived stable cyclic peptides could be used as vectors to enhance the stability and oral activity of bioactive peptides (Craik et al., 2013).

7. Conclusion and outlook

In this study the interaction between the immunosuppressive peptide T20K-CF and cells has been examined. It was confirmed that the anti-proliferative peptide penetrates through the cellular membrane of CD3 isolated primary T-cells and Jurkat cells. It was determined that the cyclotide interacted firstly with the cellular membrane and then it penetrated through the lipid bilayer.

Furthermore, prolonging of the incubation time and increasing of the peptide concentration correlated with the raising of the amount of internalized peptide. This lead to increased cytotoxicity, however concentrations between 1 - 4 µM T20K-CF have been determined to be non-cytotoxic for shorter incubation time.

Moreover, the result of the study with CD3 / CD28 or PMA / ionomycin stimulated Jurkat cells showed that there is no morphological difference by their activation and there is now alteration in the internalization of T20K-CF when comparing them with unstimulated Jurkat cells.

Additionally, we examined the temperature dependence in the internalization of T20K-CF. However the penetration of the peptide was not completely inhibited at 4°C. These results strongly supported the involvement of both active cellular uptake by endocytosis and passive membrane passage for the internalization of T20K-CF.

Although this study supports the progress in the examination of the interaction between T20K-CF and T-cells, the target of [T20K] kalata B1 remains still unknown and further analyses are required to determine the molecular mechanism of the physiologic effect of [T20K] kalata B1.

8. References

Abraham, R. T. and A. Weiss. "Jurkat T Cells and Development of the T-Cell Receptor Signalling Paradigm." *Nat Rev Immunol* 4, no. 4 (2004): 301-8.

Alberts B, Johnson A, Lewis J, et al. Molecular Biology of the Cell. 4th edition. New York: Garland Science; 2002. Available from: http://www.ncbi.nlm.nih.gov/books/NBK21054/

Alewood, D., L. C. Birinyi-Strachan, P. K. Pallaghy, R. S. Norton, G. M. Nicholson and P. F. Alewood. "Synthesis and Characterization of Delta-Atracotoxin-Ar1a, the Lethal Neurotoxin from Venom of the Sydney Funnel-Web Spider (Atrax Robustus)." *Biochemistry* 42, no. 44 (2003): 12933-40.

Alves, I. D., C. Bechara, A. Walrant, Y. Zaltsman, C. Y. Jiao and S. Sagan. "Relationships between Membrane Binding, Affinity and Cell Internalization Efficacy of a Cell-Penetrating Peptide: Penetratin as a Case Study." *PLoS One* 6, no. 9 (2011): e24096.

Alves, I. D., N. Goasdoue, I. Correia, S. Aubry, C. Galanth, S. Sagan, S. Lavielle and G. Chassaing. "Membrane Interaction and Perturbation Mechanisms Induced by Two Cationic Cell Penetrating Peptides with Distinct Charge Distribution." *Biochim Biophys Acta* 1780, no. 7-8 (2008): 948-59.

Amand, H. L., K. Fant, B. Norden and E. K. Esbjorner. "Stimulated Endocytosis in Penetratin Uptake: Effect of Arginine and Lysine." *Biochem Biophys Res Commun* 371, no. 4 (2008): 621-5.

Arnison, P. G., M. J. Bibb, G. Bierbaum, A. A. Bowers, T. S. Bugni, G. Bulaj, J. A. Camarero, D. J. Campopiano, G. L. Challis, J. Clardy, P. D. Cotter, D. J. Craik, M. Dawson, E. Dittmann, S. Donadio, P. C. Dorrestein, K. D. Entian, M. A. Fischbach, J. S. Garavelli, U. Goransson, C. W. Gruber, D. H. Haft, T. K. Hemscheidt, C. Hertweck, C. Hill, A. R. Horswill, M. Jaspars, W. L. Kelly, J. P. Klinman, O. P. Kuipers, A. J. Link, W. Liu, M. A. Marahiel, D. A. Mitchell, G. N. Moll, B. S. Moore, R. Muller, S. K. Nair, I. F. Nes, G. E. Norris, B. M. Olivera, H. Onaka, M. L. Patchett, J. Piel, M. J. Reaney, S. Rebuffat, R. P. Ross, H. G. Sahl, E. W. Schmidt, M. E. Selsted, K. Severinov, B. Shen, K. Sivonen, L. Smith, T. Stein, R. D. Sussmuth, J. R. Tagg, G. L. Tang, A. W. Truman, J. C. Vederas, C. T. Walsh, J. D. Walton, S. C. Wenzel, J. M. Willey and W. A. van der Donk. "Ribosomally Synthesized and Post-Translationally Modified Peptide

Natural Products: Overview and Recommendations for a Universal Nomenclature." *Nat Prod Rep* 30, no. 1 (2013): 108-60.

Barbeta, B. L., A. T. Marshall, A. D. Gillon, D. J. Craik and M. A. Anderson. "Plant Cyclotides Disrupt Epithelial Cells in the Midgut of Lepidopteran Larvae." *Proc Natl Acad Sci U S A* 105, no. 4 (2008): 1221-5.

Baxter, A. G. and P. D. Hodgkin. "Activation Rules: The Two-Signal Theories of Immune Activation." *Nat Rev Immunol* 2, no. 6 (2002): 439-46.

Boisseau, S., K. Mabrouk, N. Ram, N. Garmy, V. Collin, A. Tadmouri, M. Mikati, J. M. Sabatier, M. Ronjat, J. Fantini and M. De Waard. "Cell Penetration Properties of Maurocalcine, a Natural Venom Peptide Active on the Intracellular Ryanodine Receptor." *Biochim Biophys Acta* 1758, no. 3 (2006): 308-19.

Burman, R., S. Gunasekera, A. A. Stromstedt and U. Goransson. "Chemistry and Biology of Cyclotides: Circular Plant Peptides Outside the Box." *J Nat Prod* 77, no. 3 (2014): 724-36.

Burman, Robert, Adam A. Strömstedt, Martin Malmsten and Ulf Göransson. "Cyclotide–Membrane Interactions: Defining Factors of Membrane Binding, Depletion and Disruption." *Biochimica et Biophysica Acta (BBA) - Biomembranes* 1808, no. 11 (2011): 2665-2673.

Cascales, L., S. T. Henriques, M. C. Kerr, Y. H. Huang, M. J. Sweet, N. L. Daly and D. J. Craik. "Identification and Characterization of a New Family of Cell-Penetrating Peptides: Cyclic Cell-Penetrating Peptides." *J Biol Chem* 286, no. 42 (2011): 36932-43.

Clark, R. J., N. L. Daly and D. J. Craik. "Structural Plasticity of the Cyclic-Cystine-Knot Framework: Implications for Biological Activity and Drug Design." *Biochem J* 394, no. Pt 1 (2006): 85-93.

Colgrave, M. L. and D. J. Craik. "Thermal, Chemical, and Enzymatic Stability of the Cyclotide Kalata B1: The Importance of the Cyclic Cystine Knot." *Biochemistry* 43, no. 20 (2004): 5965-75.

Colgrave, M. L., A. Jones and D. J. Craik. "Peptide Quantification by Matrix-Assisted Laser Desorption Ionisation Time-of-Flight Mass Spectrometry: Investigations of the Cyclotide Kalata B1 in Biological Fluids." *J Chromatogr A* 1091, no. 1-2 (2005): 187-93.

Colgrave, M. L., A. C. Kotze, Y. H. Huang, J. O'Grady, S. M. Simonsen and D. J. Craik. "Cyclotides: Natural, Circular Plant Peptides That Possess Significant Activity against Gastrointestinal Nematode Parasites of Sheep." *Biochemistry* 47, no. 20 (2008): 5581-9.

Colgrave, M. L., A. C. Kotze, S. Kopp, J. S. McCarthy, G. T. Coleman and D. J. Craik. "Anthelmintic Activity of Cyclotides: In Vitro Studies with Canine and Human Hookworms." *Acta Trop* 109, no. 2 (2009): 163-6.

Conner, S. D. and S. L. Schmid. "Regulated Portals of Entry into the Cell." *Nature* 422, no. 6927 (2003): 37-44.

Contreras, J., A. Y. Elnagar, S. F. Hamm-Alvarez and J. A. Camarero. "Cellular Uptake of Cyclotide Mcoti-I Follows Multiple Endocytic Pathways." *J Control Release* 155, no. 2 (2011): 134-43.

Costello, P. S., M. Gallagher and D. A. Cantrell. "Sustained and Dynamic Inositol Lipid Metabolism inside and Outside the Immunological Synapse." *Nat Immunol* 3, no. 11 (2002): 1082-9.

Cragg, G. M. and D. J. Newman. "Natural Products: A Continuing Source of Novel Drug Leads." *Biochim Biophys Acta* 1830, no. 6 (2013): 3670-95.

Craik, D. J. "The Folding of Disulfide-Rich Proteins." *Antioxid Redox Signal* 14, no. 1 (2011): 61-4.

Craik, David J., David P. Fairlie, Spiros Liras and David Price. "The Future of Peptide-Based Drugs." *Chemical Biology & Drug Design* 81, no. 1 (2013): 136-147.

D'Souza, C., S. T. Henriques, C. K. Wang and D. J. Craik. "Structural Parameters Modulating the Cellular Uptake of Disulfide-Rich Cyclic Cell-Penetrating Peptides: Mcoti-Ii and Sfti-1." *Eur J Med Chem*, (2014).

Daly, N. L., S. Love, P. F. Alewood and D. J. Craik. "Chemical Synthesis and Folding Pathways of Large Cyclic Polypeptides: Studies of the Cystine Knot Polypeptide Kalata B1." *Biochemistry* 38, no. 32 (1999): 10606-14.

Daly, N. L., K. J. Rosengren and D. J. Craik. "Discovery, Structure and Biological Activities of Cyclotides." *Adv Drug Deliv Rev* 61, no. 11 (2009): 918-30.

Davidson, A. and B. Diamond. "Autoimmune Diseases." *N Engl J Med* 345, no. 5 (2001): 340-50.

de Mattos, Angelo M., Ali J. Olyaei and William M. Bennett. "Nephrotoxicity of Immunosuppressive Drugs: Long-Term Consequences and Challenges for the Future." *American Journal of Kidney Diseases* 35, no. 2 (2000): 333-346.

de Planque, M. R., B. B. Bonev, J. A. Demmers, D. V. Greathouse, R. E. Koeppe, 2nd, F. Separovic, A. Watts and J. A. Killian. "Interfacial Anchor Properties of Tryptophan Residues in Transmembrane Peptides Can Dominate over Hydrophobic Matching Effects in Peptide-Lipid Interactions." *Biochemistry* 42, no. 18 (2003): 5341-8.

Derossi, D., S. Calvet, A. Trembleau, A. Brunissen, G. Chassaing and A. Prochiantz. "Cell Internalization of the Third Helix of the Antennapedia Homeodomain Is Receptor-Independent." *J Biol Chem* 271, no. 30 (1996): 18188-93.

Duchardt, F., M. Fotin-Mleczek, H. Schwarz, R. Fischer and R. Brock. "A Comprehensive Model for the Cellular Uptake of Cationic Cell-Penetrating Peptides." *Traffic* 8, no. 7 (2007): 848-66.

Escoubas, P. "Molecular Diversification in Spider Venoms: A Web of Combinatorial Peptide Libraries." *Mol Divers* 10, no. 4 (2006): 545-54.

Escoubas, P., B. Sollod and G. F. King. "Venom Landscapes: Mining the Complexity of Spider Venoms Via a Combined Cdna and Mass Spectrometric Approach." *Toxicon* 47, no. 6 (2006): 650-63.

Farrokhi, N., J. P. Whitelegge and J. A. Brusslan. "Plant Peptides and Peptidomics." *Plant Biotechnol J* 6, no. 2 (2008): 105-34.

Felizmenio-Quimio, M. E., N. L. Daly and D. J. Craik. "Circular Proteins in Plants: Solution Structure of a Novel Macrocyclic Trypsin Inhibitor from Momordica Cochinchinensis." *J Biol Chem* 276, no. 25 (2001): 22875-82.

Firn, R. D. and C. G. Jones. "Natural Products--a Simple Model to Explain Chemical Diversity." *Nat Prod Rep* 20, no. 4 (2003): 382-91.

Fischer, R., T. Waizenegger, K. Kohler and R. Brock. "A Quantitative Validation of Fluorophore-Labelled Cell-Permeable Peptide Conjugates: Fluorophore and Cargo Dependence of Import." *Biochim Biophys Acta* 1564, no. 2 (2002): 365-74.

Fox, J. W. and S. M. Serrano. "Approaching the Golden Age of Natural Product Pharmaceuticals from Venom Libraries: An Overview of Toxins and Toxin-Derivatives Currently Involved in Therapeutic or Diagnostic Applications." *Curr Pharm Des* 13, no. 28 (2007): 2927-34.

Frankel, A. D. and C. O. Pabo. "Cellular Uptake of the Tat Protein from Human Immunodeficiency Virus." *Cell* 55, no. 6 (1988): 1189-93.

Fretz, M. M., N. A. Penning, S. Al-Taei, S. Futaki, T. Takeuchi, I. Nakase, G. Storm and A. T. Jones. "Temperature-, Concentration- and Cholesterol-Dependent Translocation of L- and D-Octa-Arginine across the Plasma and Nuclear Membrane of Cd34+ Leukaemia Cells." *Biochem J* 403, no. 2 (2007): 335-42.

Fridriksson, E. K., P. A. Shipkova, E. D. Sheets, D. Holowka, B. Baird and F. W. McLafferty. "Quantitative Analysis of Phospholipids in Functionally Important Membrane Domains from Rbl-2h3 Mast Cells Using Tandem High-Resolution Mass Spectrometry." *Biochemistry* 38, no. 25 (1999): 8056-63.

Futaki, S., T. Suzuki, W. Ohashi, T. Yagami, S. Tanaka, K. Ueda and Y. Sugiura. "Arginine-Rich Peptides. An Abundant Source of Membrane-Permeable Peptides Having Potential as Carriers for Intracellular Protein Delivery." *J Biol Chem* 276, no. 8 (2001): 5836-40.

Gerlach, S. L., R. Rathinakumar, G. Chakravarty, U. Goransson, W. C. Wimley, S. P. Darwin and D. Mondal. "Anticancer and Chemosensitizing Abilities of Cycloviolacin 02 from Viola Odorata and Psyle Cyclotides from Psychotria Leptothyrsa." *Biopolymers* 94, no. 5 (2010): 617-25.

Gerlach, Samantha and Debasis Mondal. *The Bountiful Biological Activities of Cyclotides*. Vol. 3, 2012.

Getts, D. R., S. Shankar, E. M. Chastain, A. Martin, M. T. Getts, K. Wood and S. D. Miller. "Current Landscape for T-Cell Targeting in Autoimmunity and Transplantation." *Immunotherapy* 3, no. 7 (2011): 853-70.

Goransson, U., M. Sjogren, E. Svangard, P. Claeson and L. Bohlin. "Reversible Antifouling Effect of the Cyclotide Cycloviolacin O2 against Barnacles." *J Nat Prod* 67, no. 8 (2004): 1287-90.

Gran, L. "On the Effect of a Polypeptide Isolated from "Kalata-Kalata" (Oldenlandia Affinis Dc) on the Oestrogen Dominated Uterus." *Acta Pharmacol Toxicol (Copenh)* 33, no. 5 (1973): 400-8.

Green, M. and P. M. Loewenstein. "Autonomous Functional Domains of Chemically Synthesized Human Immunodeficiency Virus Tat Trans-Activator Protein." *Cell* 55, no. 6 (1988): 1179-88.

Greenwood, Kathryn P., Norelle L. Daly, Darren L. Brown, Jennifer L. Stow and David J. Craik. "The Cyclic Cystine Knot Miniprotein Mcoti-Ii Is Internalized into Cells by Macropinocytosis." *The International Journal of Biochemistry & Cell Biology* 39, no. 12 (2007): 2252-2264.

Gruber, C. W., A. G. Elliott, D. C. Ireland, P. G. Delprete, S. Dessein, U. Goransson, M. Trabi, C. K. Wang, A. B. Kinghorn, E. Robbrecht and D. J. Craik. "Distribution and Evolution of Circular Miniproteins in Flowering Plants." *Plant Cell* 20, no. 9 (2008): 2471-83.

Gruber, C. W., M. Muttenthaler and M. Freissmuth. "Ligand-Based Peptide Design and Combinatorial Peptide Libraries to Target G Protein-Coupled Receptors." *Curr Pharm Des* 16, no. 28 (2010): 3071-88.

Grundemann, C., K. Thell, K. Lengen, M. Garcia-Kaufer, Y. H. Huang, R. Huber, D. J. Craik, G. Schabbauer and C. W. Gruber. "Cyclotides Suppress Human T-Lymphocyte Proliferation by an Interleukin 2-Dependent Mechanism." *PLoS One* 8, no. 6 (2013): e68016.

Gründemann, Carsten, Johannes Koehbach, Roman Huber and Christian W. Gruber. "Do Plant Cyclotides Have Potential as Immunosuppressant Peptides?" *Journal of Natural Products* 75, no. 2 (2012): 167-174.

Hancock, R. E. and G. Diamond. "The Role of Cationic Antimicrobial Peptides in Innate Host Defences." *Trends Microbiol* 8, no. 9 (2000): 402-10.

Hendrich, A. B. and K. Michalak. "Lipids as a Target for Drugs Modulating Multidrug Resistance of Cancer Cells." *Curr Drug Targets* 4, no. 1 (2003): 23-30.

Henriques, S. T., J. Costa and M. A. Castanho. "Translocation of Beta-Galactosidase Mediated by the Cell-Penetrating Peptide Pep-1 into Lipid Vesicles and Human Hela Cells Is Driven by Membrane Electrostatic Potential." *Biochemistry* 44, no. 30 (2005): 10189-98.

Henriques, S. T. and D. J. Craik. "Importance of the Cell Membrane on the Mechanism of Action of Cyclotides." *ACS Chem Biol* 7, no. 4 (2012): 626-36.

Henriques, S. T., Y. H. Huang, K. J. Rosengren, H. G. Franquelim, F. A. Carvalho, A. Johnson, S. Sonza, G. Tachedjian, M. A. Castanho, N. L. Daly and D. J. Craik. "Decoding the Membrane Activity of the Cyclotide Kalata B1: The Importance of Phosphatidylethanolamine Phospholipids and Lipid Organization on Hemolytic and Anti-Hiv Activities." *J Biol Chem* 286, no. 27 (2011): 24231-41.

Hirose, H., T. Takeuchi, H. Osakada, S. Pujals, S. Katayama, I. Nakase, S. Kobayashi, T. Haraguchi and S. Futaki. "Transient Focal Membrane Deformation Induced by Arginine-Rich Peptides Leads to Their Direct Penetration into Cells." *Mol Ther* 20, no. 5 (2012): 984-93.

Huang, Y. H., M. L. Colgrave, R. J. Clark, A. C. Kotze and D. J. Craik. "Lysine-Scanning Mutagenesis Reveals an Amendable Face of the Cyclotide Kalata B1 for the Optimization of Nematocidal Activity." *J Biol Chem* 285, no. 14 (2010): 10797-805.

Huang, Y. H., M. L. Colgrave, N. L. Daly, A. Keleshian, B. Martinac and D. J. Craik. "The Biological Activity of the Prototypic Cyclotide Kalata B1 Is Modulated by the Formation of Multimeric Pores." *J Biol Chem* 284, no. 31 (2009): 20699-707.

Ireland, D. C., C. K. Wang, J. A. Wilson, K. R. Gustafson and D. J. Craik. "Cyclotides as Natural Anti-Hiv Agents." *Biopolymers* 90, no. 1 (2008): 51-60.

Ireland, David C., Richard J. Clark, Norelle L. Daly and David J. Craik. "Isolation, Sequencing, and Structure−Activity Relationships of Cyclotides." *Journal of Natural Products* 73, no. 9 (2010): 1610-1622.

Jacobson, D. L., S. J. Gange, N. R. Rose and N. M. Graham. "Epidemiology and Estimated Population Burden of Selected Autoimmune Diseases in the United States." *Clin Immunol Immunopathol* 84, no. 3 (1997): 223-43.

Jiao, C. Y., D. Delaroche, F. Burlina, I. D. Alves, G. Chassaing and S. Sagan. "Translocation and Endocytosis for Cell-Penetrating Peptide Internalization." *J Biol Chem* 284, no. 49 (2009): 33957-65.

Jones, A. T. "Macropinocytosis: Searching for an Endocytic Identity and Role in the Uptake of Cell Penetrating Peptides." *J Cell Mol Med* 11, no. 4 (2007): 670-84.

Kamimori, H., K. Hall, D. J. Craik and M. I. Aguilar. "Studies on the Membrane Interactions of the Cyclotides Kalata B1 and Kalata B6 on Model Membrane Systems by Surface Plasmon Resonance." *Anal Biochem* 337, no. 1 (2005): 149-53.

Kaplan, I. M., J. S. Wadia and S. F. Dowdy. "Cationic Tat Peptide Transduction Domain Enters Cells by Macropinocytosis." *J Control Release* 102, no. 1 (2005): 247-53.

Kimura, R. H., A. T. Tran and J. A. Camarero. "Biosynthesis of the Cyclotide Kalata B1 by Using Protein Splicing." *Angew Chem Int Ed Engl* 45, no. 6 (2006): 973-6.

Koehn, F. E. and G. T. Carter. "The Evolving Role of Natural Products in Drug Discovery." *Nat Rev Drug Discov* 4, no. 3 (2005): 206-20.

Korecka, A., A. Duszota and G. Korczak-Kowalska. "[the Role of the Cd28 Molecule in Immunological Tolerance]." *Postepy Hig Med Dosw (Online)* 61, (2007): 74-82.

Korhonen, H. and A. Pihlanto. "Technological Options for the Production of Health-Promoting Proteins and Peptides Derived from Milk and Colostrum." *Curr Pharm Des* 13, no. 8 (2007): 829-43.

Kosuge, M., T. Takeuchi, I. Nakase, A. T. Jones and S. Futaki. "Cellular Internalization and Distribution of Arginine-Rich Peptides as a Function of Extracellular Peptide Concentration, Serum, and Plasma Membrane Associated Proteoglycans." *Bioconjug Chem* 19, no. 3 (2008): 656-64.

Latham, P. W. "Therapeutic Peptides Revisited." *Nat Biotechnol* 17, no. 8 (1999): 755-7.

Lee, M. T., W. C. Hung, F. Y. Chen and H. W. Huang. "Many-Body Effect of Antimicrobial Peptides: On the Correlation between Lipid's Spontaneous Curvature and Pore Formation." *Biophys J* 89, no. 6 (2005): 4006-16.

Leta Aboye, T., R. J. Clark, D. J. Craik and U. Goransson. "Ultra-Stable Peptide Scaffolds for Protein Engineering-Synthesis and Folding of the Circular Cystine Knotted Cyclotide Cycloviolacin O2." *Chembiochem* 9, no. 1 (2008): 103-13.

Lindholm, P., U. Goransson, S. Johansson, P. Claeson, J. Gullbo, R. Larsson, L. Bohlin and A. Backlund. "Cyclotides: A Novel Type of Cytotoxic Agents." *Mol Cancer Ther* 1, no. 6 (2002): 365-9.

Lundberg, P., S. El-Andaloussi, T. Sutlu, H. Johansson and U. Langel. "Delivery of Short Interfering Rna Using Endosomolytic Cell-Penetrating Peptides." *Faseb j* 21, no. 11 (2007): 2664-71.

Lundin, P., H. Johansson, P. Guterstam, T. Holm, M. Hansen, U. Langel and E. L. Andaloussi S. "Distinct Uptake Routes of Cell-Penetrating Peptide Conjugates." *Bioconjug Chem* 19, no. 12 (2008): 2535-42.

Macian, F. "Nfat Proteins: Key Regulators of T-Cell Development and Function." *Nat Rev Immunol* 5, no. 6 (2005): 472-84.

Madani, F., S. Lindberg, U. Langel, S. Futaki and A. Graslund. "Mechanisms of Cellular Uptake of Cell-Penetrating Peptides." *J Biophys* 2011, (2011): 414729.

Mai, J. C., H. Shen, S. C. Watkins, T. Cheng and P. D. Robbins. "Efficiency of Protein Transduction Is Cell Type-Dependent and Is Enhanced by Dextran Sulfate." *J Biol Chem* 277, no. 33 (2002): 30208-18.

Malek, T. R. "The Biology of Interleukin-2." *Annu Rev Immunol* 26, (2008): 453-79.

Mano, M., A. Henriques, A. Paiva, M. Prieto, F. Gavilanes, S. Simoes and M. C. Pedroso de Lima. "Cellular Uptake of S413-Pv Peptide Occurs Upon Conformational Changes Induced by Peptide-Membrane Interactions." *Biochim Biophys Acta* 1758, no. 3 (2006): 336-46.

Martin, P. J., J. A. Hansen, A. W. Siadak and R. C. Nowinski. "Monoclonal Antibodies Recognizing Normal Human T Lymphocytes and Malignant Human B Lymphocytes: A Comparative Study." *J Immunol* 127, no. 5 (1981): 1920-3.

Matsuda, S. and S. Koyasu. "Mechanisms of Action of Cyclosporine." *Immunopharmacology* 47, no. 2-3 (2000): 119-25.

Matsuzaki, K., S. Yoneyama, O. Murase and K. Miyajima. "Transbilayer Transport of Ions and Lipids Coupled with Mastoparan X Translocation." *Biochemistry* 35, no. 25 (1996): 8450-6.

Mayor, S. and R. E. Pagano. "Pathways of Clathrin-Independent Endocytosis." *Nat Rev Mol Cell Biol* 8, no. 8 (2007): 603-12.

Meuer, S. C., K. A. Fitzgerald, R. E. Hussey, J. C. Hodgdon, S. F. Schlossman and E. L. Reinherz. "Clonotypic Structures Involved in Antigen-Specific Human T Cell Function. Relationship to the T3 Molecular Complex." *J Exp Med* 157, no. 2 (1983): 705-19.

Mishra, Bhuwan B. and Vinod K. Tiwari. "Natural Products: An Evolving Role in Future Drug Discovery." *European Journal of Medicinal Chemistry* 46, no. 10 (2011): 4769-4807.

Mitchell, A. A., A. J. Sapienza-Crawford, K. L. Hanley, K. J. Lokey, L. Wells, G. C. McDowell, 2nd and M. Stanton-Hicks. "Administering Ziconotide and Monitoring Patients Treated with Ziconotide: Expert Opinions." *Pain Manag Nurs* 14, no. 3 (2013): e84-94.

Mitchell, D. J., D. T. Kim, L. Steinman, C. G. Fathman and J. B. Rothbard. "Polyarginine Enters Cells More Efficiently Than Other Polycationic Homopolymers." *J Pept Res* 56, no. 5 (2000): 318-25.

Mukherjee, Sushmita, Richik N Ghosh and Frederick R Maxfield. "Endocytosis." *Physiological reviews* 77, no. 3 (1997): 759-803.

Nakase, I., M. Niwa, T. Takeuchi, K. Sonomura, N. Kawabata, Y. Koike, M. Takehashi, S. Tanaka, K. Ueda, J. C. Simpson, A. T. Jones, Y. Sugiura and S. Futaki. "Cellular Uptake of Arginine-Rich Peptides: Roles for Macropinocytosis and Actin Rearrangement." *Mol Ther* 10, no. 6 (2004): 1011-22.

Nawae, Wanapinun, Supa Hannongbua and Marasri Ruengjitchatchawalya. "Defining the Membrane Disruption Mechanism of Kalata B1 Via Coarse-Grained Molecular Dynamics Simulations." *Sci. Rep.* 4, (2014).

Newman, D. J., G. M. Cragg and K. M. Snader. "Natural Products as Sources of New Drugs over the Period 1981-2002." *J Nat Prod* 66, no. 7 (2003): 1022-37.

Norton, R. S. and B. M. Olivera. "Conotoxins Down Under." *Toxicon* 48, no. 7 (2006): 780-98.

Panchuk-Voloshina, N., R. P. Haugland, J. Bishop-Stewart, M. K. Bhalgat, P. J. Millard, F. Mao, W. Y. Leung and R. P. Haugland. "Alexa Dyes, a Series of New Fluorescent Dyes That Yield Exceptionally Bright, Photostable Conjugates." *J Histochem Cytochem* 47, no. 9 (1999): 1179-88.

Plan, M. R., I. Saska, A. G. Cagauan and D. J. Craik. "Backbone Cyclised Peptides from Plants Show Molluscicidal Activity against the Rice Pest Pomacea Canaliculata (Golden Apple Snail)." *J Agric Food Chem* 56, no. 13 (2008): 5237-41.

Pope, J. E. and T. R. Deer. "Ziconotide: A Clinical Update and Pharmacologic Review." *Expert Opin Pharmacother* 14, no. 7 (2013): 957-66.

Possani, L. D., B. Becerril, M. Delepierre and J. Tytgat. "Scorpion Toxins Specific for Na+-Channels." *Eur J Biochem* 264, no. 2 (1999): 287-300.

Pouny, Y., D. Rapaport, A. Mor, P. Nicolas and Y. Shai. "Interaction of Antimicrobial Dermaseptin and Its Fluorescently Labeled Analogues with Phospholipid Membranes." *Biochemistry* 31, no. 49 (1992): 12416-23.

Reuter, J., I. Merfort and C. M. Schempp. "Botanicals in Dermatology: An Evidence-Based Review." *Am J Clin Dermatol* 11, no. 4 (2010): 247-67.

Richard, J. P., K. Melikov, E. Vives, C. Ramos, B. Verbeure, M. J. Gait, L. V. Chernomordik and B. Lebleu. "Cell-Penetrating Peptides. A Reevaluation of the Mechanism of Cellular Uptake." *J Biol Chem* 278, no. 1 (2003): 585-90.

Saether, O., D. J. Craik, I. D. Campbell, K. Sletten, J. Juul and D. G. Norman. "Elucidation of the Primary and Three-Dimensional Structure of the Uterotonic Polypeptide Kalata B1." *Biochemistry* 34, no. 13 (1995): 4147-58.

Sandberg, F. "[Symposium on Medicinal Plants in Kandy]." *Sven Farm Tidskr* 69, no. 15 (1965): 511-6.

Sando, L., S. T. Henriques, F. Foley, S. M. Simonsen, N. L. Daly, K. N. Hall, K. R. Gustafson, M. I. Aguilar and D. J. Craik. "A Synthetic Mirror Image of Kalata B1 Reveals That Cyclotide Activity Is Independent of a Protein Receptor." *Chembiochem* 12, no. 16 (2011): 2456-62.

Sarmadi, B. H. and A. Ismail. "Antioxidative Peptides from Food Proteins: A Review." *Peptides* 31, no. 10 (2010): 1949-56.

Sato, A. K., M. Viswanathan, R. B. Kent and C. R. Wood. "Therapeutic Peptides: Technological Advances Driving Peptides into Development." *Curr Opin Biotechnol* 17, no. 6 (2006): 638-42.

Scott, R. E. "Plasma Membrane Vesiculation: A New Technique for Isolation of Plasma Membranes." *Science* 194, no. 4266 (1976): 743-5.

Seydel, P., C. W. Gruber, D. J. Craik and H. Dornenburg. "Formation of Cyclotides and Variations in Cyclotide Expression in Oldenlandia Affinis Suspension Cultures." *Appl Microbiol Biotechnol* 77, no. 2 (2007): 275-84.

Shan, X., M. J. Czar, S. C. Bunnell, P. Liu, Y. Liu, P. L. Schwartzberg and R. L. Wange. "Deficiency of Pten in Jurkat T Cells Causes Constitutive Localization of Itk to the Plasma Membrane and Hyperresponsiveness to Cd3 Stimulation." *Mol Cell Biol* 20, no. 18 (2000): 6945-57.

Shenkarev, Z. O., K. D. Nadezhdin, E. N. Lyukmanova, V. A. Sobol, L. Skjeldal and A. S. Arseniev. "Divalent Cation Coordination and Mode of Membrane Interaction in Cyclotides: Nmr Spatial Structure of Ternary Complex Kalata B7/Mn2+/Dpc Micelle." *J Inorg Biochem* 102, no. 5-6 (2008): 1246-56.

Shenkarev, Z. O., K. D. Nadezhdin, V. A. Sobol, A. G. Sobol, L. Skjeldal and A. S. Arseniev. "Conformation and Mode of Membrane Interaction in Cyclotides. Spatial Structure of Kalata B1 Bound to a Dodecylphosphocholine Micelle." *Febs j* 273, no. 12 (2006): 2658-72.

Simonsen, S. M., L. Sando, D. C. Ireland, M. L. Colgrave, R. Bharathi, U. Goransson and D. J. Craik. "A Continent of Plant Defense Peptide Diversity: Cyclotides in Australian Hybanthus (Violaceae)." *Plant Cell* 17, no. 11 (2005): 3176-89.

Simonsen, S. M., L. Sando, K. J. Rosengren, C. K. Wang, M. L. Colgrave, N. L. Daly and D. J. Craik. "Alanine Scanning Mutagenesis of the Prototypic Cyclotide Reveals a Cluster of Residues Essential for Bioactivity." *J Biol Chem* 283, no. 15 (2008): 9805-13.

Sinha, A. A., M. T. Lopez and H. O. McDevitt. "Autoimmune Diseases: The Failure of Self Tolerance." *Science* 248, no. 4961 (1990): 1380-8.

St Georgiev, V. "Immunomodulatory Activity of Small Peptides." *Trends Pharmacol Sci* 11, no. 9 (1990): 373-8.

Strömstedt, Adam A, Lovisa Ringstad, Artur Schmidtchen and Martin Malmsten. "Interaction between Amphiphilic Peptides and Phospholipid Membranes." *Current Opinion in Colloid & Interface Science* 15, no. 6 (2010): 467-478.

Svangard, E., R. Burman, S. Gunasekera, H. Lovborg, J. Gullbo and U. Goransson. "Mechanism of Action of Cytotoxic Cyclotides: Cycloviolacin O2 Disrupts Lipid Membranes." *J Nat Prod* 70, no. 4 (2007): 643-7.

Svangard, E., U. Goransson, Z. Hocaoglu, J. Gullbo, R. Larsson, P. Claeson and L. Bohlin. "Cytotoxic Cyclotides from Viola Tricolor." *J Nat Prod* 67, no. 2 (2004): 144-7.

Tam, J. P., Y. A. Lu, J. L. Yang and K. W. Chiu. "An Unusual Structural Motif of Antimicrobial Peptides Containing End-to-End Macrocycle and Cystine-Knot Disulfides." *Proc Natl Acad Sci U S A* 96, no. 16 (1999): 8913-8.

Theakston, R. D. and A. S. Kamiguti. "A List of Animal Toxins and Some Other Natural Products with Biological Activity." *Toxicon* 40, no. 5 (2002): 579-651.

Thell, K., R. Hellinger, G. Schabbauer and C. W. Gruber. "Immunosuppressive Peptides and Their Therapeutic Applications." *Drug Discov Today* 19, no. 5 (2014): 645-53.

Thoren, P. E., D. Persson, P. Isakson, M. Goksor, A. Onfelt and B. Norden. "Uptake of Analogs of Penetratin, Tat(48-60) and Oligoarginine in Live Cells." *Biochem Biophys Res Commun* 307, no. 1 (2003): 100-7.

Torcato, I. M., Y. H. Huang, H. G. Franquelim, D. D. Gaspar, D. J. Craik, M. A. Castanho and S. T. Henriques. "The Antimicrobial Activity of Sub3 Is Dependent on Membrane Binding and Cell-Penetrating Ability." *Chembiochem* 14, no. 15 (2013): 2013-22.

Truneh, A., F. Albert, P. Golstein and A. M. Schmitt-Verhulst. "Early Steps of Lymphocyte Activation Bypassed by Synergy between Calcium Ionophores and Phorbol Ester." *Nature* 313, no. 6000 (1985): 318-20.

Utsugi, T., A. J. Schroit, J. Connor, C. D. Bucana and I. J. Fidler. "Elevated Expression of Phosphatidylserine in the Outer Membrane Leaflet of Human Tumor Cells and Recognition by Activated Human Blood Monocytes." *Cancer Res* 51, no. 11 (1991): 3062-6.

Vives, E. "Cellular Uptake [Correction of Utake] of the Tat Peptide: An Endocytosis Mechanism Following Ionic Interactions." *J Mol Recognit* 16, no. 5 (2003): 265-71.

Vlieghe, P., V. Lisowski, J. Martinez and M. Khrestchatisky. "Synthetic Therapeutic Peptides: Science and Market." *Drug Discov Today* 15, no. 1-2 (2010): 40-56.

Wang, C. K., M. L. Colgrave, D. C. Ireland, Q. Kaas and D. J. Craik. "Despite a Conserved Cystine Knot Motif, Different Cyclotides Have Different Membrane Binding Modes." *Biophys J* 97, no. 5 (2009): 1471-81.

Wang, C. K., H. P. Wacklin and D. J. Craik. "Cyclotides Insert into Lipid Bilayers to Form Membrane Pores and Destabilize the Membrane through Hydrophobic and Phosphoethanolamine-Specific Interactions." *J Biol Chem* 287, no. 52 (2012): 43884-98.

Wang, X., A. Gjorloff-Wingren, M. Saxena, N. Pathan, J. C. Reed and T. Mustelin. "The Tumor Suppressor Pten Regulates T Cell Survival and Antigen Receptor Signaling by Acting as a Phosphatidylinositol 3-Phosphatase." *J Immunol* 164, no. 4 (2000): 1934-9.

Webster, L. R., K. L. Fakata, S. Charapata, R. Fisher and M. MineHart. "Open-Label, Multicenter Study of Combined Intrathecal Morphine and Ziconotide: Addition of Morphine in Patients Receiving Ziconotide for Severe Chronic Pain." *Pain Med* 9, no. 3 (2008): 282-90.

Weiss, A., R. L. Wiskocil and J. D. Stobo. "The Role of T3 Surface Molecules in the Activation of Human T Cells: A Two-Stimulus Requirement for Il 2

Production Reflects Events Occurring at a Pre-Translational Level." *J Immunol* 133, no. 1 (1984): 123-8.

Wender, P. A., D. J. Mitchell, K. Pattabiraman, E. T. Pelkey, L. Steinman and J. B. Rothbard. "The Design, Synthesis, and Evaluation of Molecules That Enable or Enhance Cellular Uptake: Peptoid Molecular Transporters." *Proc Natl Acad Sci U S A* 97, no. 24 (2000): 13003-8.

Wimley, W. C. "Describing the Mechanism of Antimicrobial Peptide Action with the Interfacial Activity Model." *ACS Chem Biol* 5, no. 10 (2010): 905-17.

Wiskocil, R., A. Weiss, J. Imboden, R. Kamin-Lewis and J. Stobo. "Activation of a Human T Cell Line: A Two-Stimulus Requirement in the Pretranslational Events Involved in the Coordinate Expression of Interleukin 2 and Gamma-Interferon Genes." *J Immunol* 134, no. 3 (1985): 1599-603.

Witherup, K. M., M. J. Bogusky, P. S. Anderson, H. Ramjit, R. W. Ransom, T. Wood and M. Sardana. "Cyclopsychotride a, a Biologically Active, 31-Residue Cyclic Peptide Isolated from Psychotria Longipes." *J Nat Prod* 57, no. 12 (1994): 1619-25.

Yeshak, M. Y., U. Goransson, R. Burman and B. Hellman. "Genotoxicity and Cellular Uptake of Cyclotides: Evidence for Multiple Modes of Action." *Mutat Res* 747, no. 2 (2012): 176-81.

Yin, Y., Y. Li and R. A. Mariuzza. "Structural Basis for Self-Recognition by Autoimmune T-Cell Receptors." *Immunol Rev* 250, no. 1 (2012): 32-48.

9. Appendices

9.1 Abstract

Cyclotides have been isolated from plants of the families of *Rubiaceae*, *Violaceae* and *Cucurbiceae* and contain 28 to 37 amino acid residues which correspond to a mass range of 2500 – 4000 Da. They are circular proteins that are characterized by a head to tail cyclized backbone. At the molecular core of the peptides are three disulfide bonds which form a cyclic cystine knot. This structural motif is responsible for the stability and for the resistance of the cyclotides to thermal, chemical and enzymatic degradation. Moreover, these cyclic peptides are hydrophobic and this leads to a typical late elution from a RP–HPLC column.

The history of cyclotides may be traced back at more than 50 years ago when Sandberg reported that African tribes have been using an extract from the plant *Oldenlandia affinis* to facilitate childbirth. Later the Norwegian doctor Lorents Gran made ethno botanical investigations and determined that it contained cyclic peptides which are responsible for the strong activity. Due to the previously investigated uterotonic activity, cyclotides got interested for scientists. Further research determined many other biological actions, including antimicrobial, insecticidal, anticancer, anti-HIV and immunosuppressive activity.

To perform all these biological properties, the cyclotide interacts firstly with the cellular membrane of the living organisms. Moreover, the different subfamilies of cyclotides possess diverse mode of action. However, for all of them there is electrostatic interaction between the peptide and the cellular membrane due to the positively charged residues of the cyclotide and the negatively charged membrane head groups.

Recent research reported that a mutant from the cyclotide kalata B1, where the threonine at position twenty is exchanged with a lysine, has an antiproliferative effect on lymphocytes. Although the main mechanism of action is still unclear,

the cyclotide [T20K] kalata B1 suppresses the proliferation of T-cells. Moreover, the aim of this study was to confirm, implementing anti-CD3 isolated primary T-cells and Jurkat cells as *in-vitro* model systems, if the fluorescently labeled [T20K] kalata B1 mutant (T20K-CF) can penetrate through the cellular membrane. The interaction has been investigated in a dose-, time- and temperature-dependent study. Moreover, with prolonging of the incubation time and increasing of the peptide concentration, higher amounts of peptide have been internalized into the cells. On the other hand, through microscopic observation it was examined that the cytotoxicity also increased. This may be due to the property of cyclotides to form pores in the cellular membrane which has been described in several papers. Furthermore, this property enables an energy-independent, direct transport through the cellular membrane. However, at low temperature the peptide penetration was reduced which is an evidence that endocytosis plays an important role for the mechanism of peptide uptake. These results strongly supported the involvement of both passive membrane passage and active cellular uptake by endocytosis of T20K-CF.

9.2 Zusammenfassung

Cyclotide wurden von den Pflanzen aus der Familien *Rubiaceae*, *Violaceae* und *Cucurbiceae* isoliert und bestehen aus zwischen 28 und 37 Aminosäuren was ein Molekulargewicht zwischen 2500 und 4000 Da entspricht. Sie sind cyclische Peptide, die eine charakteristische 3D Struktur besitzen, welche durch drei hoch konservierte Disulfidbrücken hervorgerufen wird. Sie wurden auch „cyclic cystine–knot (CCK)“ genannt. Dieses strukturelle Motiv ist verantwortlich für die besondere Stabilität und Widerstandsfähigkeit der Cyclotide zu einem thermischen, chemischen oder enzymatischen Abbau. Weiteres sind sie eher hydrophob wodurch sie an einer RP–HPLC Säule relativ spät eluieren.

Vor mehr als 50 Jahre hat Sandberg berichtet, dass die afrikanischen Stämme ein Extrakt von der Pflanze *Oldenlandia affinis* verwendet haben, damit sie die Geburtswehen erleichtern. Später hat der norwegische Doktor Lorents Gran ethno botanische Untersuchungen gemacht und er hat entdeckt, dass der pflanzliche Extrakt cyclische Peptide enthalte, die für die starke biologische Aktivität verantwortlich waren. Wegen dieser uterotonischen Wirkung sind die Cyclotide interessant für die Forscher geworden. Weitere Untersuchungen haben viele andere biologische Aktivitäten wie antimikrobille, insektizide, antikrebs, anti-HIV und immunosuppressive Wirkung festgestellt.

Um alle diese Effekte auszuüben, soll das Cyclotid zuerst mit den zellulären Membranen der lebenden Organismen interagieren. Dafür existiert eine elektrostatische Interaktion zwischen die Peptide und die zelluläre Membran, die durch die Wechselwirkung zwischen die positiv geladenen Reste der Cyclotide und die negativ geladenen Membrankopfgruppen entstanden ist.

Die kalata B1 Mutante [T20K] kalata B1, wo das Threonin an der Position zwanzig mit einem Lysin ausgetauscht worden ist, zeigte in vorangegangenen Studien einen antiproliferativen Effekt auf Lymphozyten. Obwohl der genaue Mechanismus, der dieser Wirkung zu Grunde liegt, bis heute unbekannt ist (Gründemann et al., 2013), unterdrückt das Cyclotid [T20K] kalata B1 die Proliferation von den T-Zellen. Ziel dieser Arbeit war zu bestätigen, dass das

Fluoreszein-getaggte Peptid T20K (T20K-CF) durch die Zellmembrane von anti-CD3 isolierten primären T-Zellen und Jurkat Zellen penetrieren kann. Die Interaktion zwischen das Peptid und die Lipiddoppelschicht wurde in einem dosis-, zeit- und temperaturabhängigen Studium untersucht. Es wurde festgestellt, dass mit Verlängerung der Inkubationszeit und Erhöhung der Konzentration größere Mengen an Peptid in die Zelle aufgenommen wurden. Zusätzlich durch mikroskopische Beobachtung wurde festgestellt, dass dadurch auch die Zytotoxizität erhöht wurde. Die Ursache für die Schädigung der Zellmembran könnte mit der Fähigkeit der Cyclotiden Poren an Lipiddoppelschichten zu bilden erklärt werden. Zusätzlich dieser Prozess könnte eine Methode sein, um Peptide direkt und energiefrei aufzunehmen. Jedoch, bei niedriger Temperatur wurde die Peptidaufnahme reduziert was ein Beweis dafür ist, dass die energieabhängige Endocytose auch beteiligt ist. Das hat zu der Schlussfolgerung geführt, dass der Aufnahmemechanismus eine Mischung zwischen direkte Penetration und Endocytose ist.

9.3 Curriculum vitae

Name Mina Vasileva

Telephone +43 681 815 26 089

E-mail: mina.vasileva@yahoo.com

Education

10/2012 to present University of Vienna (Austria): Master's course in Molecular Biology

10/2008 to 08/2012 Dresden University of Technology (Germany): Bachelor Degree in Molecular Biotechnology;

09/2003 - 07/2008 35th foreign language school "Dobri Voinikov", Sofia, Bulgaria

Work exprerience

09/2013 to present	Master thesis: „Chemical derivatization and cellular imaging of immunosuppressive peptides"; Center for Pharmacology and Physiology to the Medical University of Vienna
08/2013 to 09/2013	Internship at the National Center of Infectious and Parasitic Diseases in Sofia, Bulgaria
03/2012 to 08/2012	Bachelor thesis: "Expression of GunA2 in *Escherichia coli"*; Department of Molecular Genetics to Dresden University of Technology;
09/2011 to 08/2012	Tutor at the International office Dresden
09/2011 to 11/2011	Student helper at the International office Dresden
09/2010 – 10/2010	Internship at the National Center of Infectious and Parasitic Diseases in Sofia, Bulgaria